



## Politecnico of Milan

School of Industrial and Information Engineering  
Master of Science in Mathematical Engineering

MASTER THESIS

# The DRPM Strikes Back: Improvements on a Bayesian Spatio-Temporal Clustering Model

Advisor

**Prof. Alessandra Guglielmi**

Coadvisor

**Prof. Alessandro Carminati**

Candidate

**Federico Angelo Mor**

Matr. 221429



*to my cats Otto  
and La Micia*



# Abstract

Clustering is a key technique for identifying patterns and structures in complex datasets, whose relevance is intensified in spatio-temporal contexts where observations are simultaneously influenced by multiple factors such as space, time, and covariates. To this end, the Dependent Random Partition Model (DRPM) is one of the most relevant bayesian models due to its explicit consideration of temporal dependence in the partitions. However, the current implementation lacks of the inclusion of covariates, the handling of missing data, and the efficiency in execution times. Therefore, in this work we improve the original DRPM model by addressing those issues trough updates on the model formulation and a brand new implementation in Julia. These advancements are then tested on synthetic and real-world datasets, including air quality data from the AgrImOnIA project in Lombardy, Italy.

KEYWORDS: bayesian modelling, clustering, spatio-temporal data, computational statistics



# Sommario

Il clustering è una tecnica fondamentale per identificare strutture e pattern in dataset complessi, la cui importanza è intensificata nei contesti spazio-temporali in cui le osservazioni sono influenzate simultaneamente da molteplici fattori come spazio, tempo e covariate. In tal senso, il modello DRPM (Dependent Random Partition Model, modello per partizioni aleatorie dipendenti) è uno dei modelli bayesiani più rilevanti in quanto tiene conto in modo esplicito della dipendenza temporale delle partizioni. Tuttavia, l'attuale implementazione manca dell'inclusione di covariate, della gestione dei dati mancanti, e di efficienza nei tempi di esecuzione. In questo lavoro abbiamo quindi migliorato l'originale modello DRPM affrontando tali problemi tramite aggiornamenti sulla formulazione del modello e una fiammante implementazione in Julia. Questi sviluppi sono stati poi testati su dataset sintetici e reali, compresi i dati sulla qualità dell'aria in Lombardia del progetto AgrImOnIA.

PAROLE CHIAVE: modello bayesiano, clustering, dati spazio-temporali, statistica computazionale



# Contents

<b>1</b>	<b>Introduction</b>	<b>1</b>
<b>2</b>	<b>Description of the model</b>	<b>3</b>
2.1	Update rules derivation . . . . .	7
2.2	Spatial cohesions analysis . . . . .	10
2.3	Covariates similarities analysis . . . . .	15
<b>3</b>	<b>Implementation and optimizations</b>	<b>21</b>
3.1	Optimizations . . . . .	22
3.1.1	Optimizing spatial cohesions . . . . .	23
3.1.2	Optimizing covariates similarities . . . . .	26
<b>4</b>	<b>Testing</b>	<b>29</b>
4.1	Assessing the equivalence of the models . . . . .	29
4.1.1	Target variable only . . . . .	30
4.1.2	Target variable plus space . . . . .	31
4.2	Performance with missing values . . . . .	35
4.2.1	Target variable only (NA case) . . . . .	38
4.2.2	Target variable plus space (NA case) . . . . .	39
4.3	Effects of the covariates . . . . .	41
4.3.1	Covariates in the likelihood . . . . .	42
4.3.2	Covariates in the clustering . . . . .	45
4.4	Scaling performances . . . . .	49
<b>5</b>	<b>Conclusion</b>	<b>57</b>
<b>A</b>	<b>Theoretical details</b>	<b>59</b>
A.1	Extended computations of the full conditionals . . . . .	59

<b>B Computational details</b>	<b>69</b>
B.1 Fitting algorithm code . . . . .	69
B.2 Interface . . . . .	84
<b>Bibliography</b>	<b>87</b>

# List of Figures

2.1	Updated DRPM model graph . . . . .	6
2.2	Partition considered for the cohesion analysis . . . . .	12
2.3	Cohesions 1, 2, and 3 illustration . . . . .	13
2.4	Cohesions 4, 5, and 6 illustration . . . . .	14
2.5	Partition considered for the similarity analysis . . . . .	16
2.6	Similarities 1, 2 and 3 illustration . . . . .	18
2.7	Similarity 4 illustration . . . . .	19
3.1	Flame graph of a test fit . . . . .	22
3.2	Cohesions 3 and 4 implementation comparison . . . . .	25
3.3	Similarity 4 annotations comparison . . . . .	27
4.1	Lagged ARI values of CDRPM and JDRPM fits, target values only	30
4.2	Clusters produced by JDRPM and CDRPM fits, target values only	31
4.3	Visual representation of the clusters of JDRPM and CDRPM fits, target values only . . . . .	32
4.4	Generated and fitted values of JDRPM and CDRPM fits, target values only . . . . .	33
4.5	Comparison of the two possible mean centering methods on the target variable . . . . .	34
4.6	Lagged ARI values of CDRPM and JDRPM fits, target plus space values . . . . .	35
4.7	Target and fitted values of JDRPM and CDRPM fits, target plus space values . . . . .	36
4.8	Clusters generated by CDRPM and JDRPM fits, target plus space values . . . . .	37
4.9	Fitted values of JDRPM fit, target values only, NA dataset . . . . .	38
4.10	Clusters produced by JDRPM fits, target values only, full vs NA dataset . . . . .	39

4.11 Lagged ARI values of JDRPM fits, target values only, full vs NA dataset . . . . .	39
4.12 Visual representation of the clusters of JDRPM fit, target values only, NA dataset . . . . .	40
4.13 Lagged ARI values of JDRPM fits, target plus space values, full vs NA dataset . . . . .	40
4.14 Fitted values of JDRPM fit, target plus space values, NA dataset . . . . .	41
4.15 Comparison of the two possible mean centering methods on a covariate	42
4.16 Regression vector of the fit with multiple covariates in the likelihood, full dataset . . . . .	44
4.17 Regression vector of the fit with multiple covariates in the likelihood, NA dataset . . . . .	45
4.18 Target and fitted values of JDRPM fits, target plus space values, NA dataset, with covariates in the likelihood . . . . .	46
4.19 Lagged ARI values of JDRPM fit, target plus space values, full vs NA dataset, with covariates in the likelihood . . . . .	47
4.20 Clusters generated by JDRPM fits, target plus space values, full vs NA dataset, with covariates in the likelihood . . . . .	48
4.21 Trace plot of the fitted values for a fit with covariates in the likelihood	49
4.22 Variables used for the fit tests with covariates in the clustering . . . . .	50
4.23 Enter Caption . . . . .	51
4.24 Execution times of JDRPM and CDRPM fits, target values only . . . . .	52
4.25 Execution times of JDRPM and CDRPM fits, target plus space values	53
4.26 Execution times of JDRPM fits, target plus space plus covariates . . . . .	53
4.27 Visual representation of all fitting performances . . . . .	55

# List of Tables

4.1	Accuracy metrics of CDRPM and JDRPM fits, target values only . . . . .	30
4.2	Accuracy metrics of CDRPM and JDRPM fits, target plus space values . . . . .	35
4.3	Accuracy metrics of JDRPM fits, target values only, full vs NA dataset . . . . .	39
4.4	Accuracy metrics of JDRPM fits, target plus space values, full vs NA dataset . . . . .	40
4.5	Accuracy metrics of JDRPM fits, target plus space values, full vs NA dataset, with vs without covariates in the likelihood . . . . .	43
4.6	Accuracy metrics of CDRPM and JDRPM fits, target plus space values, with vs without covariates in the clustering process . . . . .	49



# Chapter 1

## Introduction

Clustering has always been a powerful tool to identify structures and patterns in data, especially in contexts where relationships between the observations are complex such as when the target variable is affected by many factors simultaneously. For this reason, clustering techniques saw lately an increase in popularity in a variety of scientific fields, including social sciences, climate and environmental analysis, economics, and healthcare. The importance of clustering becomes even more noticeable when dealing with spatio-temporal data, in which observations are collected over time and across different spatial locations, possibly concealing trends behind both information levels. This type of data, in fact, is inherently complex due to this dependence and interaction between spatial and temporal dimensions; a complexity that is further increased if covariates are also available. For that reason, an effective analysis of such data demands models that can account for this dependence, while maintaining reasonable computational loads to be possibly applied on large scale datasets, which in this context are frequently accessible.

Recently, the use of bayesian methods to perform clustering has gained some attention, particularly in this field of spatio-temporal datasets. Bayesian clustering, in fact, allows to incorporate prior information into the model, enhancing the flexibility and interpretability of the results with respect, for example, to more traditional frequentist methods. Throughout the years, several models have been developed, but one of the most relevant in this context is the Dependent Random Partition Model (DRPM), which stands out for being able to handle explicitly the temporal dependence of partitions into the model formulation while also possibly accounting for the spatial information. However, the current DRPM implementation, written in C and available trough an R interface, lacks of some relevant utilities such as the inclusion of covariates, which could further enhance the generation and informativity of the clusters, the handling of missing data, and an efficient implementation, which would speed up the model fitting to e.g. run multiple chains in parallel or be more easily applied on large scale datasets.

In this work, we aim to address these three issues by enlarging the original model, that is, preserving the original idea of the formulation but making it richer trough the insertion of new components. We will show how this updated model can perform better than the original one, under the same testing conditions, and

improve the clustering accuracy and interpretation through the inclusion of covariates. All this while also providing faster execution times. In fact, implementing the model into code using the Julia language, rather than C, we took advantage of its high-performance capabilities and well-equipped statistical ecosystem.

Our comparison will focus on both synthetic datasets and real-world applications, with the latter involving air quality measurements from the AgrImOnIA dataset, a comprehensive record of air pollutant levels and other environmental variables measured across the Lombardy region of Italy.

Chapter 2 will briefly review the literature about bayesian clustering models and then dive deeply into the analysis and description of DRPM, and of our updated version, about their core aspects of sampling algorithm, spatial cohesions, and covariates similarities.

Chapter 3 will provide some insights about the computational aspects of the model implementation, motivating the choice of the Julia language and reporting the optimizations possibilities emerged when developing the algorithm.

Chapter 4 will be devoted to test and compare the original DRPM formulation and implementation to our updated version. We will check if they perform similarly at a common testing level, and assess the performances of the fits of our model when we employ the new updates, i.e. the handling of missing data and the insertion of covariates at clustering and/or likelihood levels. An analysis about expected execution times will also be provided.

Finally, in Chapter 5, we will briefly review the benefits and drawbacks that this work revealed and suggest possible further improvements or development paths.

# Chapter 2

## Description of the model

*“Come on, gentlemen, why shouldn’t we get rid of all this calm reasonableness with one good kick, just so as to send all these logarithms to the devil and be able to live our own lives at our own sweet will?”*  
— Fëdor Dostoevskij, *Notes from the Underground*

In the bayesian framework, clustering is possible by employing a random probability measure of discrete type that induces a distribution over random partitions. This discreteness is obtained with the Dirichlet Process (DP), which several clustering models implement either through the stick-breaking representation [Bar+12] [AW15] [GMR16] [Jo+16] [KG18] [DK18] [De +19] or through the Pólya urn scheme [Car+17]. However, these classical bayesian methods rely on modelling the dependence in the random partitions by modelling the dependence inside the random probability measures, i.e. on the parameters which underlie those DP representations rather than to the clusters themselves. This approach is therefore kind of a “step back” from the main object of interest, the clusters, which are then only *induced* by the random partition model. As a consequence, there is no guarantee that the correlation that appears in the parameters would subsequently reflect into correlation among the partitions, often producing counterintuitive behaviours in the results. The Dependent Random Partition Model (DRPM) [PQD22], on the other hand, models *directly* the sequence of partitions, thus providing a more reasonable, accurate, and interpretable temporal evolution of the clusters.

Before diving into the model description, we define some notation conventions. We setup in a spatio-temporal context with  $i = 1, \dots, n$  and  $t = 1, \dots, T$  being the indexes for units and time instants. We will denote with  $\rho_t = \{S_{1t}, \dots, S_{kt_t}\}$  the partition at time  $t$  of the  $n$  experimental units, composed by  $k_t$  cluster. Another possible representation of the partition is through cluster membership labels  $\mathbf{c}_t = \{c_{1t}, \dots, c_{nt}\}$ , where  $c_{it} = j$  if unit  $i$  belongs to cluster  $S_{jt}$ . Finally, we will denote with a  $\star$  superscript all the variables or quantities which are cluster-specific.

To implement dependence in the random partitions model, one could simply propose a joint probability model for  $(\rho_1, \dots, \rho_T)$ , denoted as  $P(\rho_1, \dots, \rho_T)$ , where each  $\rho_t$  is set to be possibly affected by all the other partitions. This principle, how-

ever, would have required even more complexity in the model; therefore the DRPM authors limited this temporal connection to a first-order Markov-chain structure, where the conditional distribution of  $\rho_t$  given all the predecessors  $\rho_{t-1}, \rho_{t-2}, \dots, \rho_1$  actually depends only on  $\rho_{t-1}$ , bringing the random partition model to the form

$$P(\rho_1, \dots, \rho_T) = P(\rho_T | \rho_{T-1}) \cdots P(\rho_2 | \rho_1) P(\rho_1) \quad (2.1)$$

To explicitly manage the relation between  $\rho_t$  and  $\rho_{t-1}$  some auxiliary variables are introduced. The idea is that if two partitions are highly time-dependent, few changes will occur between them. In turn, partitions which are quite independent will possibly exhibit very different configurations. To express this fixity or flexibility concept, for each unit  $i = 1, \dots, n$  the following variable is introduced<sup>1</sup>

$$\gamma_{it} = \begin{cases} 1 & \text{if unit } i \text{ is } \textit{not} \text{ reallocated when moving from time } t-1 \text{ to } t \\ 0 & \text{otherwise (i.e. unit } i \text{ is reallocated)} \end{cases} \quad (2.2)$$

By construction, we set  $\gamma_{i1} = 0$  for all  $i$ , meaning that at the first time instant all units get reallocated since they have no partition to which they could be possibly fixed at. Regarding their modelling, the authors proposed  $\gamma_{it} \stackrel{\text{ind}}{\sim} \text{Ber}(\alpha_t)$ , with  $\alpha_t \in [0, 1]$  behaving as a temporal dependence parameter. At the two extremes,  $\alpha_t = 1$  will denote perfect temporal dependence, with  $\rho_t = \rho_{t-1}$ , while  $\alpha_t = 0$  will imply full independence of  $\rho_t$  from  $\rho_{t-1}$ . For the sake of clarity, the vector  $\boldsymbol{\gamma}_t = (\gamma_{1t}, \dots, \gamma_{nt})$  is created, and the augmented joint model now becomes in the form

$$P(\boldsymbol{\gamma}_1, \rho_1, \dots, \boldsymbol{\gamma}_T, \rho_T) = P(\rho_T | \boldsymbol{\gamma}_T, \rho_{T-1}) P(\boldsymbol{\gamma}_T) \cdots P(\rho_2 | \boldsymbol{\gamma}_2, \rho_1) P(\boldsymbol{\gamma}_2) P(\rho_1) \quad (2.3)$$

The insertion of these additional variables make the model very powerful in describing the temporal dependence and relation of the partitions, but slightly hinders the design of the sampling algorithm. To outline it, we firstly need a

**Definition 2.1** (compatibility). Two partitions  $\rho_t$  and  $\rho_{t-1}$  are *compatible* with respect to  $\boldsymbol{\gamma}_t$  if  $\rho_t$  can be obtained from  $\rho_{t-1}$  by reallocating items as indicated by  $\boldsymbol{\gamma}_t$ ; i.e. only moving the units  $i$  with  $\gamma_{it} = 0$ .

To perform this compatibility check, it is enough to ensure that the reduced partitions from  $\rho_t$  and  $\rho_{t-1}$  are the same, with reduced meaning their restriction to the units which cannot move. Indeed, if those fixed units are clustered in the same ways, then surely the free-movers from  $\rho_t$  can be set to match the labels assigned by partition  $\rho_{t-1}$ . Denoting as  $\mathfrak{R}_t = \{i : \gamma_{it} = 1\}$  the set of fixed units, this check translates into asking that  $\rho_t^{\mathfrak{R}_t} = \rho_{t-1}^{\mathfrak{R}_t}$ .

Then, the sampling algorithm requires that when we are drawing the new sample for the  $\gamma_{it}$  parameters, or also for the cluster labels  $c_{it}$ , we firstly need to check if these draws can actually be valid, i.e. if they would keep compatible and coherent all the partitions and parameters involved. For example, when updating  $\gamma_{it}$  during

---

<sup>1</sup>a quick way to remind this convention is thinking that  $\gamma_{it}$  answers to the question “do I stay fixed?” asked from unit’s  $i$  perspective.

each iteration  $d$  of the algorithm, the only case which can raise problems is when we pass from  $\gamma_{it}^{(d-1)} = 0$  to  $\gamma_{it}^{(d)} = 1$ . This step corresponds to the case in which a unit  $i$  that was initially (i.e. according to the previous iteration parameters) free to be reassigned is now instead deemed to stay fixed in her cluster. However, this change may not align to the current sampled values of the partitions  $\rho_{t-1}^{(d)}$  and  $\rho_t^{(d-1)}$ . Therefore, compatibility between their reductions to the units in the set  $\mathfrak{R}_t \cup \{i\}$  needs to be checked, and if the check is not positive the tentative update  $\gamma_{it}^{(d-1)} = 0 \rightarrow \gamma_{it}^{(d)} = 1$  is not allowed to be executed and we force  $\gamma_{it}^{(d)} = 0$  in the sampling algorithm. Similar checks are conducted when  $\rho_t$  is updated. In this step, only the units that can actually move, i.e. that have  $\gamma_{it} = 0$ , are updated, and therefore there are no compatibility problems between  $\rho_{t-1}$  and  $\rho_t$ . However, since the update of  $\gamma_{it}$  occurs before the one of the partition, compatibility needs to be checked between  $\rho_t$  and  $\rho_{t+1}$ .

In any case, once the partition model is specified, there is great flexibility in how to setup the rest of the hierarchical model. To allow temporal dependence to propagate through the model, an optionally autoregressive AR(1) component is also added to the formulation of the model, both at the data and cluster-specific parameters level. All this led the authors to the following complete model

$$\begin{aligned}
Y_{it}|Y_{it-1}, \boldsymbol{\mu}_t^*, \boldsymbol{\sigma}_t^{2*}, \boldsymbol{\eta}, \mathbf{c}_t &\stackrel{\text{ind}}{\sim} \mathcal{N}(\mu_{c_{it}}^* + \eta_{1i} Y_{it-1}, \sigma_{c_{it}}^{2*}(1 - \eta_{1i}^2)) \\
Y_{i1} &\stackrel{\text{ind}}{\sim} \mathcal{N}(\mu_{c_{i1}}^*, \sigma_{c_{i1}}^{2*}) \\
\xi_i = \text{Logit}(\frac{1}{2}(\eta_{1i} + 1)) &\stackrel{\text{ind}}{\sim} \text{Laplace}(a, b) \\
(\mu_{jt}^*, \sigma_{jt}^*) &\stackrel{\text{ind}}{\sim} \mathcal{N}(\vartheta_t, \tau_t^2) \times \mathcal{U}(0, A_\sigma) \\
\vartheta_t | \vartheta_{t-1} &\stackrel{\text{ind}}{\sim} \mathcal{N}((1 - \varphi_1)\varphi_0 + \varphi_1\vartheta_{t-1}, \lambda^2(1 - \varphi_1^2)) \\
(\vartheta_1, \tau_1) &\stackrel{\text{iid}}{\sim} \mathcal{N}(\varphi_0, \lambda^2) \times \mathcal{U}(0, A_\tau) \\
(\varphi_0, \varphi_1, \lambda) &\sim \mathcal{N}(m_0, s_0^2) \times \mathcal{U}(-1, 1) \times \mathcal{U}(0, A_\lambda) \\
\{\mathbf{c}_t, \dots, \mathbf{c}_T\} &\sim \text{tRPM}(\boldsymbol{\alpha}, M) \text{ with } \alpha_t \stackrel{\text{iid}}{\sim} \text{Beta}(a_\alpha, b_\alpha)
\end{aligned} \tag{2.4}$$

where tRPM represents the temporal random partition model (2.3).

Moving towards our update, we decided to refine some parts of that formulation. Regarding the variances  $\sigma_{jt}^{2*}$ ,  $\tau_t^2$ , and  $\lambda^2$ , we chose to model them through an invGamma distribution rather than the  $\mathcal{U}$  employed originally. This is indeed a more sophisticated choice, since the tuning of the parameters of an  $\text{invGamma}(a, b)$  are a bit more difficult than simply setting the bounds of a uniform law, but should guarantee a better mixing in the chain. In fact, the invGamma distributions recovers conjugacy in the model, through the normal law assigned to the other parameters, allowing the update step of the variances to be performed through the analytically exact Gibbs sampler rather than the acceptance-rejection method of the Metropolis algorithm employed in the original model with the uniform laws. Finally, to improve the accuracy in fitting the target values we added a regression parameter  $\beta_t$  in the likelihood. We decided to make it only time-dependent, and not also unit-dependent, to lighten the already quite-heavy formulation.

The final updated model is now proposed, with highlighted in dark red the

changes and insertions that we made.

$$\begin{aligned}
Y_{it} | Y_{it-1}, \boldsymbol{\mu}_t^*, \boldsymbol{\sigma}_t^{2*}, \boldsymbol{\eta}, \mathbf{c}_t &\stackrel{\text{ind}}{\sim} \mathcal{N}(\mu_{c_{it}t}^* + \eta_{1i} Y_{it-1} + \mathbf{x}_{it}^T \boldsymbol{\beta}_t, \sigma_{c_{it}t}^{2*}(1 - \eta_{1i}^2)) \\
Y_{i1} &\stackrel{\text{ind}}{\sim} \mathcal{N}(\mu_{c_{i1}1}^* + \mathbf{x}_{i1}^T \boldsymbol{\beta}_1, \sigma_{c_{i1}1}^{2*}) \\
\boldsymbol{\beta}_t &\stackrel{\text{ind}}{\sim} \mathcal{N}_p(\mathbf{b}, s^2 I) \\
\xi_i &= \text{Logit}(\frac{1}{2}(\eta_{1i} + 1)) \stackrel{\text{ind}}{\sim} \text{Laplace}(a, b) \\
(\mu_{jt}^*, \sigma_{jt}^{2*}) &\stackrel{\text{ind}}{\sim} \mathcal{N}(\vartheta_t, \tau_t^2) \times \text{invGamma}(a_\sigma, b_\sigma) \\
\vartheta_t | \vartheta_{t-1} &\stackrel{\text{ind}}{\sim} \mathcal{N}((1 - \varphi_1)\varphi_0 + \varphi_1 \vartheta_{t-1}, \lambda^2(1 - \varphi_1^2)) \\
(\vartheta_1, \tau_t^2) &\stackrel{\text{iid}}{\sim} \mathcal{N}(\varphi_0, \lambda^2) \times \text{invGamma}(a_\tau, b_\tau) \\
(\varphi_0, \varphi_1, \lambda^2) &\sim \mathcal{N}(m_0, s_0^2) \times \mathcal{U}(-1, 1) \times \text{invGamma}(a_\lambda, b_\lambda) \\
\{\mathbf{c}_t, \dots, \mathbf{c}_T\} &\sim \text{tRPM}(\boldsymbol{\alpha}, M) \text{ with } \alpha_t \stackrel{\text{iid}}{\sim} \text{Beta}(a_\alpha, b_\alpha)
\end{aligned} \tag{2.5}$$

A visual representation of this new version of the DRPM model is also present in Figure 2.1, to more clearly appreciate the hierarchical structure and the relations among the parameters.

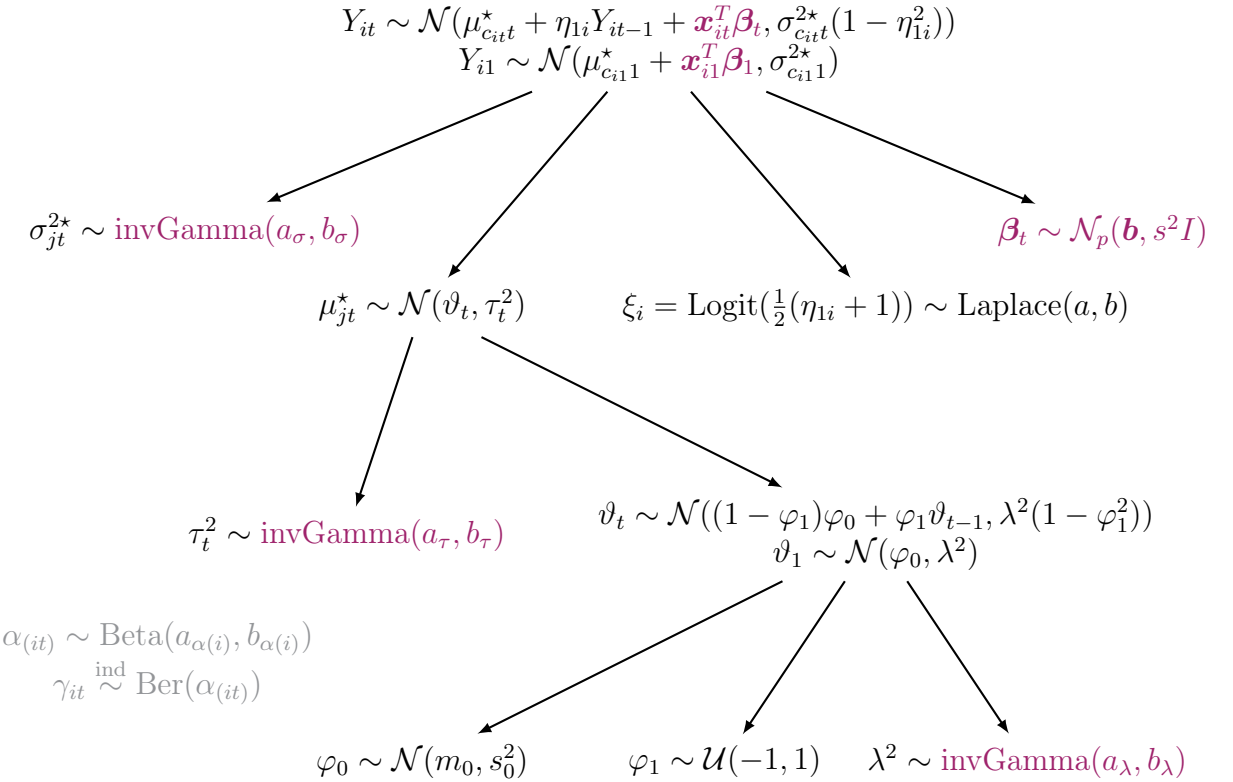


**Figure 2.1:** Graph visualization of the DRPM model, with highlighted in dark red the changes that we made to the original formulation and in gray the internal variables of the model.

In the course of this work, for the sake of clarity, we will refer to CDRPM for the original model formulation of [PQD22], and to JDRPM for our updated version.

We will now dive more deeply into the characteristics of the models, deriving the update rules for the parameters which will be used to implement the MCMC fitting

algorithm, and subsequently inspecting the behaviours of the spatial cohesions and covariates similarities.

## 2.1 Update rules derivation

We now briefly report the full conditionals derivation for the parameters which had a conjugacy in the model (for the full computations see Appendix A). The other variables not included here, namely  $\eta_{1i}$  and  $\varphi_1$ , involved instead the classical Metropolis update.

- update  $\sigma_{jt}^{2\star}$

for  $t = 1$ :  $f(\sigma_{jt}^{2\star}|-) \propto$  kernel of a  $\text{invGamma}(a_{\sigma(\text{post})}, b_{\sigma(\text{post})})$  with

$$a_{\tau(\text{post})} = a_\sigma + \frac{|S_{jt}|}{2} \quad b_{\tau(\text{post})} = b_\sigma + \frac{1}{2} \sum_{i \in S_{jt}} (Y_{it} - \mu_{jt}^* - \mathbf{x}_{it}^T \boldsymbol{\beta}_t)^2$$

for  $t > 1$ :  $f(\sigma_{jt}^{2\star}|-) \propto$  kernel of a  $\text{invGamma}(a_{\sigma(\text{post})}, b_{\sigma(\text{post})})$  with

$$a_{\tau(\text{post})} = a_\sigma + \frac{|S_{jt}|}{2} \quad b_{\tau(\text{post})} = b_\sigma + \frac{1}{2} \sum_{i \in S_{jt}} (Y_{it} - \mu_{jt}^* - \eta_{1i} Y_{it-1} - \mathbf{x}_{it}^T \boldsymbol{\beta}_t)^2$$

(2.6)

- update  $\mu_{jt}^*$

for  $t = 1$ :  $f(\mu_{jt}^*|-) \propto$  kernel of a  $\mathcal{N}(\mu_{\mu_{jt}^*(\text{post})}, \sigma_{\mu_{jt}^*(\text{post})}^2)$  with

$$\sigma_{\mu_{jt}^*(\text{post})}^2 = \frac{1}{\frac{1}{\tau_t^2} + \frac{|S_{jt}|}{\sigma_{jt}^{2\star}}} \quad \mu_{\mu_{jt}^*(\text{post})} = \sigma_{\mu_{jt}^*(\text{post})}^2 \left( \frac{\vartheta_t}{\tau_t^2} + \frac{\sum_{i \in S_{jt}} (Y_{i1} - \mathbf{x}_{i1}^T \boldsymbol{\beta}_t)}{\sigma_{jt}^{2\star}} \right)$$

for  $t > 1$ :  $f(\mu_{jt}^*|-) \propto$  kernel of a  $\mathcal{N}(\mu_{\mu_{jt}^*(\text{post})}, \sigma_{\mu_{jt}^*(\text{post})}^2)$  with

$$\sigma_{\mu_{jt}^*(\text{post})}^2 = \frac{1}{\frac{1}{\tau_t^2} + \frac{\sum_{i \in S_{jt}} \frac{1}{1 - \eta_{1i}^2}}{\sigma_{jt}^{2\star}}} \quad \mu_{\mu_{jt}^*(\text{post})} = \sigma_{\mu_{jt}^*(\text{post})}^2 \left( \frac{\vartheta_t}{\tau_t^2} + \frac{\sum_{i \in S_{jt}} \frac{Y_{it} - \eta_{1i} Y_{i,t-1} - \mathbf{x}_{it}^T \boldsymbol{\beta}_t}{1 - \eta_{1i}^2}}{\sigma_{jt}^{2\star}} \right)$$

(2.7)

- update  $\boldsymbol{\beta}_t$

for  $t = 1$ :  $f(\boldsymbol{\beta}_t|-) \propto$  kernel of a  $\mathcal{N}(\mathbf{b}_{(\text{post})}, A_{(\text{post})})$  with

$$A_{(\text{post})} = \left( \frac{1}{s^2} I + \sum_{i=1}^n \frac{\mathbf{x}_{it} \mathbf{x}_{it}^T}{\sigma_{c_{it}t}^{2\star}} \right)^{-1} \quad \mathbf{b}_{(\text{post})} = A_{(\text{post})} \left( \frac{\mathbf{b}}{s^2} + \sum_{i=1}^n \frac{(Y_{it} - \mu_{c_{it}t}^*) \mathbf{x}_{it}}{\sigma_{c_{it}t}^{2\star}} \right)$$

i.e.  $f(\boldsymbol{\beta}_t|-) \propto$  kernel of a  $\mathcal{N}\text{Canon}(\mathbf{h}_{(\text{post})}, J_{(\text{post})})$  with

$$\mathbf{h}_{(\text{post})} = \left( \frac{\mathbf{b}}{s^2} + \sum_{i=1}^n \frac{(Y_{it} - \mu_{c_{it}t}^*) \mathbf{x}_{it}}{\sigma_{c_{it}t}^{2\star}} \right) \quad J_{(\text{post})} = \left( \frac{1}{s^2} I + \sum_{i=1}^n \frac{\mathbf{x}_{it} \mathbf{x}_{it}^T}{\sigma_{c_{it}t}^{2\star}} \right)$$

for  $t > 1$ :  $f(\boldsymbol{\beta}_t|-) \propto$  kernel of a  $\mathcal{N}(\mathbf{b}_{(\text{post})}, A_{(\text{post})})$  with

$$A_{(\text{post})} = \left( \frac{1}{s^2} I + \sum_{i=1}^n \frac{\mathbf{x}_{it} \mathbf{x}_{it}^T}{\sigma_{c_{it}t}^{2\star}} \right)^{-1} \quad \mathbf{b}_{(\text{post})} = A_{(\text{post})} \left( \frac{\mathbf{b}}{s^2} + \sum_{i=1}^n \frac{(Y_{it} - \mu_{c_{it}t}^* - \eta_{1i} Y_{it-1}) \mathbf{x}_{it}}{\sigma_{c_{it}t}^{2\star}} \right)$$

i.e.  $f(\boldsymbol{\beta}_t | -) \propto \text{kernel of a } \mathcal{N}\text{Canon}(\mathbf{h}_{(\text{post})}, J_{(\text{post})})$  with

$$\mathbf{h}_{(\text{post})} = \left( \frac{\mathbf{b}}{s^2} + \sum_{i=1}^n \frac{(Y_{it} - \mu_{c_{it}t}^* - \eta_{1i} Y_{it-1}) \mathbf{x}_{it}}{\sigma_{c_{it}t}^{2\star}} \right) \quad J_{(\text{post})} = \left( \frac{1}{s^2} I + \sum_{i=1}^n \frac{\mathbf{x}_{it} \mathbf{x}_{it}^T}{\sigma_{c_{it}t}^{2\star}} \right) \quad (2.8)$$

Here  $\mathcal{N}\text{Canon}(\mathbf{h}, J)$  is the canonical formulation of the  $\mathcal{N}(\boldsymbol{\mu}, \Sigma)$ , with  $\mathbf{h} = \Sigma^{-1} \boldsymbol{\mu}$  and  $J = \Sigma^{-1}$ . This other distribution facilitates the sampling, since these full conditional computations allow to derive directly the parameters of the canonical one, e.g. the inverse of the variance matrix rather than the variance matrix itself; and therefore sampling through it does not require any inversion of matrices which would produce more computational load, numerical instabilities, and loss of accuracy. So in Julia we can write `rand(MvNormalCanon(h_star, J_star))`, rather than the riskier one `rand(MvNormal(inv(J_star)*h_star, inv(J_star)))`; which apart from the previously mentioned disadvantages would be a statistically equivalent form.

- update  $\tau_t^2$

$f(\tau_t^2 | -) \propto \text{kernel of a } \text{invGamma}(a_{\tau(\text{post})}, b_{\tau(\text{post})})$  with

$$a_{\tau(\text{post})} = \frac{k_t}{2} + a_\tau \quad b_{\tau(\text{post})} = \frac{\sum_{j=1}^{k_t} (\mu_{jt}^* - \vartheta_t)^2}{2} + b_\tau \quad (2.9)$$

- update  $\vartheta_t$

for  $t = T$ :  $f(\vartheta_t | -) \propto \text{kernel of a } \mathcal{N}(\mu_{\vartheta_t(\text{post})}, \sigma_{\vartheta_t(\text{post})}^2)$  with

$$\sigma_{\vartheta_t(\text{post})}^2 = \frac{1}{\frac{1}{\lambda^2(1-\varphi_1^2)} + \frac{k_t}{\tau_t^2}}$$

$$\mu_{\vartheta_t(\text{post})} = \sigma_{\vartheta_t(\text{post})}^2 \left( \frac{\sum_{j=1}^{k_t} \mu_{jt}^*}{\tau_t^2} + \frac{(1-\varphi_1)\varphi_0 + \varphi_1 \vartheta_{t-1}}{\lambda^2(1-\varphi_1^2)} \right)$$

for  $1 < t < T$ :  $f(\vartheta_t | -) \propto \text{kernel of a } \mathcal{N}(\mu_{\vartheta_t(\text{post})}, \sigma_{\vartheta_t(\text{post})}^2)$  with

$$\sigma_{\vartheta_t(\text{post})}^2 = \frac{1}{\frac{1+\varphi_1^2}{\lambda^2(1-\varphi_1^2)} + \frac{k_t}{\tau_t^2}}$$

$$\mu_{\vartheta_t(\text{post})} = \sigma_{\vartheta_t(\text{post})}^2 \left( \frac{\sum_{j=1}^{k_t} \mu_{jt}^*}{\tau_t^2} + \frac{\varphi_1(\vartheta_{t-1} + \vartheta_{t+1}) + \varphi_0(1-\varphi_1)^2}{\lambda^2(1-\varphi_1^2)} \right)$$

for  $t = 1$ :  $f(\vartheta_t | -) \propto \text{kernel of a } \mathcal{N}(\mu_{\vartheta_t(\text{post})}, \sigma_{\vartheta_t(\text{post})}^2)$  with

$$\sigma_{\vartheta_t(\text{post})}^2 = \frac{1}{\frac{1}{\lambda^2} + \frac{\varphi_1^2}{\lambda^2(1-\varphi_1^2)} + \frac{k_t}{\tau_t^2}}$$

$$\mu_{\vartheta_t(\text{post})} = \sigma_{\vartheta_t(\text{post})}^2 \left( \frac{\varphi_0}{\lambda^2} + \frac{\varphi_1(\vartheta_{t+1} - (1-\varphi_1)\varphi_0)}{\lambda^2(1-\varphi_1^2)} + \frac{\sum_{j=1}^{k_t} \mu_{jt}^*}{\tau_t^2} \right) \quad (2.10)$$

- update  $\varphi_0$

$$f(\varphi_0|-) \propto \text{kernel of a } \mathcal{N}(\mu_{\varphi_0(\text{post})}, \sigma_{\varphi_0(\text{post})}^2) \text{ with}$$

$$\sigma_{\varphi_0(\text{post})}^2 = \frac{1}{\frac{1}{s_0^2} + \frac{1}{\lambda^2} + \frac{(T-1)(1-\varphi_1)^2}{\lambda^2(1-\varphi_1^2)}}$$

$$\mu_{\varphi_0(\text{post})} = \sigma_{\varphi_0(\text{post})}^2 \left( \frac{m_0}{s_0^2} + \frac{\vartheta_1}{\lambda^2} + \frac{1-\varphi_1}{\lambda^2(1-\varphi_1^2)} \sum_{t=2}^T (\vartheta_t - \varphi_1 \vartheta_{t-1}) \right) \quad (2.11)$$

- update  $\lambda^2$

$$f(\lambda^2|-) \propto \text{kernel of a } \text{invGamma}(a_{\lambda(\text{post})}, b_{\lambda(\text{post})}) \text{ with}$$

$$a_{\lambda(\text{post})} = \frac{T}{2} + a_\lambda$$

$$b_{\lambda(\text{post})} = \frac{(\vartheta_1 - \varphi_0)^2}{2} + \sum_{t=2}^T \frac{(\vartheta_t - (1-\varphi_1)\varphi_0 - \varphi_1 \vartheta_{t-1})^2}{2} + b_\lambda \quad (2.12)$$

- update  $\alpha$

if global  $\alpha$ :  $f(\alpha|-) \propto \text{kernel of a } \text{Beta}(a_{\alpha(\text{post})}, b_{\alpha(\text{post})})$  with

$$a_{\alpha(\text{post})} = a_\alpha + \sum_{i=1}^n \sum_{t=1}^T \gamma_{it} \quad b_{\alpha(\text{post})} = b_\alpha + nT - \sum_{i=1}^n \sum_{t=1}^T \gamma_{it}$$

if time specific  $\alpha$ :  $f(\alpha_t|-) \propto \text{kernel of a } \text{Beta}(a_{\alpha(\text{post})}, b_{\alpha(\text{post})})$  with

$$a_{\alpha(\text{post})} = a_\alpha + \sum_{i=1}^n \gamma_{it} \quad b_{\alpha(\text{post})} = b_\alpha + n - \sum_{i=1}^n \gamma_{it}$$

if unit specific  $\alpha$ :  $f(\alpha_i|-) \propto \text{kernel of a } \text{Beta}(a_{\alpha(\text{post})}, b_{\alpha(\text{post})})$  with

$$a_{\alpha(\text{post})} = a_{\alpha i} + \sum_{t=1}^T \gamma_{it} \quad b_{\alpha(\text{post})} = b_{\alpha i} + T - \sum_{t=1}^T \gamma_{it}$$

if time and unit specific  $\alpha$ :  $f(\alpha_{it}|-) \propto \text{kernel of a } \text{Beta}(a_{\alpha(\text{post})}, b_{\alpha(\text{post})})$  with

$$a_{\alpha(\text{post})} = a_{\alpha i} + \gamma_{it} \quad b_{\alpha(\text{post})} = b_{\alpha i} + 1 - \gamma_{it} \quad (2.13)$$

- update a missing observation  $Y_{it}$

for  $t = 1$ :  $f(Y_{it}|-) \propto \text{kernel of a } \mathcal{N}(\mu_{Y_{it}(\text{post})}, \sigma_{Y_{it}(\text{post})}^2)$  with

$$\sigma_{Y_{it}(\text{post})}^2 = \frac{1}{\frac{1}{\sigma_{c_{it} t}^{2*}} + \frac{\eta_{1i}^2}{2\sigma_{c_{it+1} t+1}^{2*}(1-\eta_{1i}^2)}}$$

$$\mu_{Y_{it}(\text{post})} = \sigma_{Y_{it}(\text{post})}^2 \left( \frac{\mu_{c_{it} t}^* + \mathbf{x}_{it}^T \boldsymbol{\beta}_t}{\sigma_{c_{it} t}^{2*}} + \frac{\eta_{1i}(Y_{it+1} - \mu_{c_{it+1} t+1}^* - \mathbf{x}_{it+1}^T \boldsymbol{\beta}_{t+1})}{\sigma_{c_{it+1} t+1}^{2*}(1-\eta_{1i}^2)} \right)$$

for  $1 < t < T$ :  $f(Y_{it}|-) \propto \text{kernel of a } \mathcal{N}(\mu_{Y_{it}(\text{post})}, \sigma_{Y_{it}(\text{post})}^2)$  with

$$\sigma_{Y_{it}(\text{post})}^2 = \frac{1 - \eta_{1i}^2}{\frac{1}{\sigma_{c_{it} t}^{2*}} + \frac{\eta_{1i}^2}{\sigma_{c_{it+1} t+1}^{2*}}}$$

$$\mu_{Y_{it}(\text{post})} = \sigma_{Y_{it}(\text{post})}^2 \left( \frac{\mu_{c_{it}}^* + \eta_{1i} Y_{it-1} + \mathbf{x}_{it}^T \boldsymbol{\beta}_t}{\sigma_{c_{it}t}^{2*}(1 - \eta_{1i}^2)} + \frac{\eta_{1i}(Y_{it+1} - \mu_{c_{it+1}t+1}^* - \mathbf{x}_{it+1}^T \boldsymbol{\beta}_{t+1})}{\sigma_{c_{it+1}t+1}^{2*}(1 - \eta_{1i}^2)} \right)$$

for  $t = T$ :  $f(Y_{it}| -)$  is just the likelihood of  $Y_{it}$  (2.14)

Finally, briefly highlight in Algorithm 1 the steps which compose the MCMC sampling algorithm. Regarding the computation of the fitting metrics LPML and WAIC, they follow familiar ideas from [Chr+10] and [GHV13] respectively.

The core of the clustering process happens in the updating steps of  $\gamma_{it}$  and  $\rho_t$ . Their update step is indeed quite complex, and as we said before involves the check of compatibility issues. In any case, the general idea is, for each unit  $i$  currently belonging to cluster  $j$ , to simulate it to be assigned to one of the existing clusters plus to a singleton cluster, and compute for each case the likelihood of this to happen, to derive probability weights to finally sample the decision for the next iteration. The key elements participating into the definition of such weights are spatial cohesions and, with the JDRPM update, covariate similarities, which we will now both investigate.

## 2.2 Spatial cohesions analysis

To include spatial information into the clustering process, the idea is to extend the PPM from being a function of just  $C(S_{jt})$  to the more informed one  $C(S_{jt}, \mathbf{s}_{jt}^*)$ , where  $S_{jt}$  is the  $j$ -th cluster at time instant  $t$  and  $\mathbf{s}_{jt}^*$  is the subset of spatial coordinates of the units inside  $S_{jt}$ . For the sake of clarity, in this section where we are just interested in analysing the cohesions we employ the  $S_h$  notation to indicate a general  $h$ -th cluster, rather than the more pedantic  $S_{jt}$ .

Regarding the computation of spatial cohesion, several choices are available [PQ15]. The main common idea of the following formulas is to favour few spatially connected clusters rather than a lot of singleton ones, to derive more interpretable and meaningful results. For this reason, most of the cohesions employ the  $M \cdot \Gamma(|S_h|)$  term, which resembles the DP partitioning method that helps in reaching that goal.

We will now describe briefly all the cohesions which are implemented in the JDRPM model, and were implemented as well in the CDRPM model, and conduct tests on each of them, to see how the tuning of their parameters reflects on the computed values.

All the tests of Figures 2.3 and 2.4 refer to the partition of Figure 2.2, taken as test case here from a general fit on the same spatio-temporal dataset of Chapter 4. The following results, as well as the ones of the next section, are presented with the logarithm applied to better highlight the differences among them, otherwise for example all values could be really close together and make the analysis less understandable, and moreover because this is the actual perspective in which the implementation works. In fact, the fitting algorithm firstly saves the log-transformed values generated by the cohesions, in order to avoid numerical problems and instabilities, and secondly exponentiates and normalizes them into proper scaled probabilities, from which finally draw the cluster assignments.

**Algorithm 1:** Pseudocode of the MCMC algorithm for the JDRPM model.

---

```

1 for  $d = 1, \dots, draws$  do
2   if target variable has missing values then
3     | update missing  $Y_{it}$  using (2.14)
4   end
5   for  $t = 1, \dots, T$  do
6     for  $i = 1, \dots, n$  do
7       if  $t = 1$  then
8         |  $\gamma_{it} = 0$ 
9       else
10        | update  $\gamma_{it}$ 
11      end
12    end
13    for  $i \in \{l : \gamma_{lt} = 0\}$  do
14      | update  $c_{it}$  (i.e. update  $\rho_t$ )
15    end
16    update  $\mu_{jt}^*$  using (2.7)
17    update  $\sigma_{jt}^{2*}$  using (2.6)
18    if are there covariates in the likelihood then
19      | update  $\beta_t$ 
20    end
21    update  $\vartheta_t$  using (2.10)
22    update  $\tau_t^2$  using (2.9)
23  end
24  if update_eta = true then
25    | update  $\eta_{1i}$  using Metropolis sampling
26  end
27  if update_alpha = true then
28    | update  $\alpha$  using (2.13)
29  end
30  update  $\varphi_0$  using Gibbs sampling
31  if update_phi1 = true then
32    | update  $\varphi_1$  using Metropolis sampling
33  end
34  update  $\lambda^2$  using (2.12)
35  if  $d > burnin$  and  $d \% thin = 0$  then
36    | save MCMC current iterate
37  end
38 end
39 compute LPML and WAIC metrics
40 if perform diagnostics then
41   | print diagnostics (ESS and  $\hat{R}$ ) on parameters  $\lambda^2, \varphi_0, \tau_t^2, \vartheta_t, \eta_{1i}, \alpha$ 
42 end

```

---

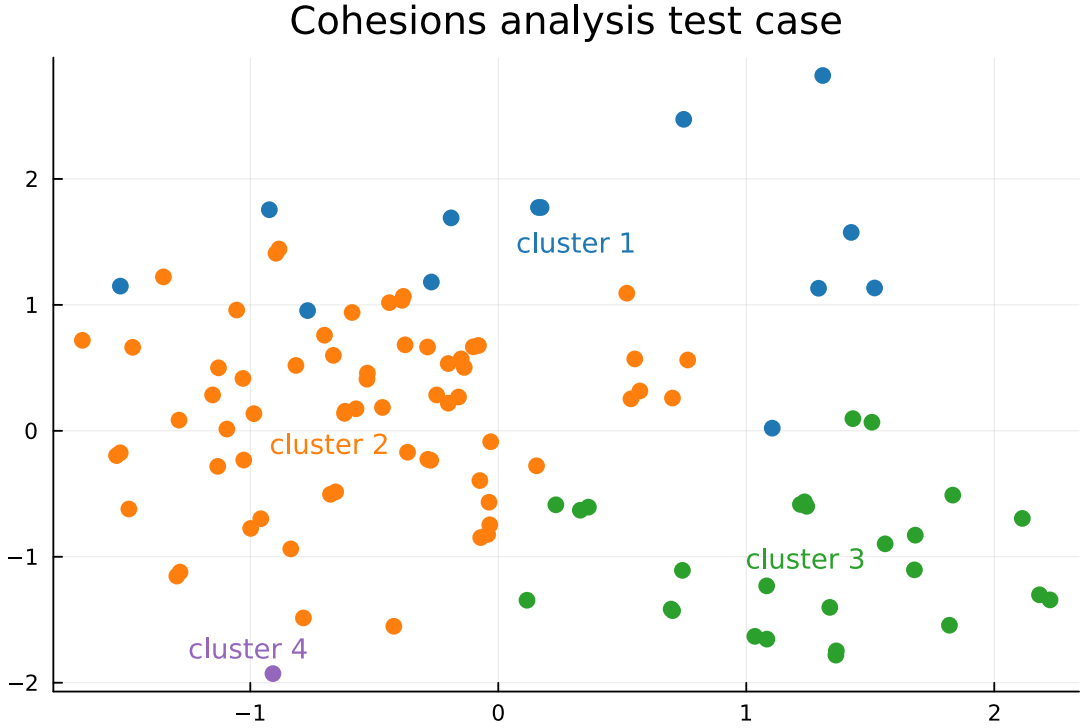


**Figure 2.2:** Partition considered to analyse the spatial cohesions.

The first cohesion uses a tessellation idea from [DH01] that considers  $\mathcal{D}_h = \sum_{i \in S_h} \|s_i - \bar{s}_h\|$  as the total distance from the units to the cluster centroid  $\bar{s}_h$ . The computation is then an adjustment of a decreasing function in terms of  $\mathcal{D}_h$ , to give an higher weight on clusters which are denser, i.e. that have lower  $\mathcal{D}_h$ , with an additional parameter  $\alpha$  to provide more control on the penalization.

$$C_1(S_h, s_h^*) = \begin{cases} \frac{M \cdot \Gamma(|S_h|)}{\Gamma(\alpha \mathcal{D}_h) \mathbb{1}_{[\mathcal{D}_h \geq 1]} + \mathcal{D}_h \mathbb{1}_{[\mathcal{D}_h < 1]}} & \text{if } |S_h| > 1 \\ M & \text{if } |S_h| = 1 \end{cases} \quad (2.15)$$

The second function provides, instead, a hard cluster boundary, where the weight is set to 1, i.e. 0 with the logarithm view, only if all the distances between all possible pairs of points inside the cluster are below the threshold parameter, i.e. if all units are “close enough” to each other. If this does not happen, even for a single pair of points, the returned value is 0, which corresponds to the maximum penalization since it would be  $-\infty$  in the logarithm perspective. The strictness of this requirement can be adjusted through the parameter  $a$ .

$$C_2(S_h, s_h^*) = M \cdot \Gamma(|S_h|) \cdot \prod_{i,j \in S_h} \mathbb{1}_{[\|s_i - s_j\| \leq a]} \quad (2.16)$$

According to this function, from Figure 2.3 we can see how the purple cluster is considered the one with the highest cohesion, being a singleton. The runner-up is the green cluster, because it’s the first among all the non-singletons which activates cohesion 2 when we increase the parameter  $a$ . The orange and blue clusters, instead,

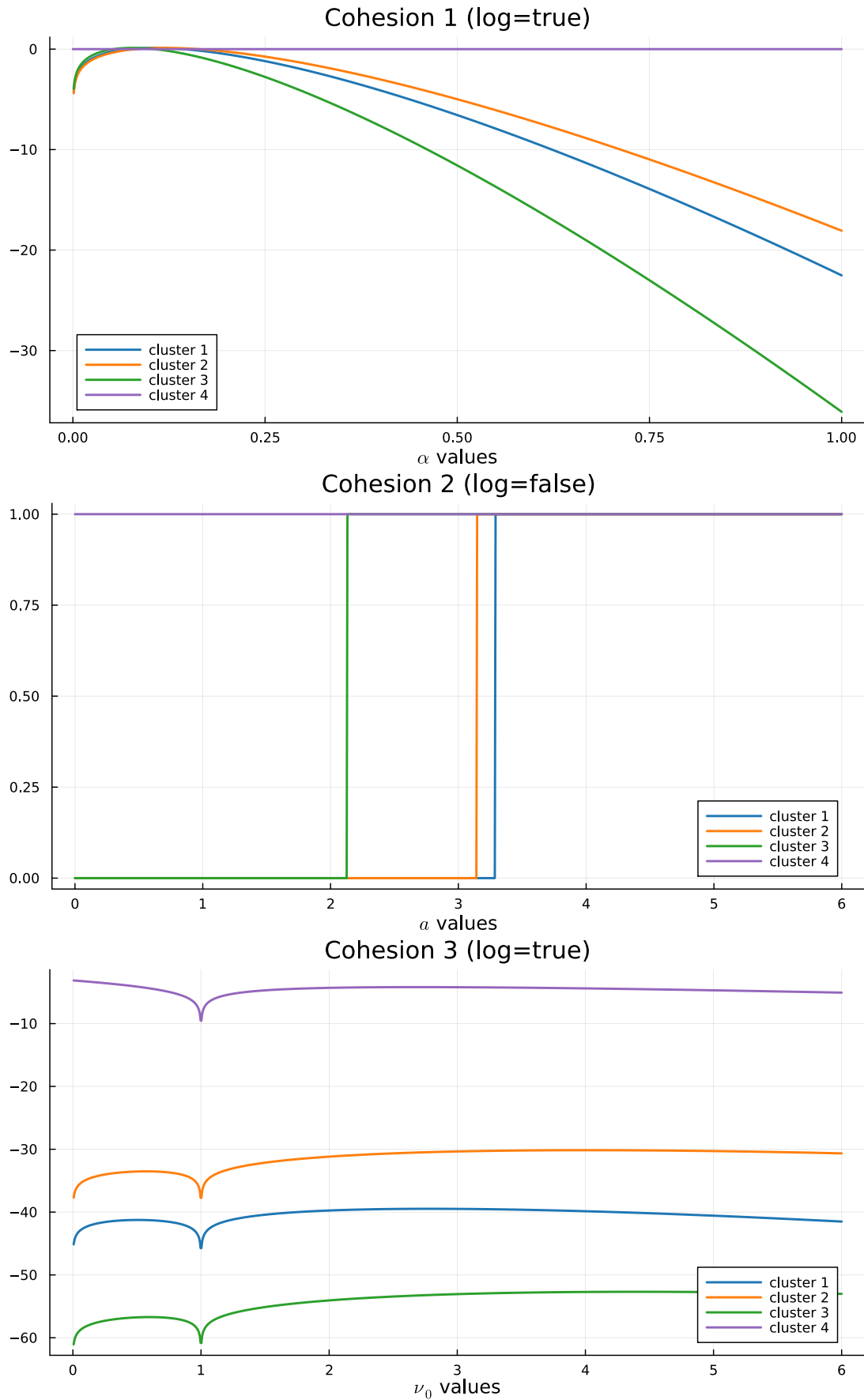


**Figure 2.3:** Cohesions 1, 2, and 3 computed on the test case partition, with respect to different values of their tuning parameter. Cohesion 2 is without the logarithm applied just for plotting purposes, since otherwise the values would have been  $-\infty$  and 0.

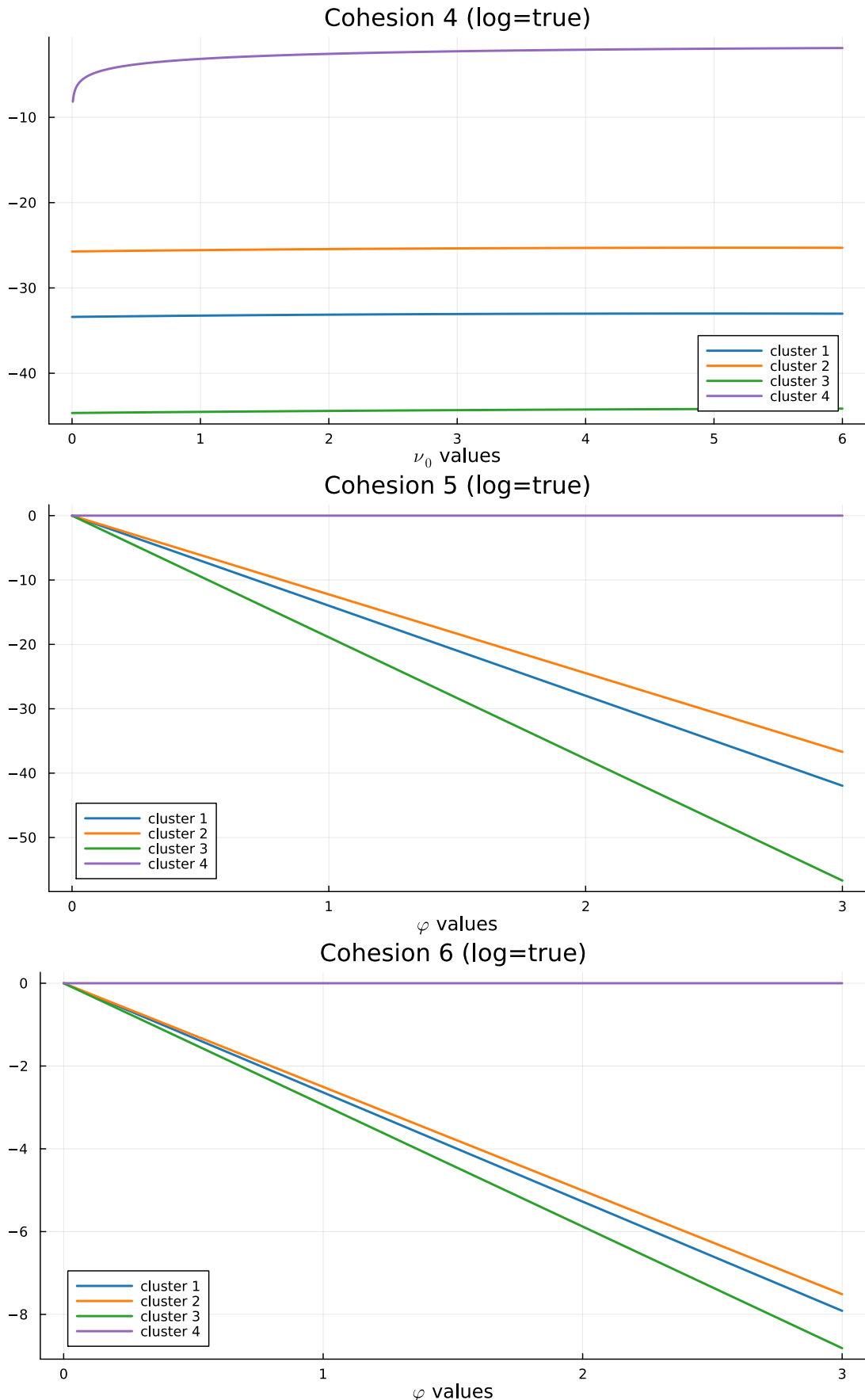


**Figure 2.4:** Cohesions 4, 5, and 6 computed on the test case partition, with respect to different values of their tuning parameter.

appear to be less dense since they require an higher value of  $a$  to “pass” the distance check.

However, cohensions  $C_1$  and  $C_2$  do not preserve the exchangeability property, meaning that if we would marginalize the random partition model over the last of  $m$  units we would not get to the same model as if we only had  $m - 1$  units. This coherence property, known as sample size consistency or addition rule [De +15], is instead often desirable, for theoretical or computational purposes, and the following two cohensions are able to provide it [MQR11].

Cohesion 3, called auxiliary similarity, treats the spatial coordinates  $\mathbf{s}^*$  as if they were random, applying on them a model such as the Normal/Normal-Inverse-Wishart with  $\boldsymbol{\xi} = (\mathbf{m}, V)$ ,  $\mathbf{s}|\boldsymbol{\xi} \sim \mathcal{N}(\mathbf{m}, V)$  and  $\boldsymbol{\xi} \sim \mathcal{NIW}(\boldsymbol{\mu}_0, \kappa_0, \nu_0, \Lambda_0)$ . The idea is to assign a larger weight on clusters which produce large marginal likelihood values, i.e. which according to the modelling are more probable to appear.

$$C_3(S_h, \mathbf{s}_h^*) = M \cdot \Gamma(|S_h|) \cdot \int \prod_{i \in S_h} q(\mathbf{s}_i | \boldsymbol{\xi}_h) q(\boldsymbol{\xi}_h) d\boldsymbol{\xi}_h \quad (2.17)$$

On the same line there is cohesion 4, the double dipper cohesion [QMP15], which now employs the posterior predictive distribution rather than the prior predictive distribution of cohesion  $C_3$ .

$$C_4(S_h, \mathbf{s}_h^*) = M \cdot \Gamma(|S_h|) \cdot \int \prod_{i \in S_h} q(\mathbf{s}_i | \boldsymbol{\xi}_h) q(\boldsymbol{\xi}_h | \mathbf{s}_h^*) d\boldsymbol{\xi}_h \quad (2.18)$$

Another final idea comes from the cluster variance/entropy similarity function, a very general methodology to measure the closeness of a set of values which in fact will be used also for the covariates case. As in cohesion  $C_1$ , the idea is to derive a summary of the closeness of the units, summing the distance of the units from the cluster centroid, and then adjust the penalization trough the parameter  $\varphi$ , to control how much penalize dissimilar values.

$$C_5(S_h, \mathbf{s}_h^*) = \exp \left\{ -\varphi \sum_{i \in S_h} \|\mathbf{s}_i - \bar{\mathbf{s}}_h\| \right\} \quad (2.19)$$

$$C_6(S_h, \mathbf{s}_h^*) = \exp \left\{ -\varphi \log \left( \sum_{i \in S_h} \|\mathbf{s}_i - \bar{\mathbf{s}}_h\| \right) \right\} \quad (2.20)$$

## 2.3 Covariates similarities analysis

A wide spectrum of choice is also available for covariates similarities [PQ18]. To account for them, the idea consists in extending the PPM to make it function of  $S_{jt}$ ,  $\mathbf{s}_{jt}^*$ , and now also of  $X_{jt}^*$ , being this the  $p \times |S_{jt}|$  matrix storing the covariates of the units belonging to cluster  $j$  at time  $t$ , i.e.  $X_{jt}^* = \{\mathbf{x}_{it}^* = (x_{it1}, \dots, x_{itp})^T : i \in S_{jt}\}$ .

For the current implementation of JDRPM we decided to treat each covariate individually, therefore the PPM will actually be function of the set of unidimensional

vectors which record the different  $p$  covariates of the units inside cluster  $S_{jt}$ , meaning  $\mathbf{x}_{jtr}^*, \dots, \mathbf{x}_{jtp}^*$ , of which all contributions will be considered independently one to each other. In this way, the final PPM form will be

$$P(\rho) \propto \prod_{h=1}^{k_t} C(S_{jt}, \mathbf{s}_{jt}^*) \left( \prod_{r=1}^p g(S_{jt}, \mathbf{x}_{jtr}^*) \right) \quad (2.21)$$

where  $\mathbf{x}_{jtr}^*$  represents the vector recording the  $r$ -th covariate values for all the units inside cluster  $S_{jt}$ , i.e. row  $r$  of matrix  $X_{jt}^*$ . This choice is lighter from the theoretical and computational perspectives, and allows a mixture of numerical and categorical covariates without any problem. A unified and multidimensional consideration of the covariates is nonetheless possible, with proper adjustments on the similarities functions, and would have lead to a PPM of the form

$$P(\rho) \propto \prod_{h=1}^{k_t} C(S_{jt}, \mathbf{s}_{jt}^*) g(S_{jt}, X_{jt}^*) \quad (2.22)$$

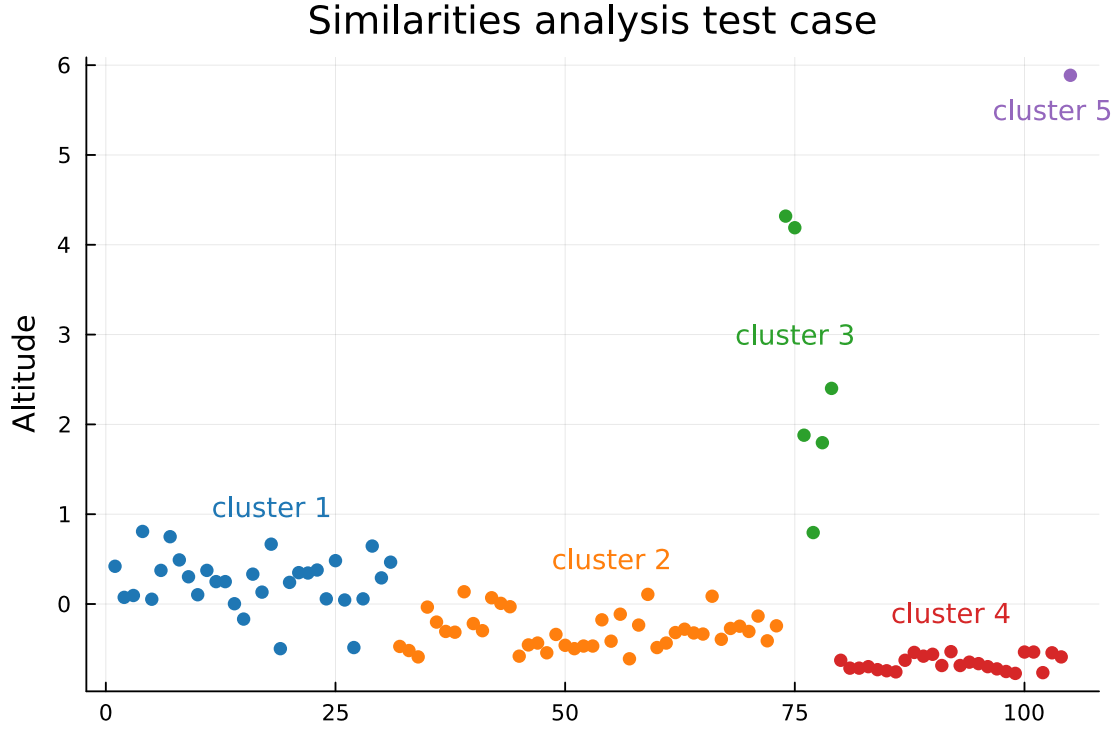


**Figure 2.5:** Partition considered to analyse the covariate similarities. The order of the units has been modified to plot together all units belonging to the same cluster.

As in the previous section, we will now discuss all the similarities implemented in the JDRPM model and perform tests on each of them. All the tests will be referred to the test case partition displayed in Figure 2.5. Regarding the notation, we will again employ the simpler and general one dropping the spatio-temporal context.

The first similarity is the cluster variance/entropy similarity function, which as the name suggest can work with both numerical and categorical variables. The

general form is

$$g_1(S_h, \mathbf{x}_h^*) = \exp \{-\varphi H(S_h, \mathbf{x}_h^*)\} \quad (2.23)$$

with  $H(S_h, \mathbf{x}_h^*) = \sum_{i \in S_h} (x_i - \bar{x}_h)^2$  for numerical covariates, being  $\bar{x}_h$  the mean value of the  $\mathbf{x}_h^*$  vector, and  $H(S_h, \mathbf{x}_h^*) = -\sum_{c=1}^C \hat{p}_c \log(\hat{p}_c)$  for categorical covariates, with  $\hat{p}_c$  indicating the relative frequency at which each factor appears. The parameter  $\varphi$  controls the amount of penalization to apply. This function can be extended quite easily to the multidimensional case, at least for the case of numerical covariates only, where the  $H$  function becomes  $H(S_h, X_h^*) = \sum_{r=1}^p \|\mathbf{x}_r - \bar{\mathbf{x}}_h\|$ .

Another popular choice is the Gower similarity function [Gow71], which was originally designed for a multivariate context, where vectors of covariates are compared to each other. As a consequence, some work was required to adapt it to the univariate case. The simple idea of comparing all cluster-specific pair-wise similarities leads to the total Gower similarity.

$$g_2(S_h, \mathbf{x}_h^*) = \exp \left\{ -\alpha \sum_{i,j \in S_h, i \neq j} d(x_i, x_j) \right\} \quad (2.24)$$

This function, however, is strictly increasing with respect to the cluster size, meaning that it will naturally tend to propose a large number of small clusters. For that reason, a correction can be applied, accounting for the size of the cluster  $S_h$ , leading to the average Gower similarity.

$$g_3(S_h, \mathbf{x}_h^*) = \exp \left\{ -\frac{2\alpha}{|S_h|(|S_h| - 1)} \sum_{i,j \in S_h, i \neq j} d(x_i, x_j) \right\} \quad (2.25)$$

In both functions,  $d(x_i, x_j)$  is the Gower dissimilarity between  $x_i$  and  $x_j$ , with  $d(x_i, x_j) = |x_i - x_j|/R$  in the case of numerical covariates, being  $R = \max(\mathbf{x}) - \min(\mathbf{x})$  the range of the covariate values, considering all the units independently from their cluster, while  $d(x_i, x_j) = \mathbb{1}_{[x_i \neq x_j]}$  in the case of categorical covariates. This is a dissimilarity since values closer to 0 refer to similar data, while values closer to 1 to dissimilar data; therefore the minus sign inside  $g_2$  and  $g_3$  exponents converts the function to a similarity. For the multidimensional design there are natural extensions of the  $d(\mathbf{x}_i, \mathbf{x}_j)$  function.

The last similarity recalls the structure of the spatial cohesion  $C_3$ , where now are the covariates to be treated as if they were random variables. However, since we chose to deal with each covariate individually, in this unidimensional setting a Normal/Normal-Inverse-Gamma model is employed, with  $\boldsymbol{\xi} = (\mu, \sigma^2)$ ,  $x|\boldsymbol{\xi} \sim \mathcal{N}(\mu, \sigma^2)$ , and  $\mu \sim \mathcal{N}(\mu_0, \sigma^2/\lambda_0)$ ,  $\sigma^2 \sim \text{invGamma}(a_0, b_0)$ , i.e.  $\boldsymbol{\xi} \sim \mathcal{N}\text{invGamma}(\mu_0, \lambda_0, a_0, b_0)$ . A multivariate extension is thus possible through the same modelling style of the spatial coordinates case.

$$g_4(S_h, \mathbf{x}_h^*) = \int \prod_{i \in S_h} q(x_i|\boldsymbol{\xi}_h) q(\boldsymbol{\xi}_h) d\boldsymbol{\xi}_h \quad (2.26)$$

All the similarities, except for  $g_2$ , agree to classify the non-singleton clusters with the red being the one with the highest similarity, followed by the orange, blue,

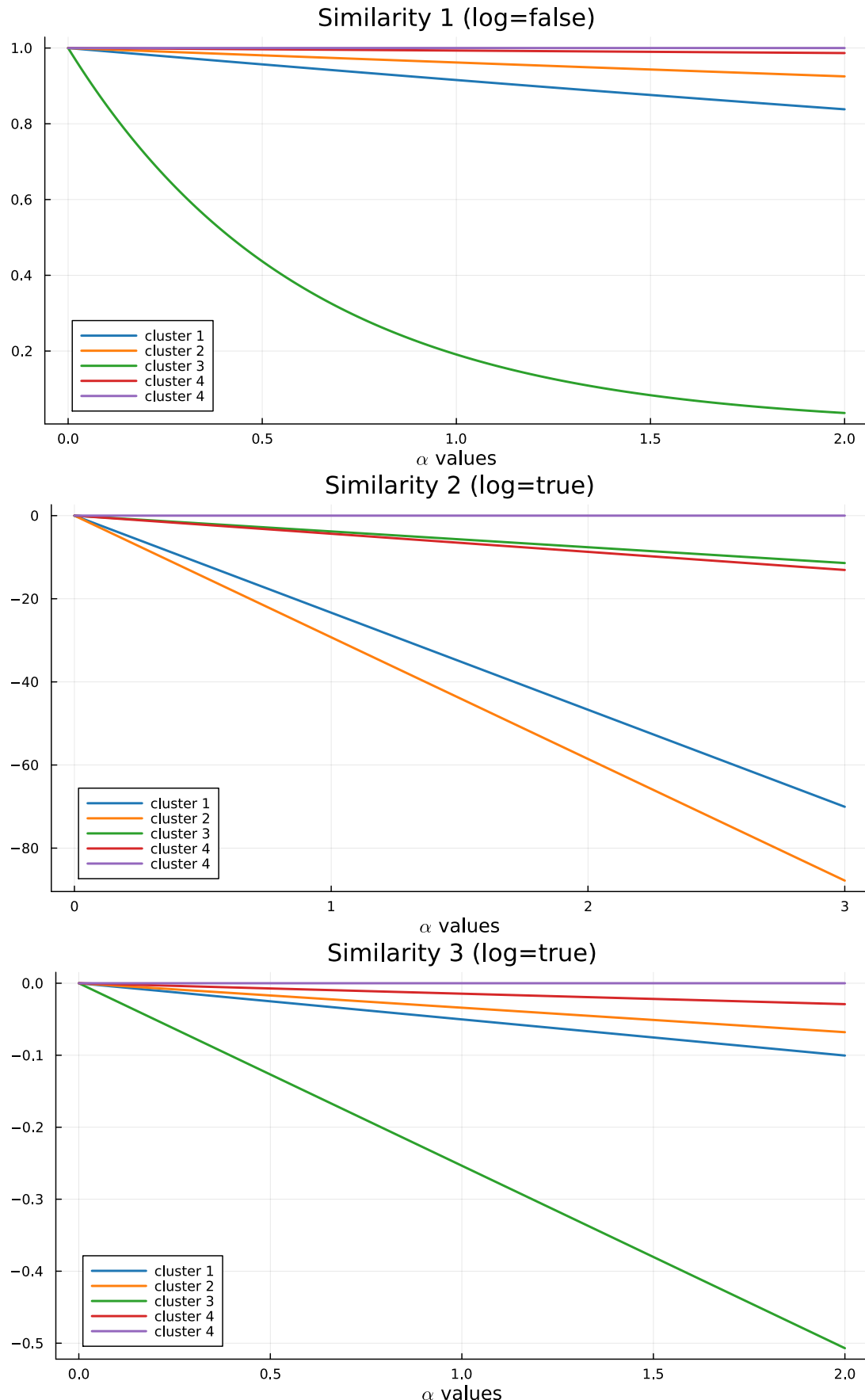


**Figure 2.6:** Similarities 1, 2 and 3 computed on the test case partition, with respect to different values of their tuning parameter. Similarity 1 is without the logarithm applied just for plotting purposes, to see more clearly the gap among the clusters.

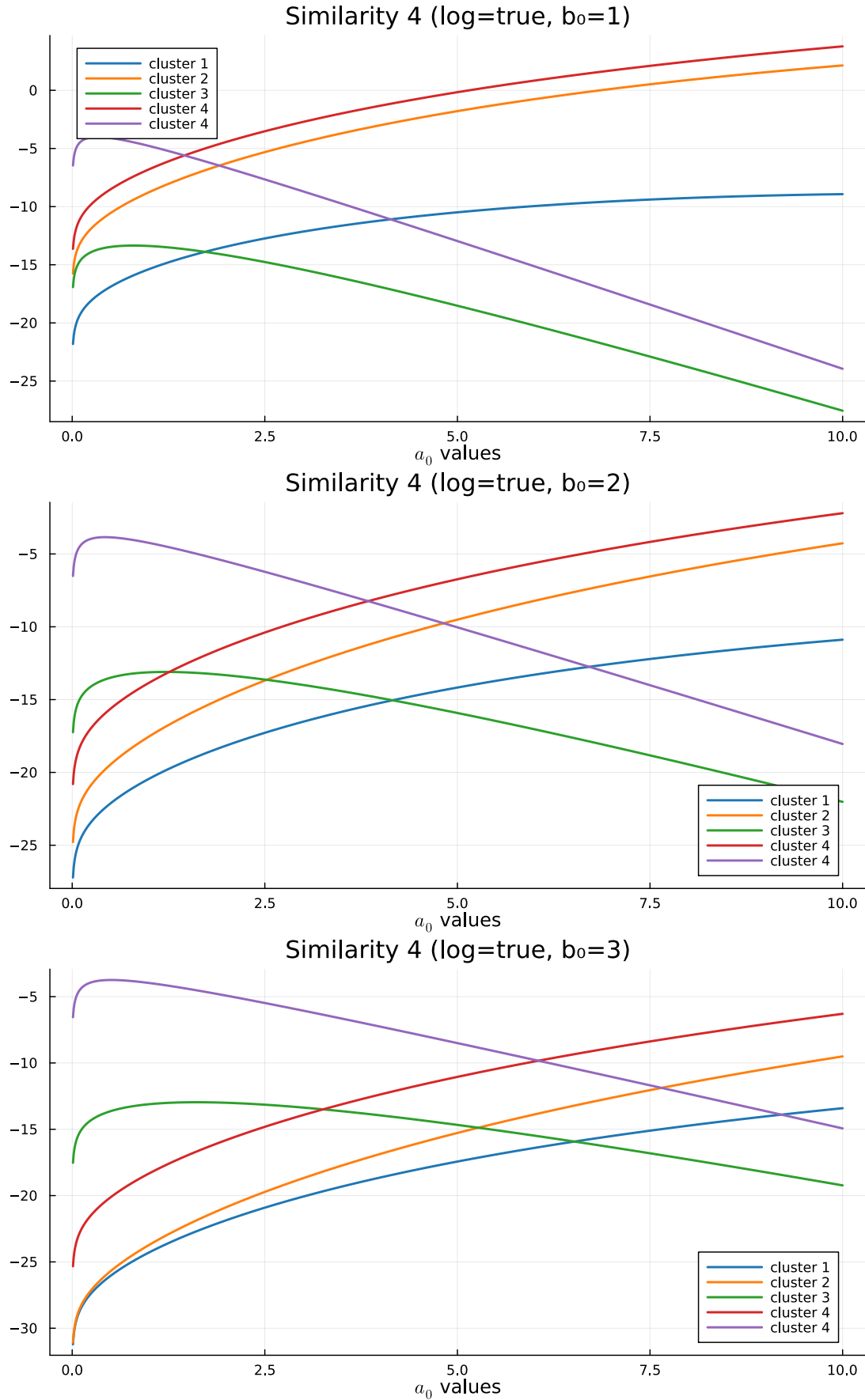


**Figure 2.7:** Similarity 4 computed on the test case partition, with respect to the different values of the tuning parameter  $a_0$  and  $b_0$ . The other parameters has been set to  $\mu_0 = 0$  and  $\lambda_0 = 1$ , with the idea to apply the similarity on scaled (centered and standardized) covariates.

and green, as we can see from Figures 2.6 and 2.7. Intuitively, Figure 2.5 seems to confirm this ranking, by visually reasoning about the sparsity of each cluster. Similarities  $g_4$  and  $g_2$  seems to be the only ones which are able to give a considerable weight also to the green partition, which is indeed sparser but collects all the large, sort of outliers, values of the covariate at test.

Regarding their flexibility, we tested their behaviour changing the testing covariate. Similarity  $g_1$  appeared to be the most adaptive one, working well (i.e. returning very reasonable orders in the clusters). However, it tends to penalize a lot sparse clusters, as we saw in the previous test case. This could suggest to maybe implement other distance metrics rather than the  $L^2$  norm in the computation of  $H(S_h, \mathbf{x}_h^*)$ . On the other hand, similarity 4 appeared to be quite sensible to the parameters regulating the invGamma distribution for  $\sigma^2$ , suggesting that each covariate that we want to include in the clustering process should have her properly-tuned pair of  $a_0$  and  $b_0$  parameters. The JDRPM implementation will provide this flexibility in assigning separately those parameters for each clustering covariate.

# Chapter 3

## Implementation and optimizations

To implement our updated model, and to do it efficiently, we decided to opt for the Julia language [Bez+17].

Julia is a relatively new programming language that combines the ease and expressiveness of high-level languages to the efficiency and performance of low-level ones. Such balance largely achieved through the just-in-time (JIT) compilation, implemented using the LLVM framework, together with many nice features like dynamic multiple dispatch and heavy code specialization against multiple types. This design choice allows Julia to be used interactively, in the same fashion to the R, Matlab, or Python consoles, while also supporting the more traditional program execution style of statically compiled languages such as C, C++ and Fortran. This solution provides faster development phases, since for examples code sections can be evaluated and tested line by line, guaranteeing and at the same time efficient implementations. Performances are further enhanced by the native integration of the optimized BLAS [Law+79] and LAPACK libraries for linear algebra operations, which are often at the core of all scientific applications. Regarding productivity, instead, Julia provides an extensive ecosystem, currently comprised by more than ten thousand packages, spanning over almost all branches of science and engineering. Moreover, most of them are already highly tested and optimized, and can therefore reduce the implementation time required to the users. As an example, in this work we employed the `Distributions` [Bes+21] [Lin+19] and `Statistics` packages, while the original C implementation had to write all the statistical functionalities from scratch. Considering all this, the Julia choice was deemed very natural.

As we will see in Section 4, even despite the higher complexity of the model we managed to get better performance in Julia compared to the original C implementation, at the reasonable cost of a smaller increase in the memory requirements, which nowadays should not be a big deal. Anyway, this improvement was possible through several refinements and optimizations, which we will now discuss.

## 3.1 Optimizations

One of the major issues encountered during the design of the fitting function in Julia was controlling the amount of memory and allocations that some functions, structures, or algorithms would require. At the beginning of the development and testing, where the correctness of the algorithm was the only priority, we saw in fact that most of the execution time was actually spent by the garbage collector of Julia, which had the burden of track all the allocated memory and reclaim the unused one in order to make it available again for new computations.

Together with avoiding useless allocations, or in general managing more precisely the memory, another important aspect to focus on to get better performance is ensuring type stability of the function. Luckily, Julia disposes of several tools to inspect and address both problems.

Regarding the second point, there are several packages such as `Cthulhu` or even the simple `@code_warntype` macro which allow to ensure that a function is type-stable, i.e. that the types of all variables can be correctly predicted by the compiler and stay consistent throughout the execution. Type stability is crucial for performance as it enables the compiler to generate optimized machine code, removing the load derived from dynamic type checks. In fact, Julia is dynamically typed, which means that variables do not have to be necessarily declared with their type, in contrast to fully statically typed languages such as C, and they could change it during execution. For example, a variable initialized as an integer could later become a float, or even a string. However, for performance purposes, these dynamicisms should be avoided, and those tools help to ensure that this happens. We managed to reduce all the useless type instabilities, but some are instead still present to guarantee some flexibility to the users, e.g. to select at run time the cohesion and similarity functions to use in the fit.

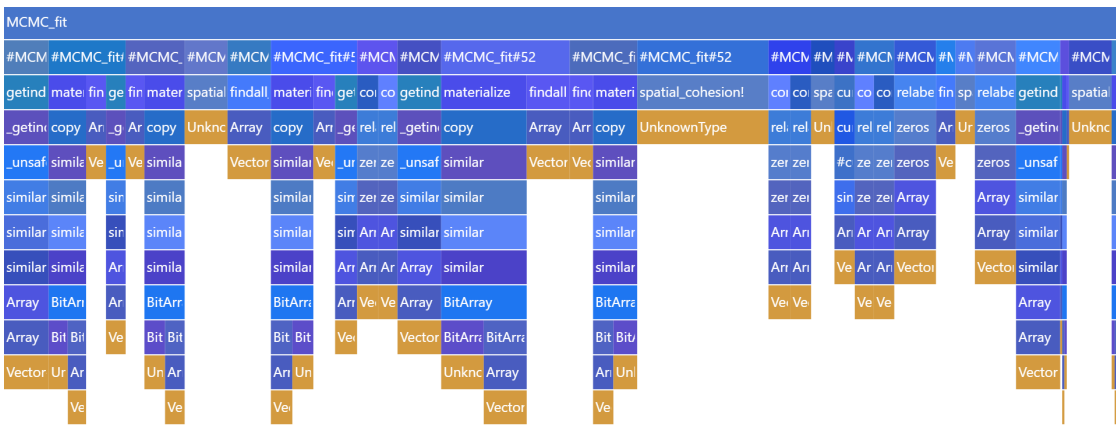


**Figure 3.1:** Flame graph derived from a simple test fit with  $n = 20$ ,  $T = 50$ , ran for 10000 iterates. Each section, identified with a colored box, represents a function call with its stack trace below, i.e. all the other subsequent function calls generated from the initial top one. The widths are proportional to allocation counts, i.e. to how many times a memory allocation was required for their corresponding box. The plot should be read from top to bottom with respect to function calls, and from left to right with respect to the fitting steps.

Regarding the first point, the memory issues, we relied on the `ProfileCanvas` package. This profiler generates a plot, the flame graph, represented in Figure 3.1, which illustrates the different sections of code with regions whose size is proportional to a certain metric, e.g. the time spent on them during execution or, in this case of memory investigation, the number or size of allocations that was required for that section. This allows to see if the running time is spent on actual useful operations or instead on “bad” ones, such as garbage collection and run-time evaluations; therefore highlighting the sections of code which could possibly be optimized. All the modelling and working variables were of course preallocated, but the key idea has been to refactor the code to make it work more *in place*, passing as arguments the variables which would be modified by the function and applying those changes directly inside the function, rather than returning some values and then use them to modify the initial variables.

More in general, also the `BenchmarkTools` [CR16] package has been a great tool to quickly analyse and compare entire fits or just small sections of code. For example, that package allows to simply test different versions of equivalent instructions to see which one could be the most efficient, as in this case

```
using BenchmarkTools
nh_tmp = rand(100)
@btime nclus_temp = sum($nh_tmp .> 0)
# 168.956 ns (2 allocations: 112 bytes)
@btime nclus_temp = count(x->(x>0), $nh_tmp)
# 11.612 ns (0 allocations: 0 bytes)
```

or this other one

```
n = 100; rho_tmp = rand((1:5),n); k = 1
@btime findall(j -> ($rho_tmp)[j]==$k, 1:n) # with anonymous function
# 272.302 ns (5 allocations: 384 bytes)
@btime findall_faster(j -> ($rho_tmp)[j]==$k, 1:n) # custom implementation
# 214.259 ns (3 allocations: 960 bytes)
@btime findall($rho_tmp .== $k) # with element-wise comparison
# 184.112 ns (3 allocations: 320 bytes)
```

where the `$` symbol is used for interpolating a variable, ensuring to treat it as a local variable inside the benchmark and therefore avoiding any performance bias caused by accessing a global variable. This was a quick and simple comparison, yet very precise and effective, which would be instead more complex to replicate in C.

During the finer and final refinements of the code we also used more low-levels analysis tools such as the `--track-allocation` option, which asks Julia to execute the code and annotate the source file to see at which lines, and of which amount, allocations occur.

### 3.1.1 Optimizing spatial cohesions

The memory allocation problem was especially visible in the spatial cohesion computation. In fact, such computation appears in both sections of updating  $\gamma_{it}$  and updating  $\rho_t$ , which are inside of outer loops on draws, time, and units, and

involve themselves some other loops on clusters. All this implied that those cohesion computations will be executed possibly millions of times during each fit. A simple and quick inspection suggests a value between  $dTn$  and  $dTn^2$ , being  $d$  the number of iterations,  $T$  the time horizon and  $n$  the number of units. We can't provide more precise estimate due to the variability and randomicity of the inside loops, which depend on the distribution of the clusters. With all that in mind, it was crucial to optimize the performance of the cohesion functions.

The only optimizing task consisted in carefully designing the cohesion function implementations. Cohesions 1, 2, 5 and 6 didn't exhibit any complication or need for optimization: the natural conversion in code from their mathematical models proved to be already optimally performing. The main problem was instead with cohesions 3 and 4, the auxiliary and double dipper, which by nature would involve some linear algebra computations with vectors and matrices.

The first implementation of those cohesions turned out to be really slow, due to the overhead generated by allocating and then freeing, at each call, the memory devoted to all vectors and matrices. This in the end meant that most of the execution time was actually spent by the garbage collector, rather than in the real and useful operations. A first solution was then to resort to a scalar implementation, which would remove the overhead of the more complex memory structures. In the end, we managed to combine the readability of the first idea with the performance of the second one into a final version, as we can see from Listing 1.

**Listing 1:** Sections of the Julia code for the three implementation cases of the spatial cohesions 3 and 4. The first one has the first-thought vector implementation derived from the mathematical formulation, the second one is the conversion to only have scalar variables, while the third one is the final version, keeping the vector form but improved using static structures.

```
# original vector version
sbar = [mean(s1), mean(s2)]
vtmp = sbar - mu_0
Mtmp = vtmp * vtmp'
Psi_n = Psi + S + (k0*sdim) / (k0+sdim) * Mtmp

# scalar-only version
sbar1 = mean(s1); sbar2 = mean(s2)
vtmp_1 = sbar1 - mu_0[1]
vtmp_2 = sbar2 - mu_0[2]
Mtmp_1 = vtmp_1^2
Mtmp_2 = vtmp_1 * vtmp_2
Mtmp_3 = copy(Mtmp_2)
Mtmp_4 = vtmp_2^2
aux1 = k0 * sdim; aux2 = k0 + sdim
Psi_n_1 = Psi[1] + S1 + aux1 / (aux2) * Mtmp_1
Psi_n_2 = Psi[2] + S2 + aux1 / (aux2) * Mtmp_2
Psi_n_3 = Psi[3] + S3 + aux1 / (aux2) * Mtmp_3
Psi_n_4 = Psi[4] + S4 + aux1 / (aux2) * Mtmp_4

# static improved version
sbar1 = mean(s1); sbar2 = mean(s2)
sbar = SVector((sbar1, sbar2))
vtmp = sbar .- mu_0
Mtmp = vtmp * vtmp'
```

```

aux1 = k0 * sdim; aux2 = k0 + sdim
Psi_n = Psi .+ S .+ aux1 / (aux2) .* Mtmp

```

This final version exploits the `StaticArrays` package of Julia, which allows to use vectors and matrices more efficiently if their size is known at compile time; which is the case of the spatial cohesions computation since working with planar spatial coordinates we will always have  $2 \times 1$  vectors and  $2 \times 2$  matrices. The benefits of this final version are that we maintain the natural mathematical form of the first one, improving the clearness of the code, together with the efficiency of the second one, since now with static structures the compiler is able to optimize all memory allocations as it was doing with the simple scalar variables.

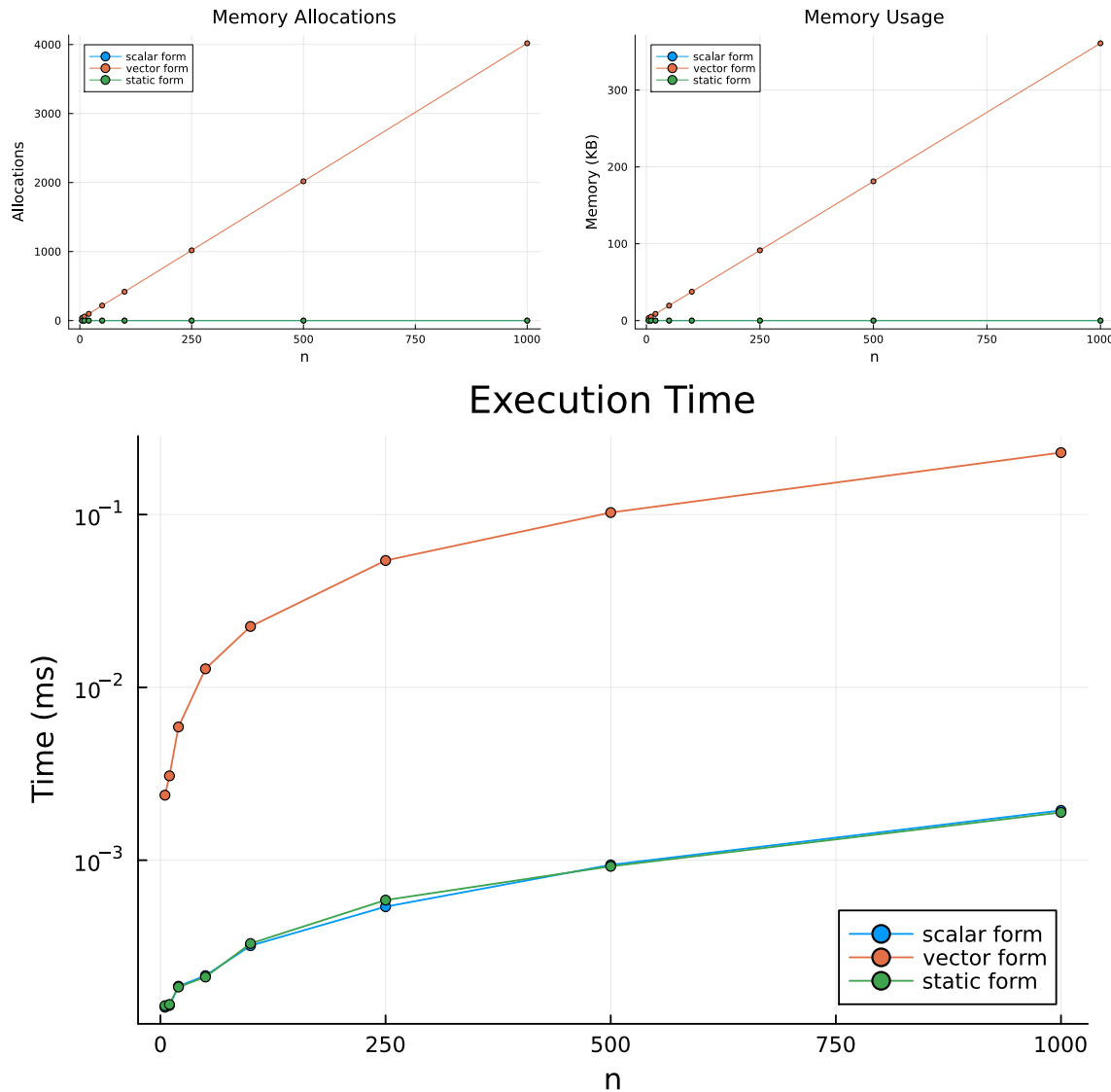


**Figure 3.2:** Performance comparison between the three versions of the cohesion 4 function. Tests ran through the `BenchmarkTools` package of Julia by randomly generating the spatial coordinates of the various test sizes  $n$ , with similar results standing for cohesion 3. The memory allocation and usage plots are constant at zero for both the scalar and vector static cases.

Figure 3.2 shows the comparison of their performances, where we can see how

the scalar and static versions indeed perform very similarly to each other, and more quickly with respect to the first version.

Noticeably, the C implementation of the model didn't have to worry about all this reasoning, since C can't natively, nor gracefully, work with vectors and matrices and was therefore forced to the scalar implementation.

### 3.1.2 Optimizing covariates similarities

Another problem has been understanding how to speed up the computation of the similarity functions, since those would also be called possibly millions of times as the cohesion ones or even more, considering that we can incorporate more than one covariate into the clustering process, and this would add an additional loop based on  $p$ , the number of covariates decided to be included.

As in the previous case, some of the functions didn't show any special need or room for relevant optimizations. The fourth one instead, the auxiliary similarity function, was essential to be optimized: not only because it is one the most common choice among the similarities, but also because it involves a computationally heavy sum of the squares of the covariate values, as we can see in Listing 2.

**Listing 2:** Version of the similarity 4 function with all the possible optimizing macros. The performance analysis will focus just on that inside loop, since the rest is not negotiable.

```
function similarity4(X_jt::AbstractVector{<:Real}, mu_c::Real, lambda_c::Real,
                     a_c::Real, b_c::Real, lg::Bool)
    n = length(X_jt)
    nm = n/2
    xbar = mean(X_jt)
    aux2 = 0.
    @inbounds @fastmath @simd for i in eachindex(X_jt)
        aux2 += X_jt[i]^2
    end
    aux1 = b_c + 0.5 * (aux2 - (n*xbar + lambda_c*mu_c)^2/(n+lambda_c) +
                         lambda_c*mu_c^2)
    out = -nm*log2pi + 0.5*log(lambda_c/(lambda_c+n)) + lgamma(a_c+nm) -
          lgamma(a_c) + a_c*log(b_c) + (-a_c-nm)*log(aux1)
    return lg ? out : exp(out)
end
```

The idea to optimize it has been to annotate the loop with some macros provided by Julia. They are the following:

- `@inbounds` eliminates the array bounds checking within expressions. This allows to skip those checks to save some execution time. This insertion is harmless as long as we are sure that in our code design no out-of-bounds or wrong accesses will occur. Otherwise some undefined behaviour will take place. The above loop is indeed very simple and safe, so this assumption is clearly satisfied.

- `@fastmath` executes a transformed version of the expression which calls functions that may violate strict IEEE semantics<sup>1</sup>. For example, its use could make  $(a + b) + c \neq a + (b + c)$ , but just in very pathological cases. Again, this is not a problem in our function, where we are just computing  $\sum X_i^2$ , since it does not have an intrinsically “right order” in which it has to be done.
- `@simd` (single instruction multiple data) annotate a for loop to allow the compiler to take extra liberties to allow loop re-ordering. This is a sort of parallelism technique, but rather than distributing the computational load on more processors we just *vectorize* the loop, i.e. we enable the CPU to perform that single instruction (summing the square of the  $i$ -th component to a reduction variable) on multiple data chunks at once, using vector registers, rather than working on each element of the vector individually.

As we can see from Figure 3.3, the actual performance difference basically derives just from the use of `@simd`, with the other two annotations making not much of a difference. For that reason, and to reassure all pure mathematicians, we decided to remove the `@fastmath` annotation, leaving just `@inbounds` and `@simd`.

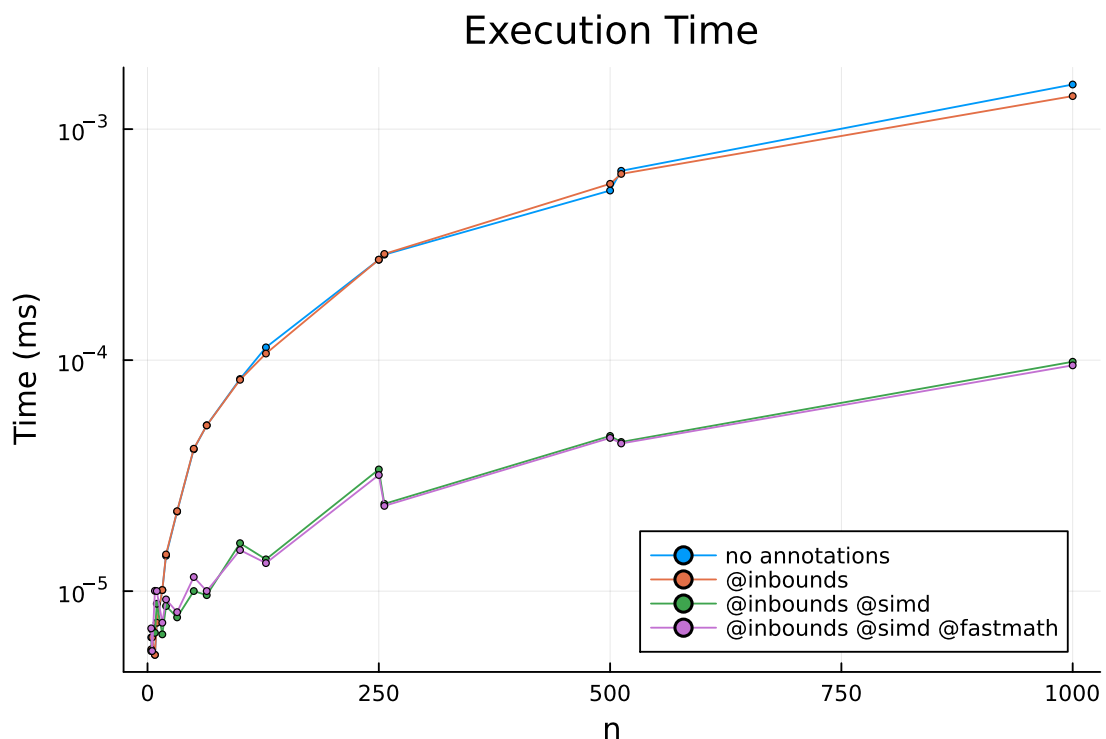


**Figure 3.3:** Comparison of the performances of the different possible loop annotations in the similarity 4 implementation. Their numerical output results are indeed the same for all cases. There are no memory allocation and usage plots since the analysis has been conducted only to evaluate the performances of the inside loop, which has no memory issues.

<sup>1</sup>Institute of Electrical and Electronics Engineers. The IEEE-754 standard defines floating-point formats, i.e. the ways to represent real numbers in hardware, and the expected behavior of arithmetic operations on them, including precision, rounding, and handling of special values (e.g. NaN (Not a Number) and infinity).

We can also notice interestingly how the tests with `@simd` annotation run quicker in the case of  $n$  being a power of two, compared to their closest rounded integers (e.g. 256 against 250 or 512 against 500), despite having relatively some more data. This is a proof of the effectiveness of the SIMD paradigm: according to the different architectures, the CPUs can provide different register sizes (e.g. 64, 128, 256 or 512 bits) and therefore the data subdivision can fit perfectly in them when the total memory occupied by the elements is a multiple of that register size (i.e. the number of data values is a power of two). Otherwise there will be some “leftovers chunks”, which will of course be processed, but will also cause, as a consequence of the imperfect fit, a bit of overhead.

# Chapter 4

## Testing

### 4.1 Assessing the equivalence of the models

Our model, and the corresponding Julia code, is just an improvement of the original DRPM with his relative C implementation. These improvements, as described in the previous chapters, refer to the insertion of covariates, both at the clustering and likelihood levels, the handling of missing values in the target variable, and the computational efficiency. In this sense, our updates are just add-ons to the original model, and therefore at a common testing level they should perform similarly by agreeing in the clusters that they produce on a given dataset.

To assess this ideally equivalent behaviour we ran two tests: the first one with only the target values, using synthetic data, while the second including spatial information, using a real spatio-temporal dataset. For the sake of clarity, also in these sections we will refer to CDRPM for the original model and implementation from [PQD22], while to JDRPM for the updated version derived from this thesis work.

In the following analysis we will heavily rely on the Adjusted Random Index (ARI) [HA85] to compare the partitions generated by the models. The ARI index is a correlation index to measure similarities between clusterings. More precisely, given two partitions  $\rho_1$  and  $\rho_2$ , the  $\text{ARI}(\rho_1, \rho_2)$  returns a value between  $[-1, 1]$  where higher values indicates higher levels of agreement between the partitions, i.e. they produced similar clusters. Being a *random* index it has an expected value and it is equal to zero, which corresponds to the case of comparing two randomly generated partitions.

We will use this index both to study the time evolution of the clusterings, to see e.g. if  $\rho_{t+k}$  is correlated to  $\rho_t$ , that is, if the clusters show the time dependent structure that the models implement, and also to check the level of agreement between the two models, comparing the clusters produced by CDRPM and JDRPM.

### 4.1.1 Target variable only

For the first test we generated a dataset of  $n = 10$  units and  $T = 12$  time instants, and fitted both models collecting 1000 iterates derived from 10000 total iterations, discarding the first 5000 as burnin and thinning by 5. Those parameters, as well as the generating function, were the same of [PQD22]. The generating function allowed to create data points with temporal dependence, which could be tuned through some dedicated parameters. Both models were fitted using the full formulation, i.e. including and updating also the optional autoregression parameters  $\eta_{1i}$ , and  $\varphi_1$ , and using a time specific  $\alpha$ .

**Table 4.1:** Summary of the comparison between the two fits on target values only. The MSE columns refer to the accuracy between the fitted values generated by the models (estimated by taking the mean and the median of the returned 1000 iterates) and the true values of the target variable. Higher LPML and lower WAIC indicate a better fit.

	MSE mean	MSE median	LPML	WAIC	exec. time
CDRPM	1.6731	1.5861	-249.61	469.69	4.8s
JDRPM	<b>1.2628</b>	<b>1.2181</b>	<b>-227.83</b>	<b>415.03</b>	<b>2.5s</b>

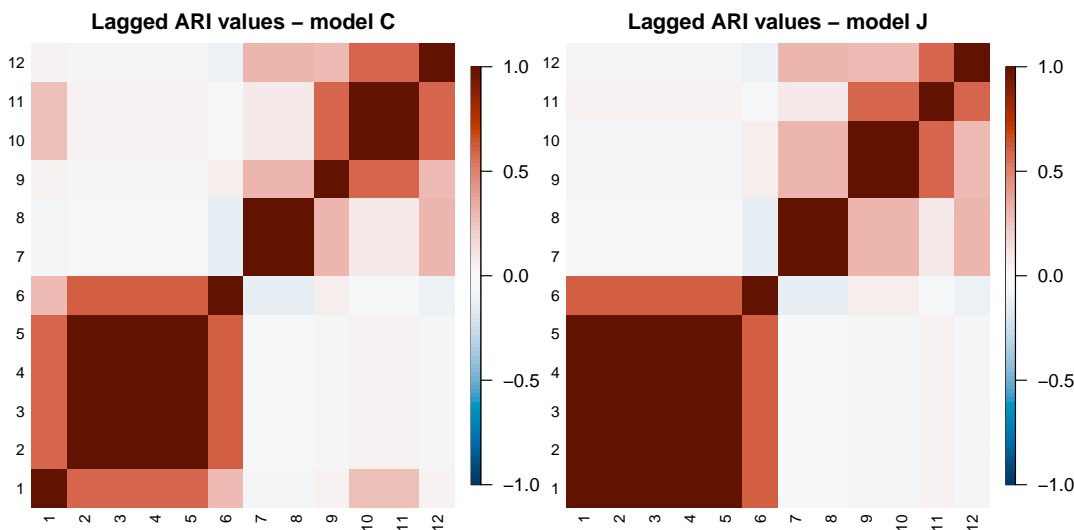


**Figure 4.1:** Lagged ARI values for the two models, on the fit with target only data. The partitions were estimated using the `salso` function from the corresponding R library.

At this testing stage there were just the target values from  $Y_{it}$  to dictate the clusters definition, and both models managed to provide good fits, as we can read from Table 4.1. The JDRPM model had better fit metrics (lower WAIC and higher LPML) and also faster execution time, which is however not really relevant in this small-sized fit. Regarding the fitted values, displayed in Figure 4.4 together with the original data, they turned out to be also more precise than the one generated by CDRPM, having lower mean squared errors.

The resulting clusters were indeed very similar. Figure 4.1 shows how they manifest the same temporal trend, while Figure 4.2 highlights how the clusters

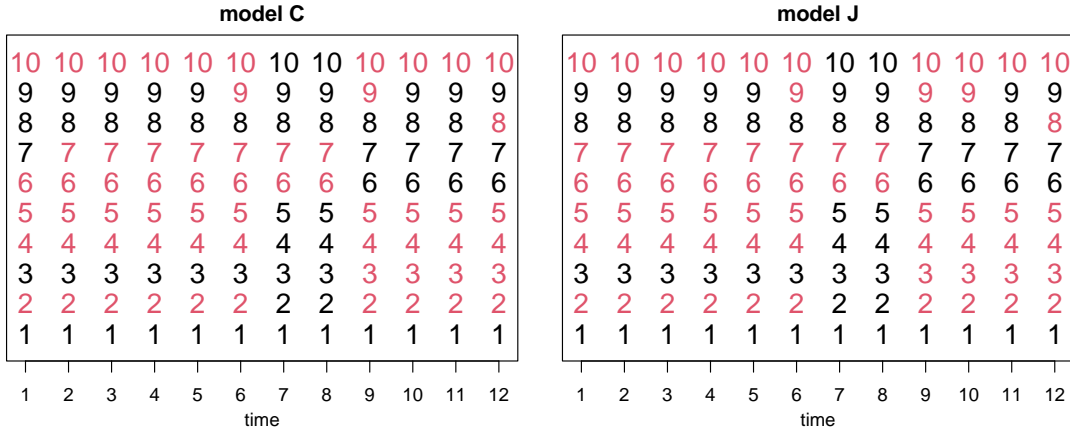


**Figure 4.2:** Clustering produced by the two models, with time points on the  $x$  axis, units indicated vertically by their number, and colors representing the cluster label.

produced are effectively the same except for two differences occurred at times 1 and 10. By visually inspecting the clusters from Figure 4.3, we can see how at  $t = 1$  the JDRPM model assigned a red label to a unit closer to the black pack, to which in fact model CDRPM assigned a black label. However, that same unit in the following time instants would be clearly part of the red cluster, thus making the JDRPM choice very reasonable. The opposite happens at  $t = 10$ , where now the CDRPM model seems to give more importance to the temporal trend, assigning a black label to a unit really closer to the red pack but that is destined to enter the black cluster in the following two time instants.

#### 4.1.2 Target variable plus space

We now consider a more realistic scenario in which we fit the models using a spatio-temporal dataset. In particular, we used the AgrImOnIA [Fas+23] dataset which stores measurements about air pollutants, together with many other environmental variables, in the Lombardy region from 2016 to 2021. For the following testing fits, we employed a summary dataset composed by weekly averages of the data from year 2018.

The chosen target variable was  $\text{PM}_{10}$  whose values had been log-transformed, to recover a normal distribution, and centered with respect to time-wise means. More precisely, each unit  $Y_{it}$  was corrected by subtracting the mean  $\bar{Y}_t$  of all the observations of that time instant. This procedure, which was the same employed by the authors of the original DRPM during their spatial tests, helps to emphasizes the variations within each time point rather than across the entire dataset. This can be particularly useful to understand how units deviate from their typical behavior at specific times, potentially highlighting temporal trends and anomalies. This method also removes any temporal bias, e.g. time instants in which all target values were particularly high or low for any particular reason. In contrast, the more traditional choice of centering with respect to the global mean  $\bar{Y}$  of the dataset would be useful to just detect global trends, without inspecting deeply into each step. From some

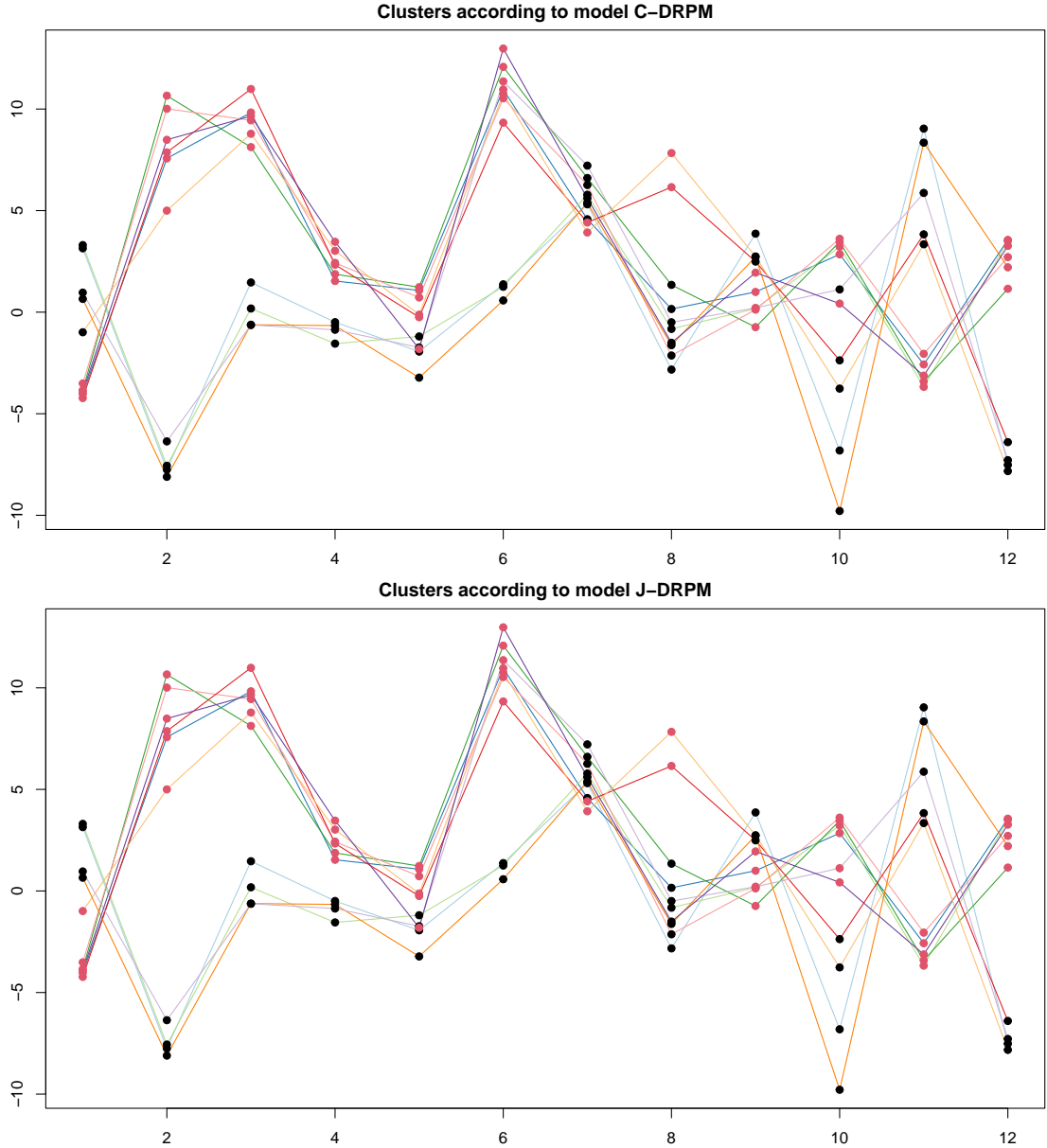


**Figure 4.3:** Visual representation of the clusters produced by the models, on the fit with target only data, with units' labels represented as colored dots overlaid to the trend of the generated target variable. The only differences occur at times 1 and 10.

test fits performed on the target values with the classical global centering indeed only three clusters appeared, for all time instants. This is of course correct, in some sense, since it's reasonable according to the trend displayed in the top image of Figure 4.5. However, as we will see shortly, the other version was able to produce several clusters, or at least different partitions at different time instants, improving the specializations of the clusters and the interpretability of the obtained results.

We took all the  $n = 105$  stations available in the dataset but we limited the time horizon to  $T = 12$ , which corresponds to a three-month monitoring period, just to reduce the time needed to perform all tests. We ran both CDRPM and JDRPM models using the same complete modelling setup, as in Section 4.1.1, and

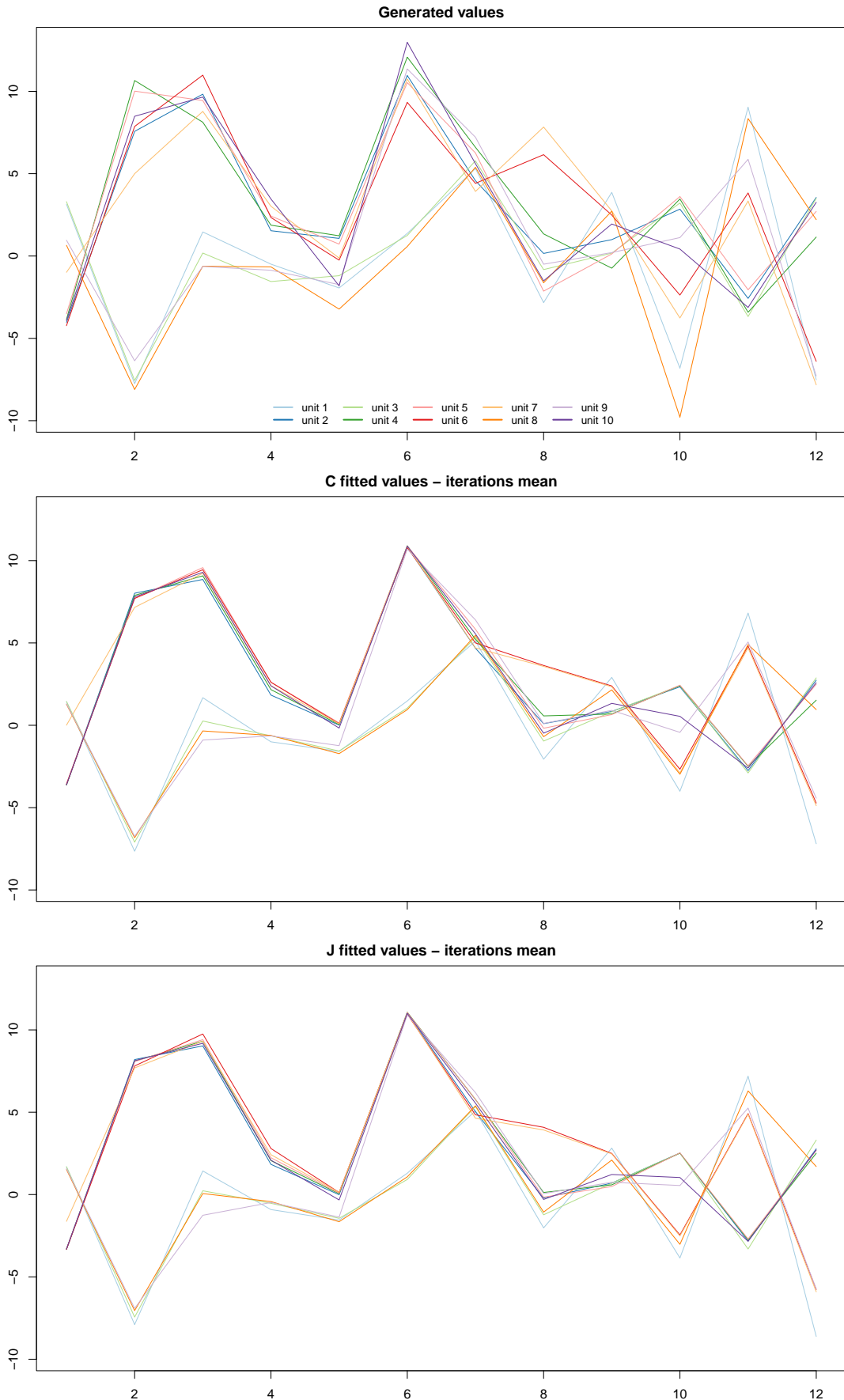


**Figure 4.4:** Generated target values (top), together with their fitted values estimate through the mean of the 1000 iterates generated by model CDRPM (middle) and JDRPM (bottom).

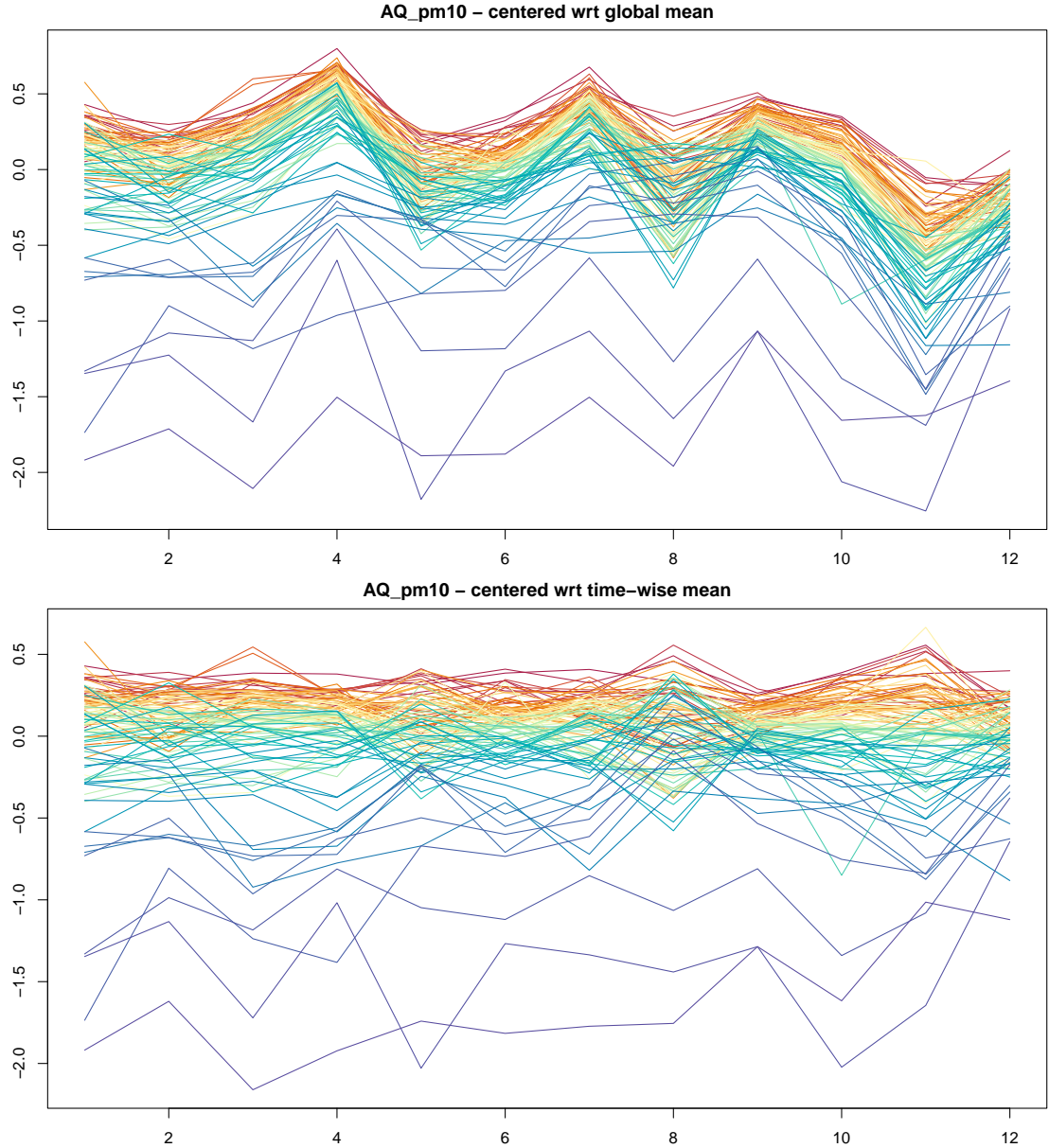


**Figure 4.5:** Values of the target variable AQ\_pm10 corrected using the global mean (top) and using the time-wise mean (bottom). This second choice helps to adjust the values range while keeping, or even highlighting, the clustering structural information. Coloring is based on the ranking of PM<sub>10</sub> values of the units according to their median, from highest (red) to lowest (blue).

using a time specific  $\alpha$ . Convergence was ensured visually by inspecting trace plots and, for the JDRPM model, by numerical diagnostics such as ESS and  $\hat{R}$ , which instead the CDRPM model is not able to provide directly from the fit. We collected 4000 iterates, from 110000 total iterates with a burnin of 90000 and thinning by 5.

Table 4.2 shows how both model managed to be accurate not only with respect to the fitting metrics of LPML and WAIC but also in terms of the fitted values. Execution times are also reported, but they are somewhat inaccurate since during the fitting I was busy in writing this thesis, meaning that not all the computational resources of my laptop were devoted to the fitting task. In any case, more precise

**Table 4.2:** Summary of the comparison between the two fits on target plus space values. The MSE columns refer to the accuracy between the fitted values generated by the models (estimated by taking the mean and the median of the returned 4000 iterates) and the true values of the target variable. Higher LPML and lower WAIC indicate a better fit.

	MSE mean	MSE median	LPML	WAIC	exec. time
CDRPM	0.0142	0.0149	<b>694.81</b>	-1768.42	1h38m
JDRPM	<b>0.0131</b>	<b>0.0138</b>	624.91	<b>-1898.05</b>	<b>56m</b>

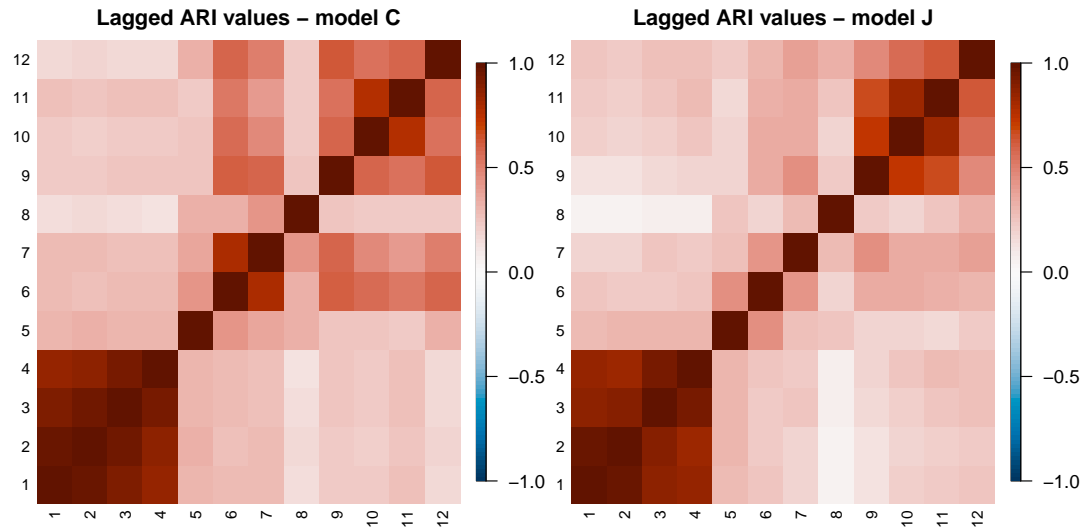


**Figure 4.6:** Lagged ARI values for the two models, on the fit with target plus space data. The partitions were estimated using the `salso` function from the corresponding R library.

performance evaluations on the timings will be conducted in Section 4.4.

From Figure 4.6 we can see how the temporal trend was very similar, confirming again the correctness of the JDRPM implementation. Regarding the similarity of the produced clusters, the partition plot as the one of Figure 4.2 would now be more crowded due to the high number of units. For this reason, in order to still convey that information, we computed  $\text{ARI}(\rho_{\text{JDRPM}}(t), \rho_{\text{CDRPM}}(t))$  for all time instants  $t = 1, \dots, 12$ , and we obtained a mean of 0.80 and a median of 0.86, denoting high levels of agreement in the clusters produced.

A visual representation of the clusters is provided in Figure 4.8, but will be further detailed and commented in Section 4.3.2 together with the fits including covariates in the clustering.

## 4.2 Performance with missing values

We now repeat the tests of the previous section on the same datasets but this time with missing values, to see how the JDRPM model reacts to the absence of a full dataset and check if it can still perform well. Based on the amount of missing values in the AgrImOnIA dataset, used for the spatio-temporal tests, we chose

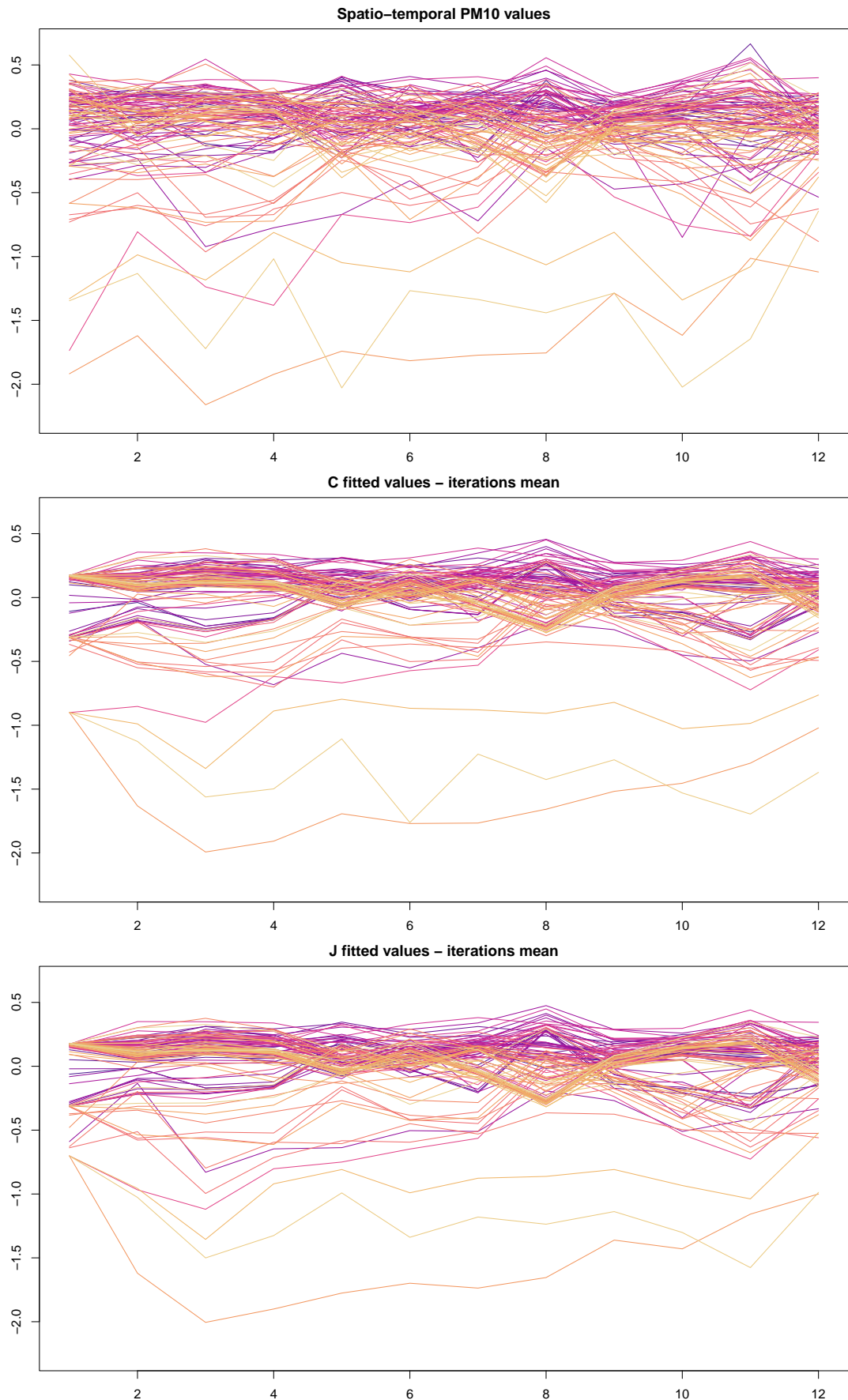


**Figure 4.7:** Target  $Y_{it}$  values (top), together with their fitted values estimate through the mean of the 4000 iterates generated by model CDRPM (middle) and JDRPM (bottom).

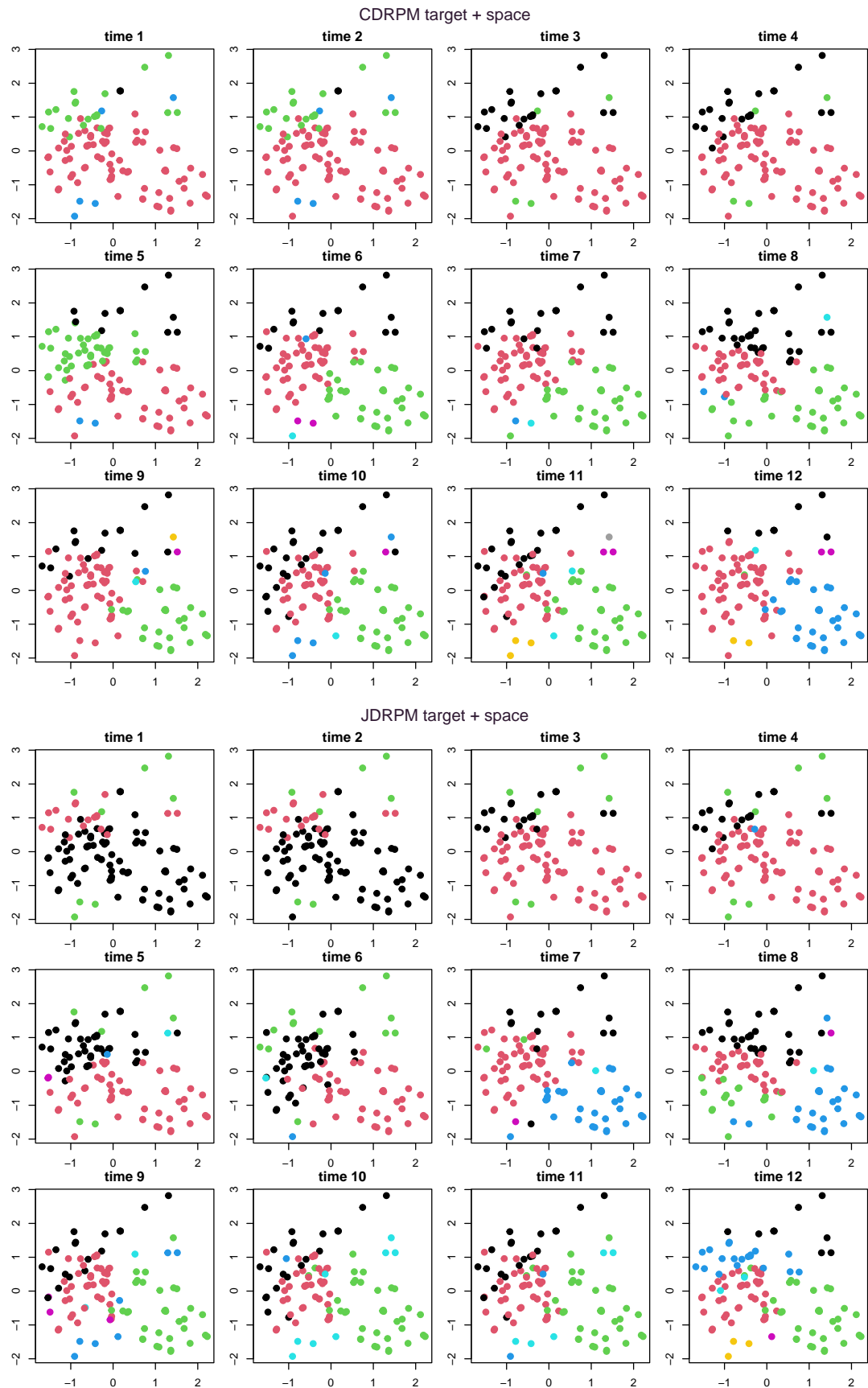


**Figure 4.8:** Clusters generated by the CDRPM and JDRPM fits with target plus space values.

to set at 10% the amount of values that would be replaced by NAs. To perform such replacements, we randomly drew  $nT/10$  indexes from the sets  $[1, \dots, n]$  and  $[1, \dots, T]$  to get all the pairs  $(i, t)$  which would become missing values in the target variable  $Y_{it}$ . The dealing of NAs was an upgrade brought by the JDRPM model, so we can't perform these tests with the original CDRPM model since it cannot handle missing data.

All the following fits have been conducted under the same conditions of their full-dataset counterpart, i.e. using the same models formulation and parameters.

#### 4.2.1 Target variable only (NA case)

The JDRPM seems to exhibit good performance also with missing values. From Table 4.3 we can see how the performances, naturally worse than the fit in the full case, are still good. The MSE is inevitably higher since the model did not have all the data points, and so we get less precise fitted values for the corresponding missing spots in the dataset, but the fitted values of Figure 4.9 are still close the one obtained with the fit on full dataset.

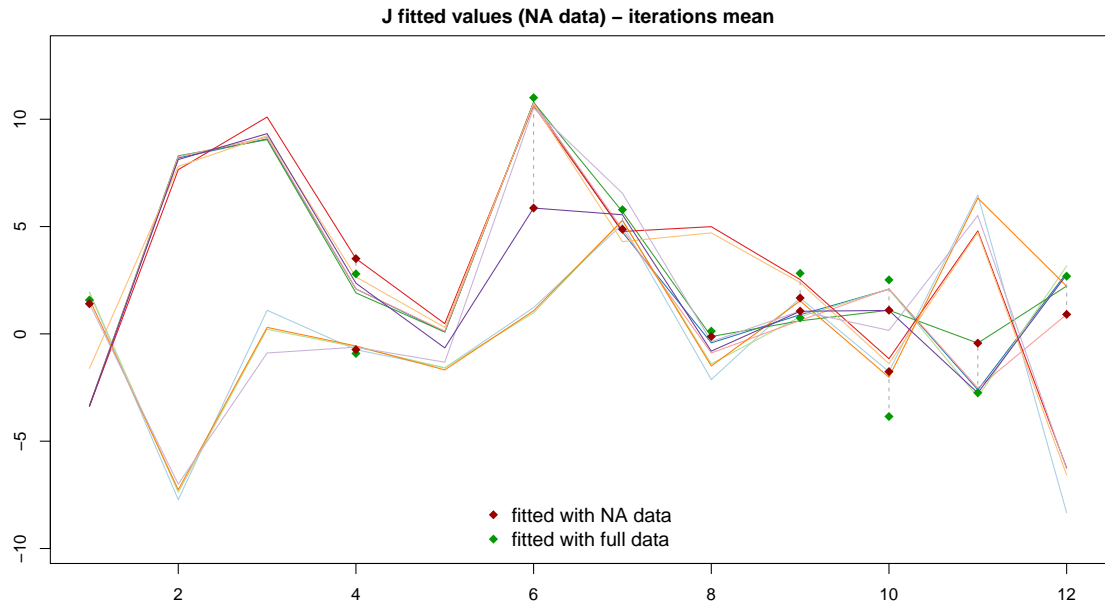


**Figure 4.9:** Fitted values estimate trough the mean of the 1000 iterates generated by model JDRPM. The generated target values were the same of Figure 4.4. Special point markers are used for the data points which were missing, to highlight the gaps between the fitted values on the full dataset (green squares) and the fitted ones on the NA dataset (red squares).

From Figures 4.11 and 4.10 we can see how we get almost the same temporal trend which we saw in the case without missing data, and indeed the assigned clusters are almost the same. The only difference occurs on a single unit at time 10, where now the JDRPM model does the same thing that CDRPM did in its corresponding fit of Section 4.1.1.

**Table 4.3:** Summary of the comparison between the two Julia fits on target values only. The MSE columns refer to the accuracy between the fitted values generated by the models (estimated by taking the mean and the median of the returned 1000 iterates) and the true values of the target variable. Higher LPML and lower WAIC indicate a better fit.

JDRPM	MSE mean	MSE median	LPML	WAIC	exec. time
NA data	2.1819	1.7876	-239.21	417.21	3.0s
full data	1.2628	1.2181	-227.83	415.03	2.5s

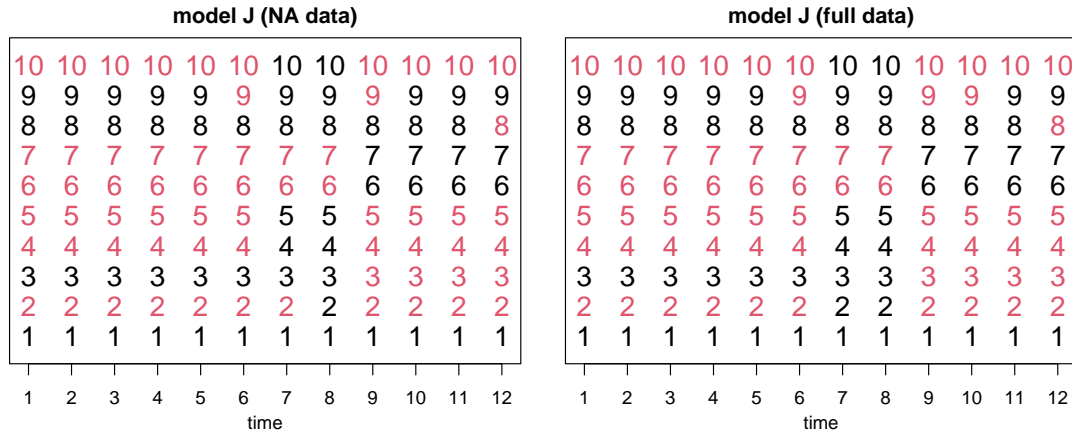


**Figure 4.10:** Clustering produced by the two tests on the JDRPM model, with time points on the  $x$  axis, units indicated vertically by their number, and colors representing the cluster label.

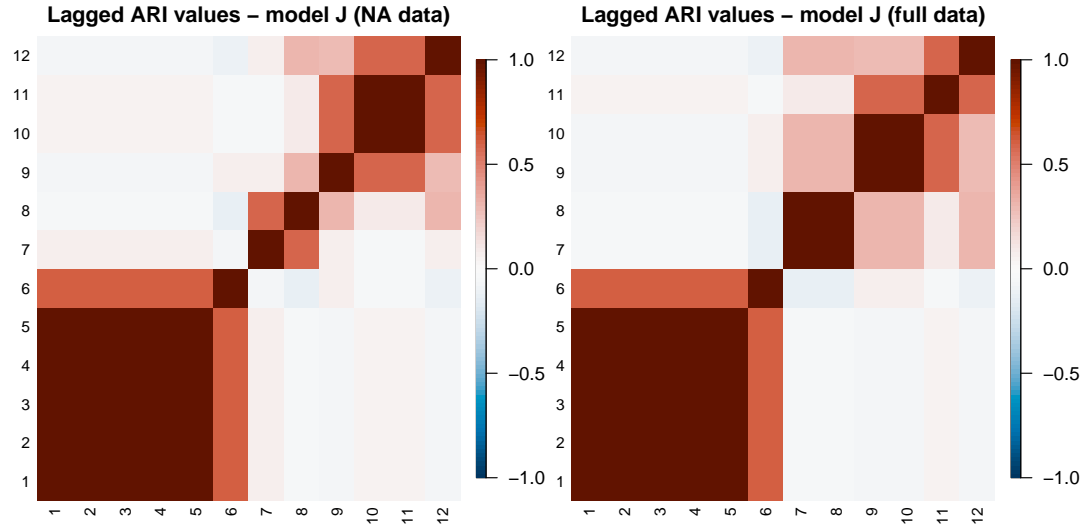


**Figure 4.11:** Lagged ARI values for the two fits on the JDRPM model with target values only. The partitions were estimated using the `salso` function from the corresponding R library.

#### 4.2.2 Target variable plus space (NA case)

The JDRPM model seems able to perform well also in the case of fits including spatial information. Table 4.4 shows how the accuracy reduces, which again is inevitable since we are fitting with missing data, but not drastically. In fact, the

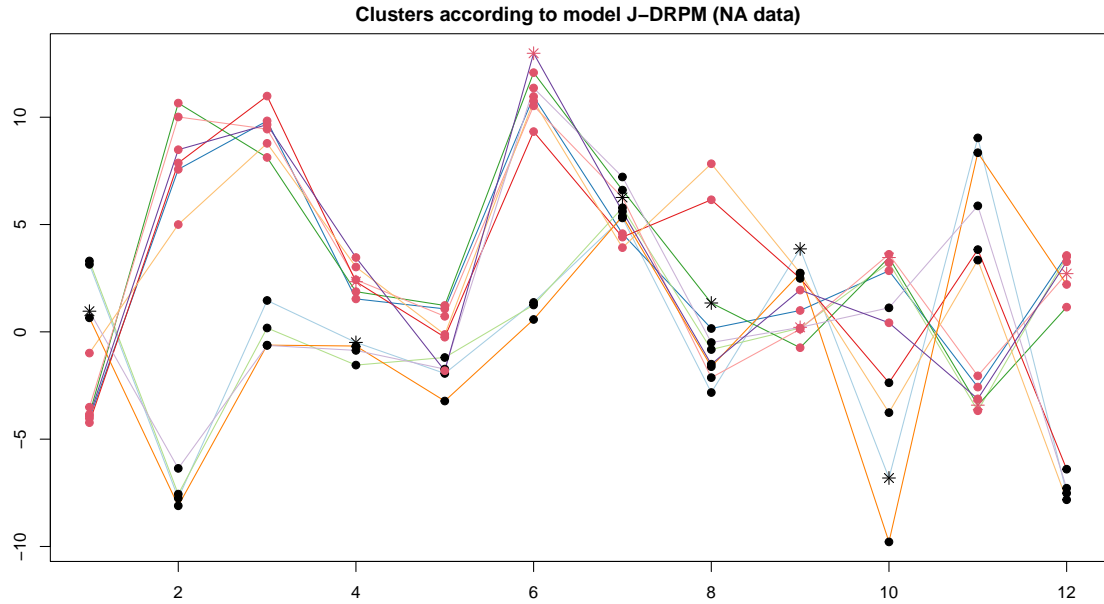


**Figure 4.12:** Visual representation of the clusters produced by the model, with units' labels represented as colored dots overlaid to the trend of the original generated target variables. Special point markers are used for the data points corresponding to missing values.

**Table 4.4:** Summary of the comparison between the two Julia fits on target plus space values. The MSE columns refer to the accuracy between the fitted values generated by the models (estimated by taking the mean and the median of the returned 4000 iterates) and the true values of the target variable. Higher LPML and lower WAIC indicate a better fit.

JDRPM	MSE mean	MSE median	LPML	WAIC	exec. time
NA data	0.0160	0.0170	502.86	-1793.64	43m
full data	0.0131	0.0138	624.91	-1898.05	56m

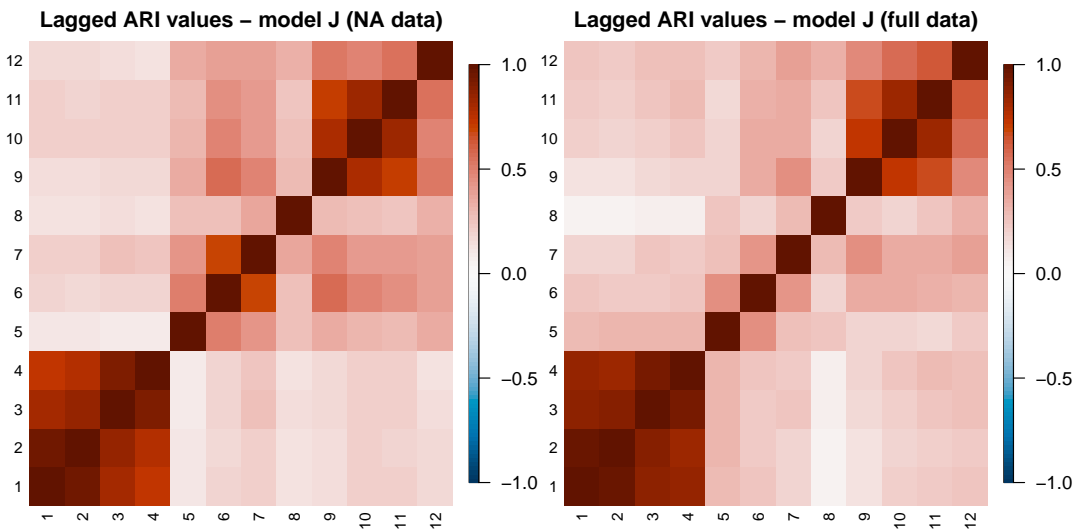


**Figure 4.13:** Lagged ARI values for the two fits on the JDRPM model with target plus space values. The partitions were estimated using the `salso` function from the corresponding R library.

drops in LPML and WAIC metrics are just of 3.16% and 0.95% respectively. Fitted values are reported in Figure 4.14. Regarding the reported execution times, they are not completely truthful, as already said before, due to the not-full commitment of my laptop resources to the fitting task. In fact, the fit with NA data appeared to be faster than the one with full data, which is somewhat implausible since in the presence of NA data there is the additional load of updating the missing  $Y_{it}$  values. Again, more accurate results will be provided in Section 4.4.

The temporal trend managed as well to remain similar to the trend we saw in Section 4.1.2, as proved by Figure 4.13. Regarding the similarity of the produced clusters, we computed the values  $\text{ARI}(\rho_{\text{JDRPM\_NA}}(t), \rho_{\text{JDRPM\_full}}(t))$  for all time instants  $t = 1, \dots, 12$ , and we obtained a mean of 0.82 and a median of 0.86, denoting still a relatively high level of agreement in the partitions despite the loss of quite some data (121 points out of the 1260 of the full dataset).

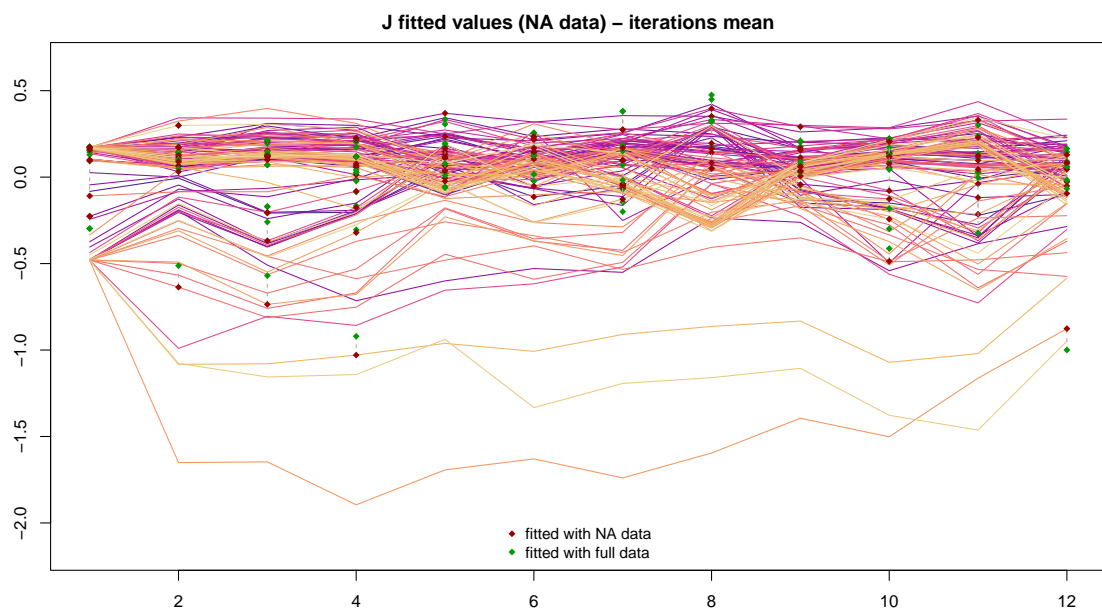


**Figure 4.14:** Fitted values estimate through the mean of the 4000 iterates generated by model JDRPM. The generated target values were the same of Figure 4.7. Special point markers are used for the data points which were missing, to highlight the gaps between the fitted values on the full dataset (green squares) and the fitted ones on the NA dataset (red squares).

## 4.3 Effects of the covariates

To perform the fits that will now follow, all the included covariates were treated in the same way as the target value, with the time-wise centering procedure and reasoning described in Section 4.1.2. Figure 4.15 provides an exemplification of the effect of this transformation on one of the covariates.

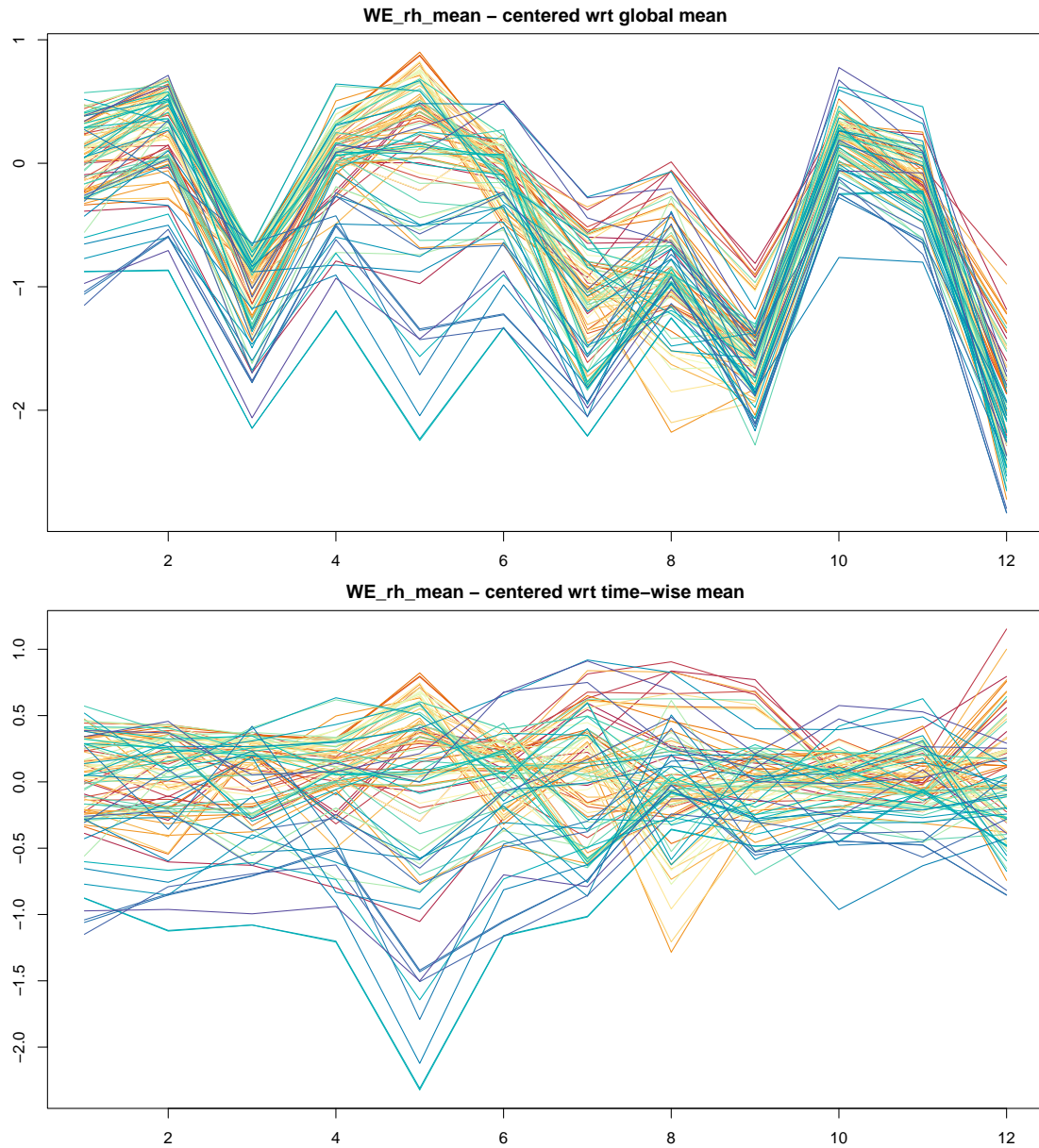


**Figure 4.15:** Values of the `WE_rh_mean` centered covariate corrected using the global mean (top) and using the time-wise mean (bottom). Coloring is based on the ranking of PM<sub>10</sub> values of the units according to their median, from highest (red) to lowest (blue).

### 4.3.1 Covariates in the likelihood

Continuing on the line of the previous section, we can test if the insertion of covariates in the likelihood can help to recover some accuracy in the case of fits with missing data. In fact, the addition of the regression parameter  $\beta_t$  had the main goal of improving the accuracy of the model when estimating the target values  $Y_{it}$ , without affecting too much the cluster generation. With that in mind, the most natural use case of such parameter would be when fitting with missing values.

Indeed, after including one or multiple covariates in the likelihood, and repeating the fit on the NA dataset under the same conditions, apart from this addition, we

saw some improvements. To better illustrate them, we also ran the corresponding fit using the same covariates set in the likelihood, but this time on the full dataset. Results are summarized in Table 4.5 which also includes, as a reference, the results of the previous fits without the regressor component. Again, the execution times have to be taken with a pinch of salt.

**Table 4.5:** Summary of the comparison between the JDRPM fits, on target plus space values, plus the fits including also covariates in the likelihood. The MSE columns refer to the accuracy between the fitted values generated by the models (estimated by taking the mean and the median of the returned 4000 iterates) and the true values of the target variable. Higher LPML and lower WAIC indicate a better fit.

JDRPM	MSE mean	MSE median	LPML	WAIC	exec. time
full data	0.0131	0.0138	624.91	-1898.05	<b>48m</b>
full data + Xlk	<b>0.0112</b>	<b>0.0113</b>	<b>778.96</b>	<b>-2029.84</b>	56m
NA data	0.0160	0.0170	502.86	-1793.64	<b>43m</b>
NA data + Xlk	<b>0.0127</b>	<b>0.0130</b>	<b>625.81</b>	<b>1902.74</b>	58m

We can see how clearly the insertion of covariates in the likelihood managed to improve all fitting metrics with, as expected, a decrease in the MSEs, especially in the fits with NA data, proving how that insertion can indeed recover some performance in the case of missing values. The regression vectors  $\beta_t$  displayed dense trace plots, as from Figures 4.16 and 4.17, proving the correctness and effectiveness of the implementation. Moreover the values at which the regressors settled seems to be reasonable and interpretable. For example, it is known that higher altitudes implies lower air pollution, due to the nearly absence of emission sources like industries and vehicles, the more intense winds, the lower atmospheric pressure which facilitates the mixing of the air, and so on; and in fact the  $\beta_t$  component referring to `Altitude` wanders around negative values, indicating a reduction impact on  $PM_{10}$  concentrations. On the other hand, the `LI_bovine` covariate, which refers to the density of bovines per  $km^2$  in the the area of the measuring station, tends to stay around positive values, since indeed the presence of livestock industries contributes to the emission of air pollutants.

Regarding the generated partitions, they remained substantially unchanged, as briefly depicted in Figure 4.20. The spatio-temporal trend was as well preserved, displayed in Figure 4.19, except for a generally higher dependence in the second part of the time interval, after the same identified “change point” at  $t = 4$ .

The JDRPM fitting function also includes a `beta_update_threshold` argument, defaulted to zero, to set after which iteration the algorithm should start to update the  $\beta_t$  parameter. This was an harmless and simple addition, which was considered useful to firstly let the model update and improve the more delicate and relevant parameters for the clustering, such as  $\mu_{jt}^*$  and  $\sigma_{jt}^{2*}$ , and secondly tune also the less impactful  $\beta_t$ . Otherwise, maybe, the initial development of the model parameters and clusterings could be biased by early inaccurate samples of the likelihood regressor.

Finally, Figure 4.18 encloses the fitted values of these two runs, with multiple

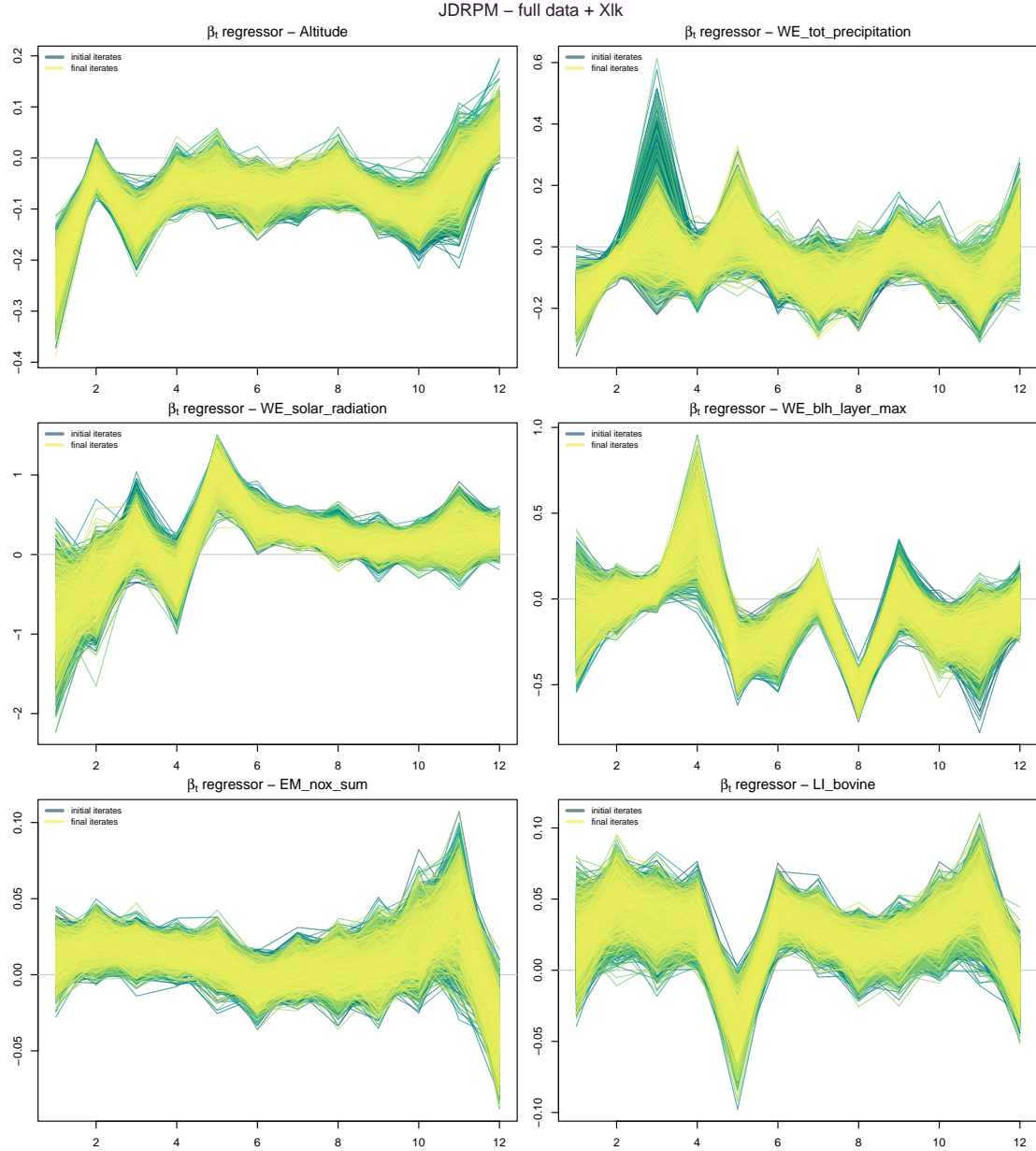


**Figure 4.16:** Regression vector  $\beta_t$  for the  $p = 6$  covariates inserted in the likelihood in the full data spatio-temporal fit test, with time instants  $t = 1, \dots, 12$  are on the  $x$  axis.

covariates in the likelihood on the NA and full datasets, with respect to the real  $\text{PM}_{10}$  values. We can see how indeed, visually but also as proved by the better MSEs, these fitted values resemble more the ones of the original target variable, especially if compared to the case of Figure 4.7, in which both fits were without any “external suggestion” of covariates in the likelihood. A further proof of this insertion can be seen in Figure 4.21, representing the trace plot of the fitted values for a problematic unit and time instant, with problematic in the sense that both the standard JDRPM and CDRPM fits didn’t manage to provide precise estimates, where we can see how now they also become more accurate. In the end, this analysis denotes how the addition of this regression parameter  $\beta_t$  could be beneficial to recover more accuracy in the results, and also help the clustering process since the

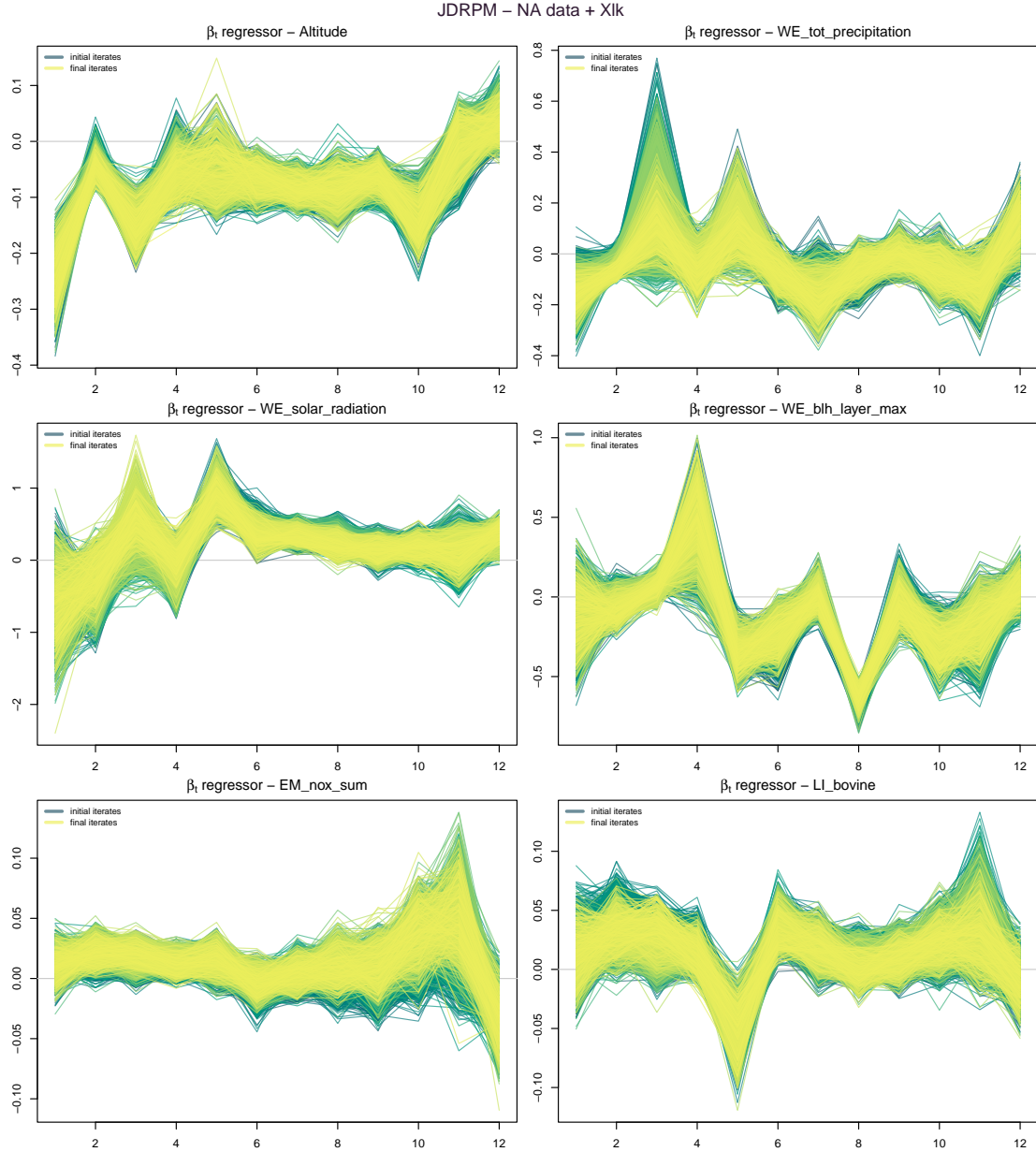


**Figure 4.17:** Regression vector  $\beta_t$  for the  $p = 6$  covariates inserted in the likelihood in the NA data spatio-temporal fit test, with time instants  $t = 1, \dots, 12$  are on the  $x$  axis.

regressor contribution manifests when using variables computed from the target values inside the update steps of the parameters.

### 4.3.2 Covariates in the clustering

Now we consider the more theoretically effective and impactful inclusion of covariates in the clustering process. For the choice of which covariates to include, we reasoned about which where the aspects that could affect more the  $\text{PM}_{10}$  concentrations, and we ended up selecting the following three covariates:

- `WE_wind_speed_10m_max`. Wind speed plays a significant role in the concen-

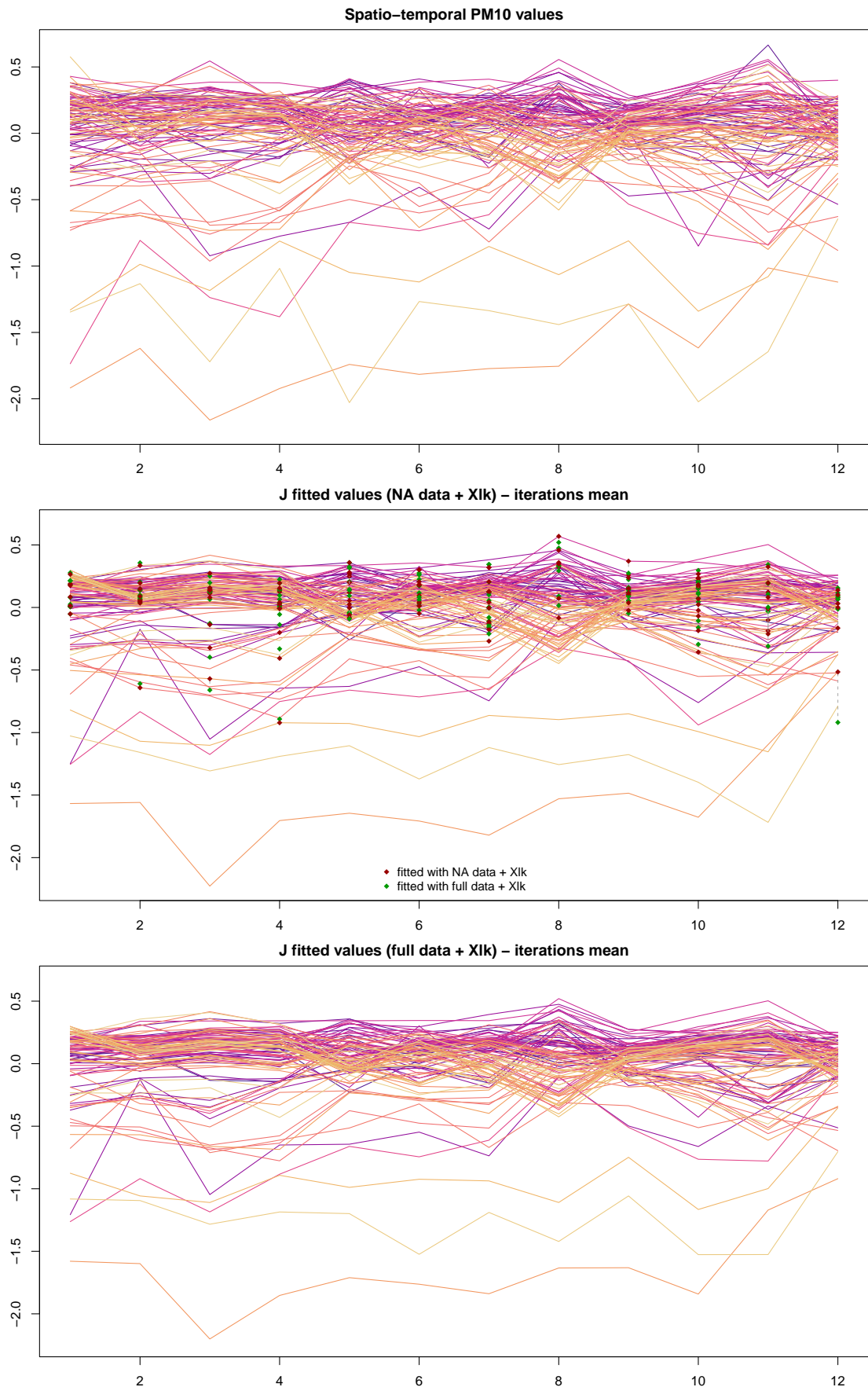


**Figure 4.18:** Target and fitted values of the JDRPM fits with target plus space values, on the NA and full dataset, to see the effects of the insertion of covariates in the likelihood.

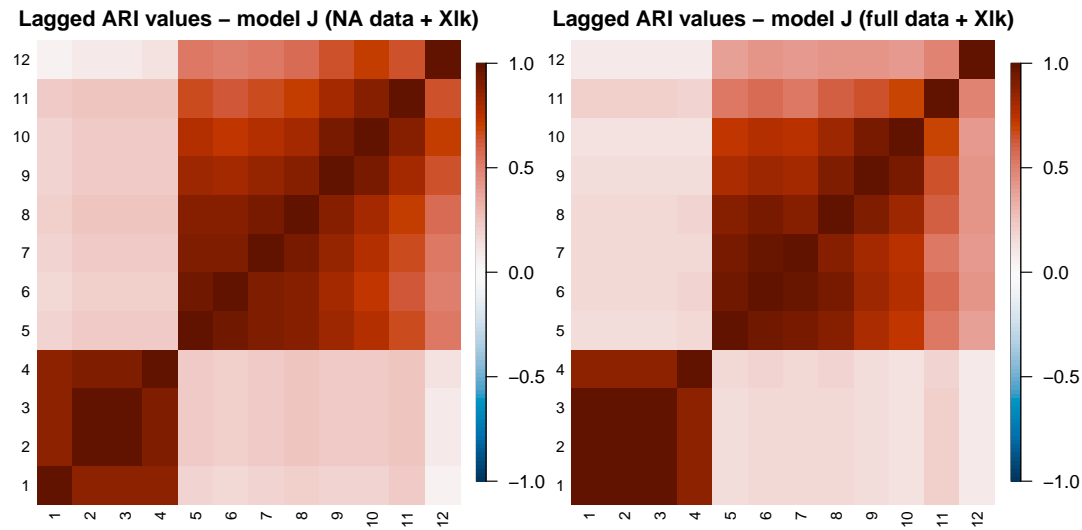


**Figure 4.19:** Lagged ARI values of the two JDRPM fits with target plus space values on the full and NA datasets, with covariates in the likelihood.

tration levels of air pollutants. Its effect is of dual: wind can disperse the pollutants away from their source, spreading them to different areas and thus locally reducing the levels, but it can also have an opposite effect, increasing the amount of contaminants in the air by resuspending the particles which were settled down on the earth surface, such as roads, soils, or buildings. This latter effect is particularly visible in dry and windy rural areas, of which Lombardy is a suitable example. The dataset offered also the wind speed at 100m, but this would be relevant for a wider analysis, where e.g. the trend of PM<sub>10</sub> concentrations are followed over multiple regions or countries. Our setup, as with the time-wise mean adjustment, was instead more focused on local and particular behaviours, on the more the ground-level perspective about Lombardy cities.

- **WE\_tot\_precipitation.** It is well known how rainwater can improve the air quality thanks to water droplets that attract aerosol particles, taking them away from the air, and bringing them to the ground. This process, known as wet deposition, precipitation, scavenging, or washout is indeed very effective in reducing the concentrations of air pollutants.
- **WE\_blh\_layer\_max.** The boundary layer height (BLH) is another relevant variable in terms of the dispersion of air contaminants. This layer defines the height at which air mixing occurs. Usually air gets colder when rising in the atmosphere; however, there could be some warm air regions on top of colder ones. At this boundary, air is not more able to mix, with the warm layer causing a sort of lid, a covering, which traps the lower cold air, with all the contaminants, below it. This reduces the quality of the air since the pollution builds up and accumulates since it has no way to disperse. This covariate, therefore, records the maximum height at which this problematic layer occurs: the lower the values, the higher we should expect the pollutants

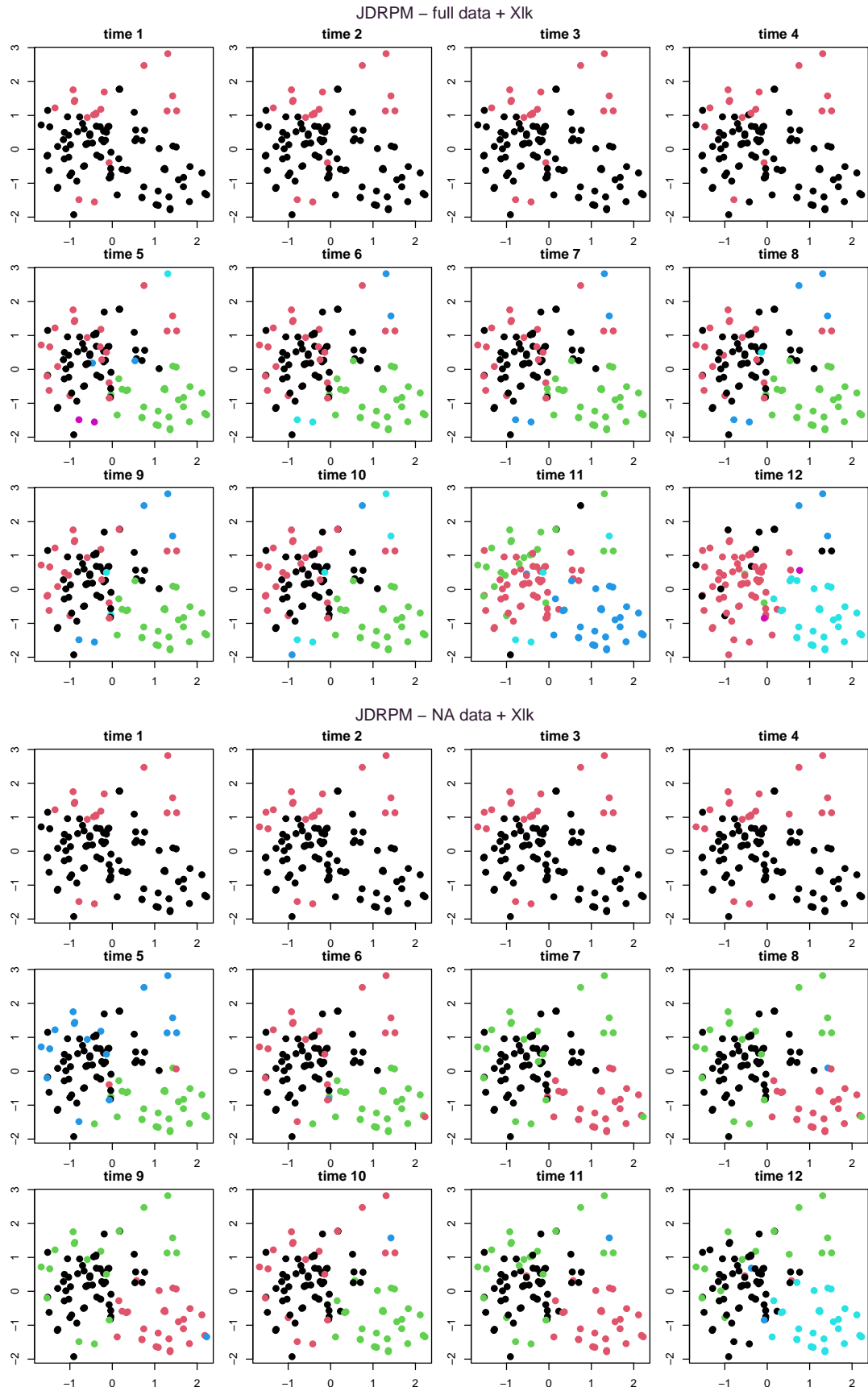


**Figure 4.20:** Clusters generated by the two JDRPM fits with target plus space values fits on the full and NA datasets, with covariates in the likelihood.

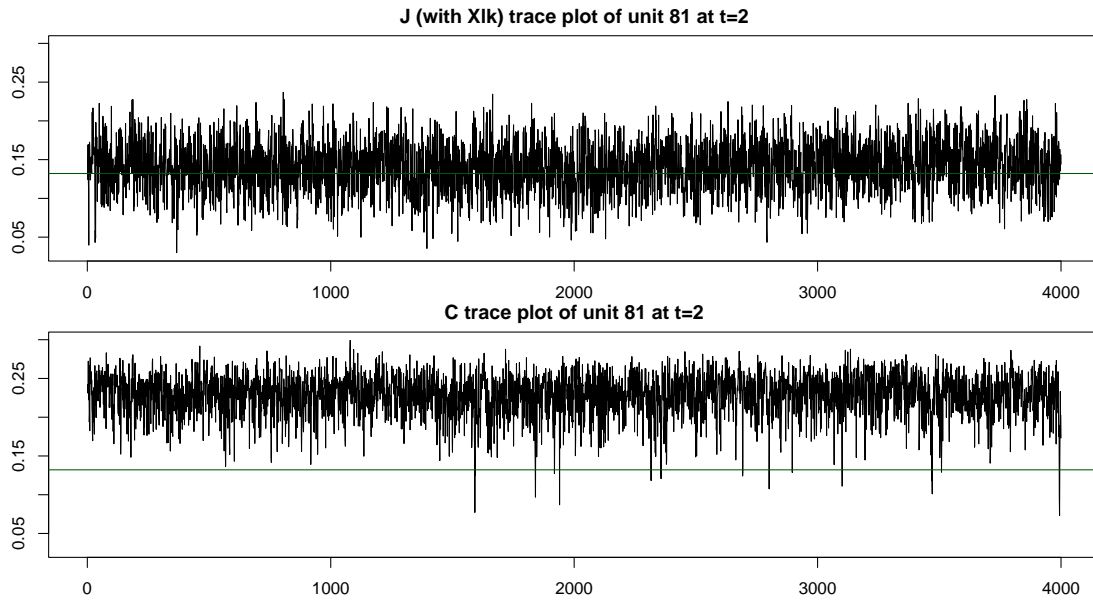


**Figure 4.21:** Example of a trace plot of the fitted values, on a problematic unit  $i$  and time instant  $t$ , comparing the JDRPM fit with covariates in the likelihood to the base (target plus space) CDRPM fit. The green line represents the true value of  $Y_{it}$ .

concentrations to be.

**Table 4.6:** Summary of the comparison between the two fits, on target plus space values, plus also the JDRPM fits including covariates in the clustering process. The MSE columns refer to the accuracy between the fitted values generated by the models (estimated by taking the mean and the median of the returned 4000 iterates) and the true values of the target variable. Higher LPML and lower WAIC indicate a better fit.

	MSE mean	MSE median	LPML	WAIC	exec. time
CDRPM	0.0142	0.0149	694.81	-1768.42	1h38m
JDRPM	0.0131	0.0138	624.91	-1898.05	<b>56m</b>
JDRPM + Xcl	<b>0.0126</b>	<b>0.0135</b>	<b>677.71</b>	<b>-1969.76</b>	1h20m

## 4.4 Scaling performances

To really assess if the goal of faster fits was reached, we setup several tests to compare the two models and the different information levels at which they could be called. The original CDRPM allowed to perform clustering using just the target values or by also including spatial information. In addition to them, the options introduced by JDRPM are the inclusion of covariates at clustering and/or likelihood levels.

Apart, of course, from the target values, all the other information levels are indeed independent: one could perform the fit ignoring space and accounting just for covariates, for example; but with an additive perspective in mind we decide to

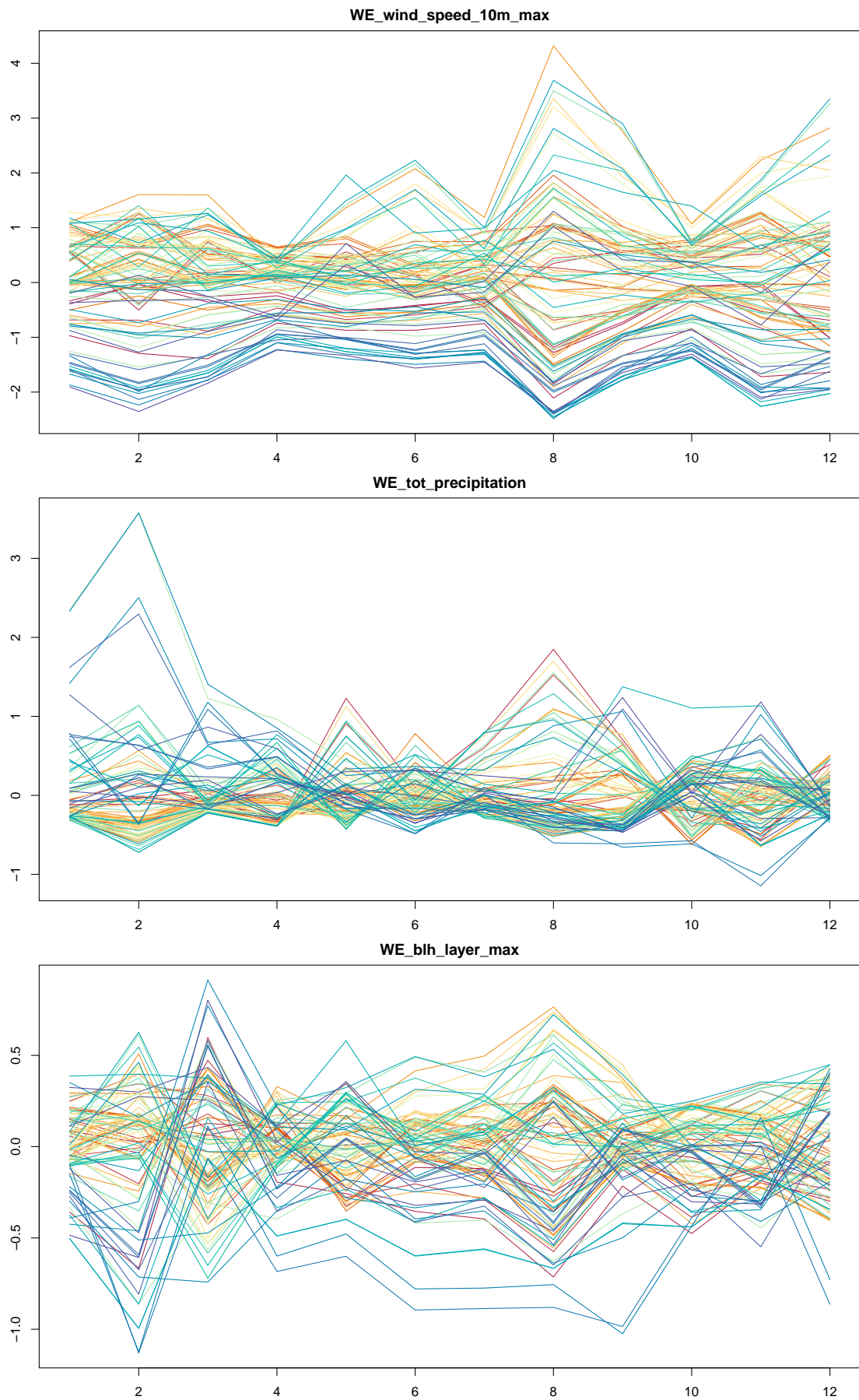


**Figure 4.22:** The three variables used to perform the test fit with covariates in the clustering. Colors are based on the ranking of PM<sub>10</sub> values of the units according to their median, from highest (red) to lowest (blue).

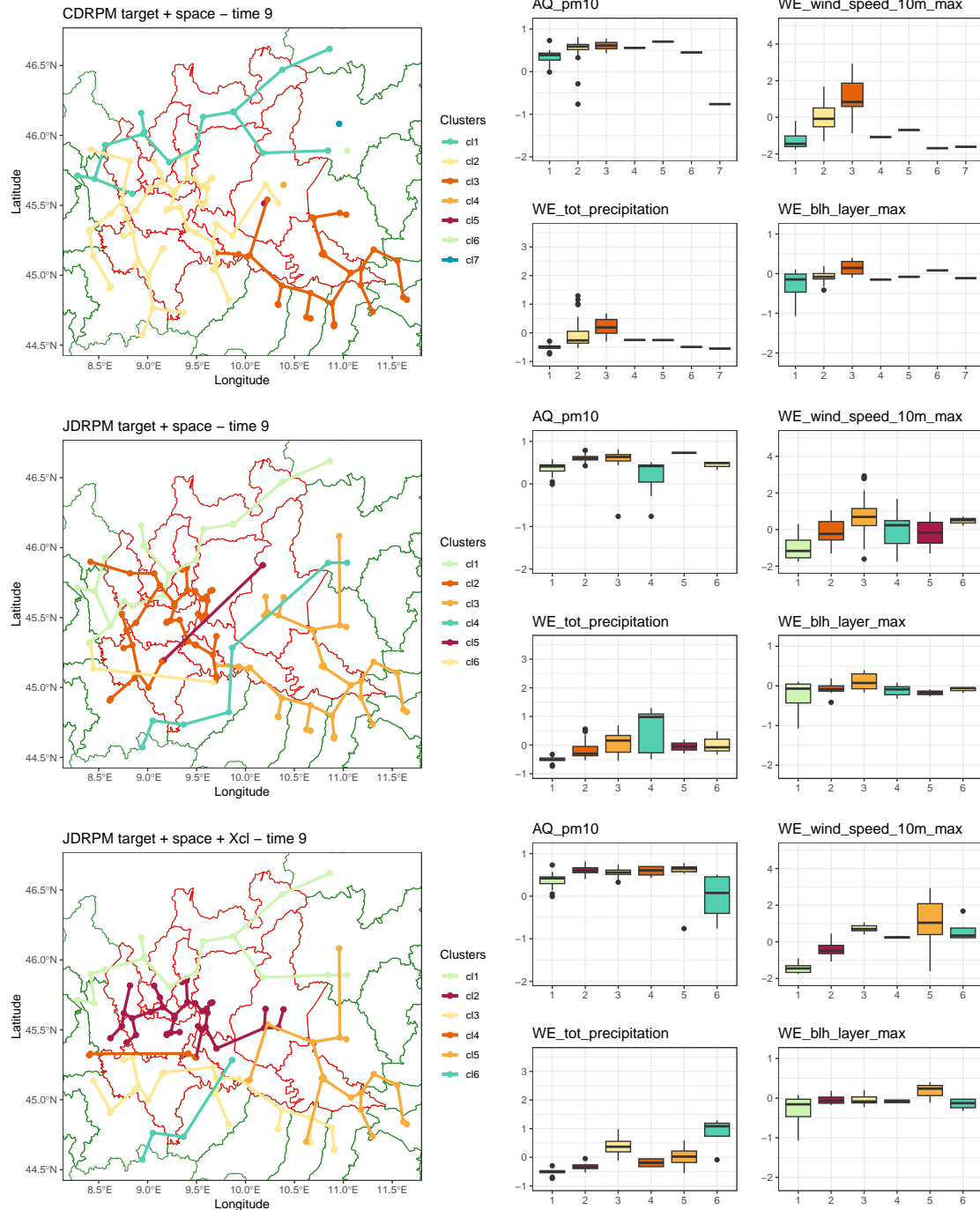


Figure 4.23: Enter Caption

perform incremental tests, adding new layers on top of the base ones. Therefore, in what follows, we will see comparisons of fits using just the target values, then those plus space, then those two plus covariates in the clustering, and finally all those plus covariates in the likelihood.

As it appeared from Section 3, the Julia implementation seemed to be a little more eager for memory than the C one. This meant that when we ran the larger tests my system could have ran out of RAM memory, resulting in some data needing

to be stored in the slower swap space on the disk, and therefore losing performance. However, on newer or just more technical-oriented machines than my simple laptop, this memory limitation should not be an issue.

Accounting all this, in what follows we should consider really accurate just the intermediate-values tests, i.e. the ones with  $n$  or  $T$  being 10, 50 or 100, and take with a pinch of salt the extreme one of 250, for which my laptop hardware limitations<sup>1</sup> could have concealed the true accurate results. Nonetheless, the analysis is really encouraging for the JDRPM model.

The tests were conducted on randomly generated values, according to  $n$  and  $T$ , for the target data  $Y_{it}$  and the spatial coordinates  $\mathbf{s}_i$ . In this way, we produced a sort of “mesh” of possible fitting parameters, ranging from small number of units and time horizons to larger ones. To record the expected execution time per iteration of each case we ran each fit with a number of iterations inversely proportional to the size of the test, e.g. 10000 iterations for the case  $(n, T) = (10, 10)$  and 16 iterations for  $(n, T) = (250, 250)$ . This ensured that each fit lasted approximately the same time. Each fit was ran four times, to then save the minimum time observed during those multiple runs. Such practice, common in benchmarking, helps to eliminate bias from the results due to the system computational demands and fluctuations, filtering in this way just the “ideal” execution time in which all the system performance are devoted to that task.

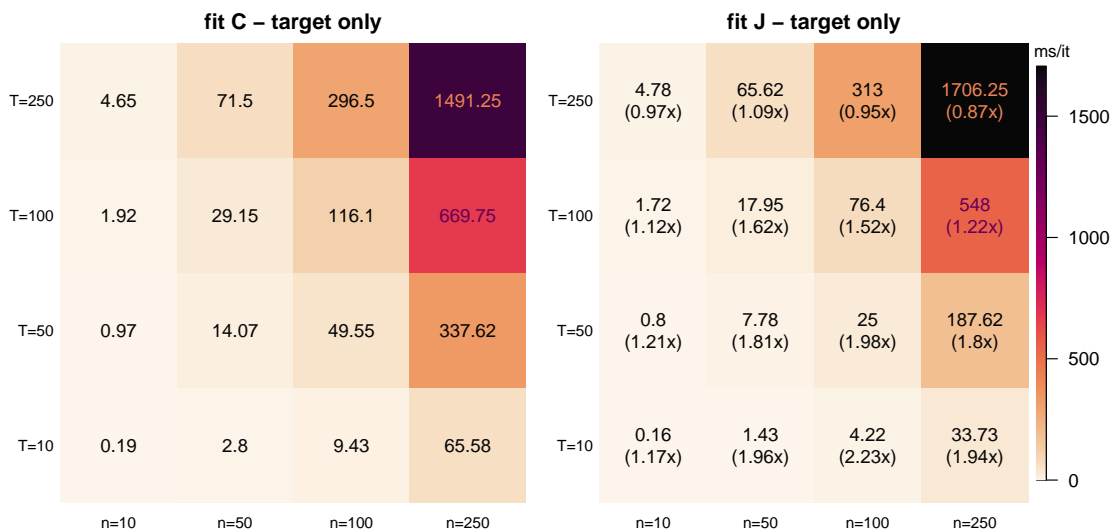


**Figure 4.24:** Execution times, measured in milliseconds per iteration, when fitting the models using just the target values to generate the clusters. On the JDRPM plot (on the right), in brackets, are reported the speedups relative to the CDRPM timings (on the left), where higher values indicate better performance.

From Figure 4.24 we can see how the basic fit, with just the target values, perform very quickly in Julia, with peaks even around a 2x speedup. Similar improvements appeared in the case of fits including also the spatial information, as

<sup>1</sup>all the tests and performances evaluations reported in this Chapter were performed on my laptop which has 8 GB of RAM and 1.80 GHz CPU base clock speed.

Figure 4.25 shows. Therefore, especially looking at the more reliable non-extreme tests, we can confidently claim that the JDRPM implementation is faster than the CDRPM one.

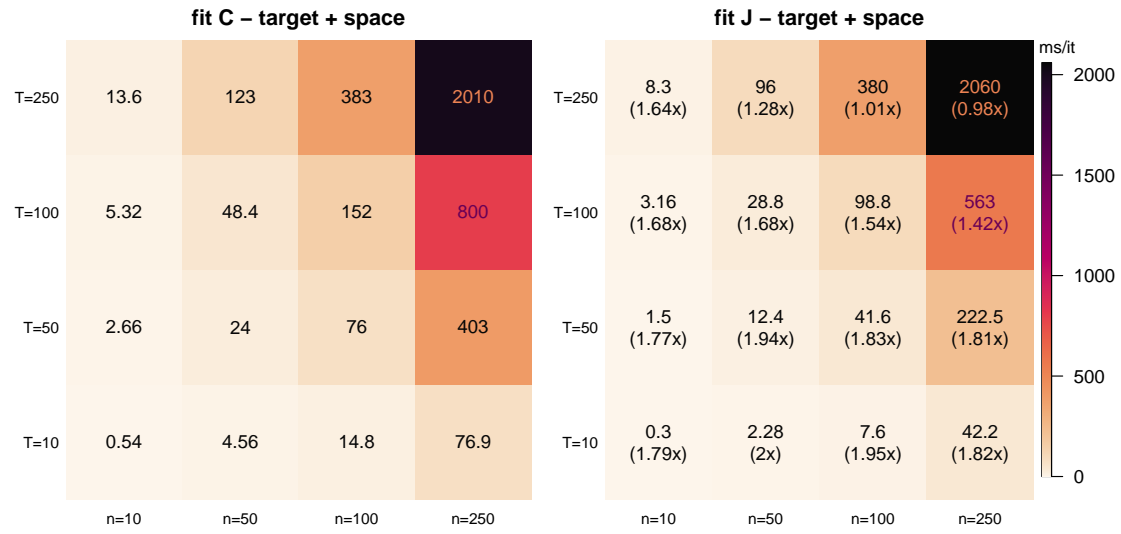


**Figure 4.25:** Execution times, measured in milliseconds per iteration, when fitting the models using the target values plus the spatial information to generate the clusters. On the JDRPM plot (on the right), in brackets, are reported the speedups relative to the CDRPM timings (on the left), where higher values indicate better performance.

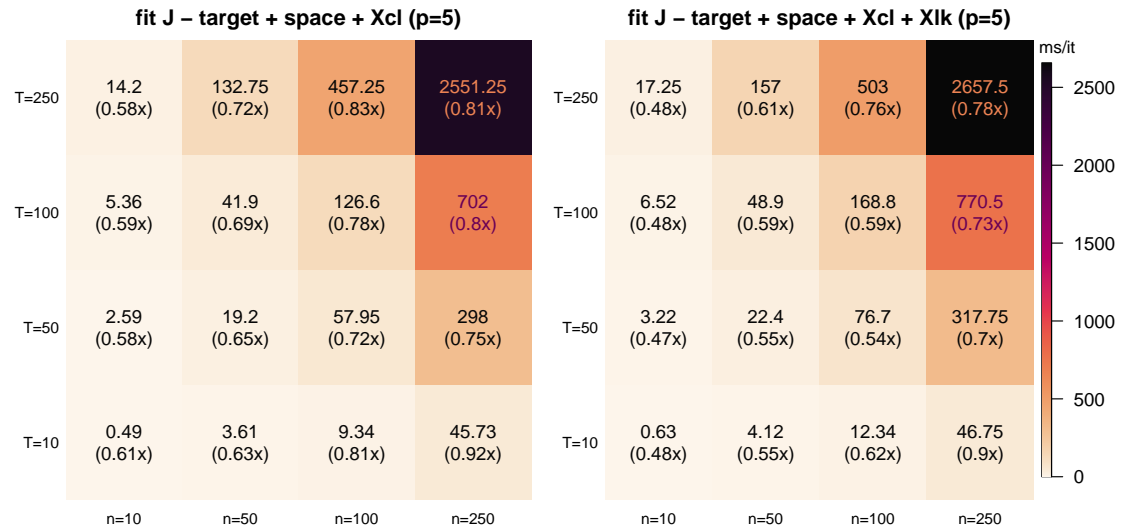


**Figure 4.26:** Execution times, measured in milliseconds per iteration, when fitting the JDRPM model using target values, spatial information, covariates in the clustering level (left), and covariates in both clustering and likelihood levels (right). In brackets are reported the speedups relative to the JDRPM timings of the fitting with target and space, with higher values still indicating better performance.

Regarding fits with covariates, we also generated them randomly by creating matrices of dimensions  $n \times p \times T$ . For these tests, we avoided to treat different values of  $p$ : the previous figures summarizing the fits up to spatial information

were in fact projection of 3d information ( $n$ ,  $T$ , and execution time), while if we extended the mesh to also account for  $p$ , the number of covariates, we would have ended up with 4d information, or even 5d if we considered separately clustering and likelihood covariates. Therefore, to keep things tidy and understandable, we just fixed  $p = 5$  for both cases.

Figure 4.26 shows how fits including covariates saw a drop of performance, which was inevitable due to the additional work to perform, but they still remain at a good performance level. Indeed, Figure 4.27 will point out how some of the fits with all information levels in Julia were actually faster than the basic fits in C.

We can also notice how with larger fits the performance drop reduces to just around 0.8x, rather than the 0.6x of the small cases: this indicates that on fits with heavy  $n$  and  $T$  the bottleneck is no more the algorithm complexity, meaning the choice of which information levels to include in the clusters generation, but rather the available hardware resources.

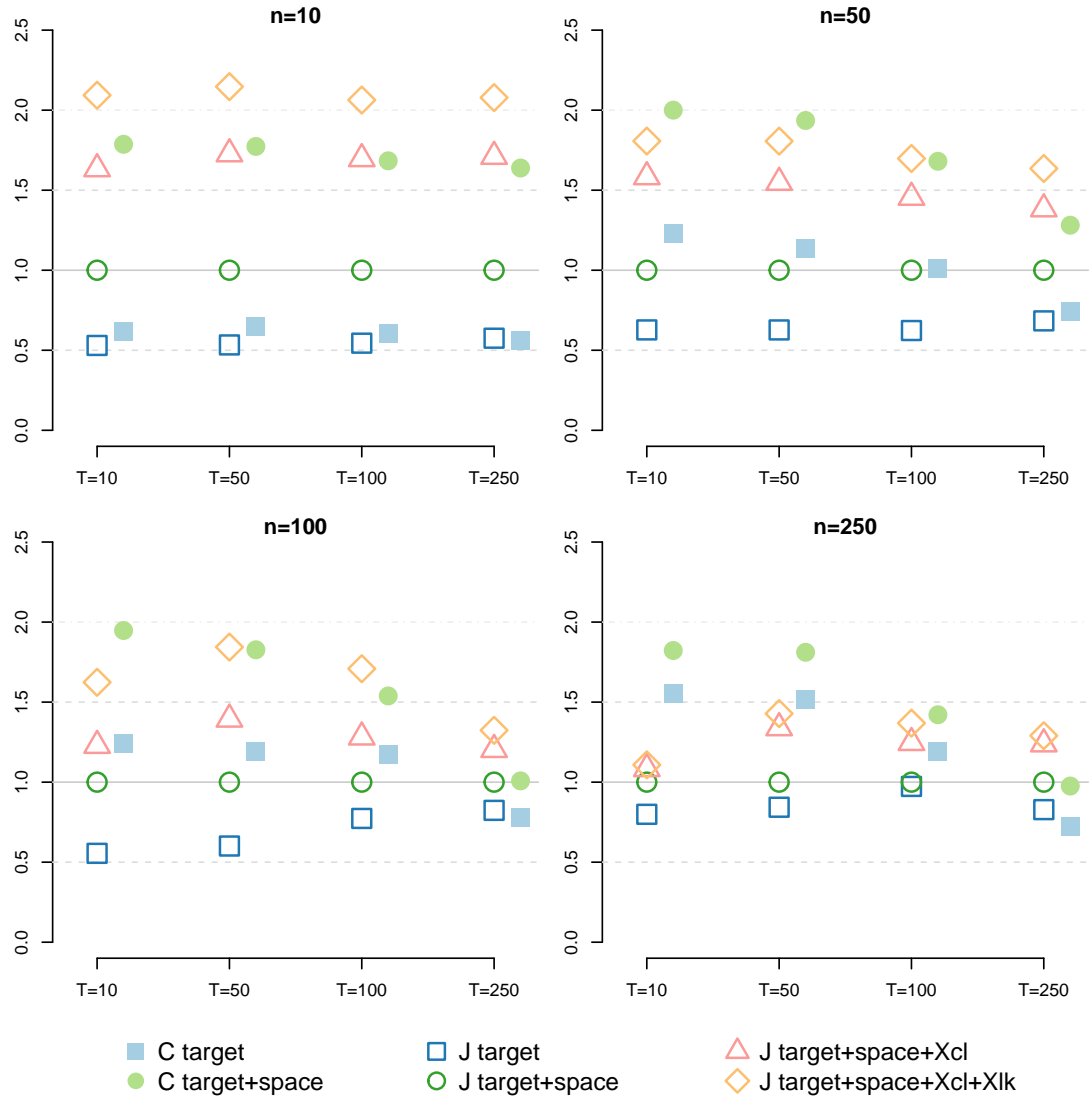


**Figure 4.27:** Visual representation of the performance of all the fits, for all the  $n$  and  $T$  cases, relatively to the JDRPM fit using target values and spatial information. Namely, the execution time per iteration metric of that fit has been taken as a reference, to which then all other fits have been compared to derive their speedup (or slowdown) factor. Points above the reference line indicate slower fits, while points below denote faster fits.



# Chapter 5

## Conclusion

*And what in human reckoning seems still afar off,  
may by the Divine ordinance be close at hand, on the  
eve of its appearance. And so be it, so be it!*

— Fëdor Dostoevskij, *Brothers Karamazov*

In the end, we can confidently assert that the JDRPM model is a valid improvement of the original DRPM formulation.

From a theoretical point of view, it offers the same base structure, just with the addition of a possible regression term in the likelihood, while also enhancing the quality of the sampled values of the parameters by having changed the laws of the variances from  $\mathcal{U}$  to invGamma. In fact, this choice recovers conjugacy in the model and therefore improves the mixing of the chain during the fitting of the model. And, of course, the insertion of covariates in the clustering should provide even more accurate results in the generation of the partitions with respect to only having the spatio-temporal information layers.

A possible drawback, inevitable with the increased model complexity, could be the tuning of the parameters, for example in the cohesions and similarities function to find the right balance between the different contributes of the information levels. However, in this regards, an hopefully helpful analysis was conducted in Chapter 2, where the effects of the tuning parameters for all cohesions and similarities have been explored. Moreover, the Julia `MCMC_fit` function provides an optional argument `cv_weight`, defaulted to 1, which can be used to scale up (or down) the contribute of the covariates similarities, e.g. to make them closer to the interval of values to which the spatial cohesions values belong.

This higher complexity appeared also in the tuning of the  $\text{invGamma}(a, b)$  parameters, which are indeed more delicate than a simple  $\mathcal{U}(l, u)$ . To this end, a possible solution could be to run an initial fit with the original CDRPM model, to see where the values of the variances tend to gather, and according to that fixing the invGamma parameters. For example, in the spatio-temporal tests of Section 4.1.2 we saw, from the CDRPM fits, very low values for the variances parameters, and as such we assigned, for  $\lambda^2$  and  $\tau_t^2$  parameters in the JDRPM model, an  $\text{invGamma}(a =$

$1.9, b = 0.4$ ), which has 90% of his density in the interval  $[0.109151, 1.58222]$ . The more relevant  $\sigma_{jt}^{2*}$  parameter had also pretty low values, however on that we attached a more uninformative prior of  $\text{invGamma}(a = 0.01, b = 0.01)$ , which despite being not always suggested [Gel04] turned out to be fine and very precise, relatively to the sampled “reference” values of CDRPM. An alternative solution, probably less theoretically appealing but possibly effective, could be to truncate the  $\text{invGamma}$  laws to a certain region in order to avoid sampling extremely high values, which can happen when uninformative priors get not properly adjusted by the data, and to resemble more the density of a  $\mathcal{U}$  random variable. This choice can be seamlessly implemented in the Julia code by e.g. swapping `rand(InverseGamma(a,b))` to `rand(truncated(InverseGamma(a,b),l,u))`, with  $l$  and  $u$  being the lower and upper bounds of the designed truncation interval.

From a computational point of view, the goal of faster fits was also reached, reducing the execution times up to a factor of two with respect to the original implementation. This at the cost of a small increase in the memory requirements which however, nowadays, is not a big deal.

A final drawback can be the time needed to convert back the results from Julia to R, since the `juliaGet` function from the `JuliaConnectoR` package can take up to some minutes, especially in fits where lots of iterations are saved. In any case, this latency becomes quite negligible with respect to the time saved from the previous implementation on the DRPM package.

Regarding some possible further improvements, from the theoretical point of view we can also consider satisfied. The complexity of the original DRPM model was already kind of daunting, and the improvements brought by the JDRPM update surely haven’t reduced it, considering all the parameters present in the model and especially the ones regulating the spatial cohesions and covariate similarities, which strongly determine the final clusters. Therefore, with this complexity in mind, some room for improvements is easily available in improving the usability of this model. To this end, the current JDRPM implementation has already some basic logging features, where some steps of the computations can be saved to a text file and analysed afterwards, but further profiling and monitoring tools could also be implemented, particularly considering the flexible possibilities offered by Julia. For example, some heuristics or suggestions about how to initialize the parameters according to the dataset at hand, or automatic online tuning of the parameters with the progression of iterations. Additionally, visualization tools could be also comfortably implemented trough the extensive plotting ecosystem of Julia, e.g. to return trace plots directly with the execution, live-monitoring the distribution of the sampled parameters, and so on.

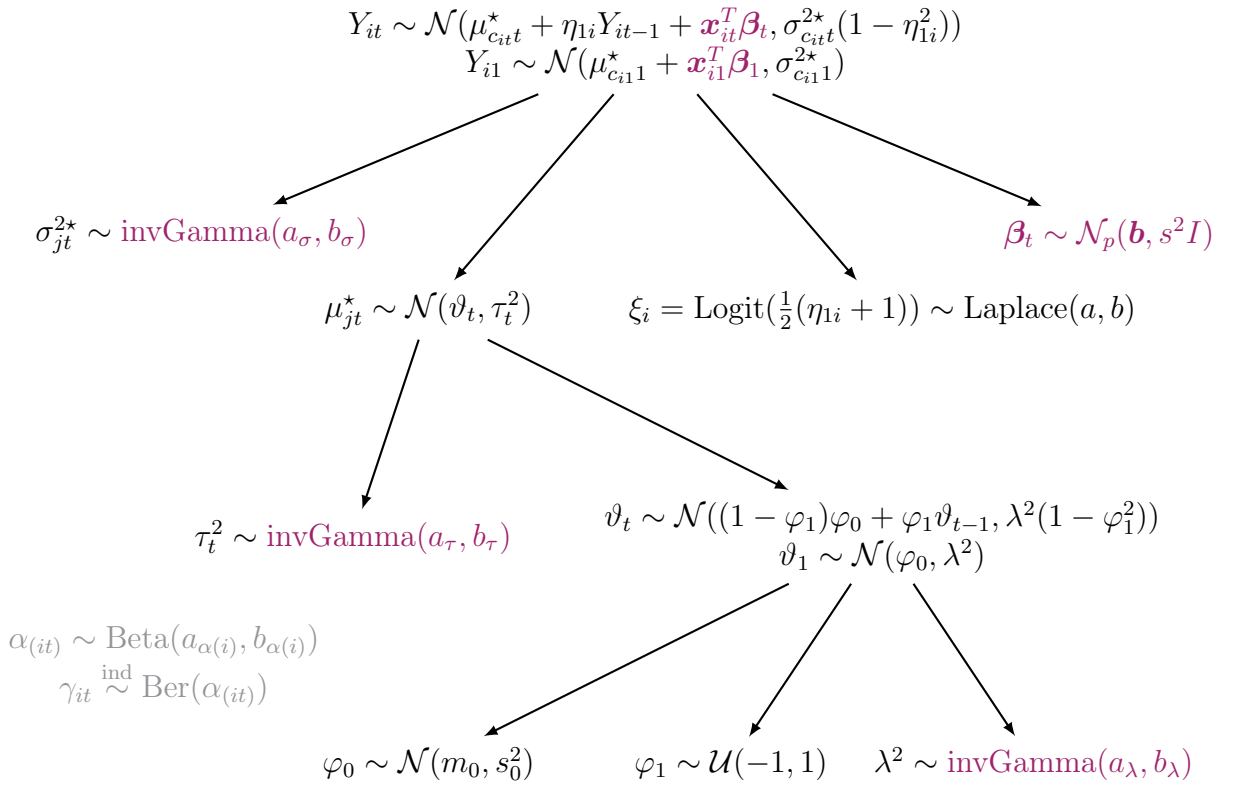
Moreover, considering the advancement in performance, a setup with multiple chains ran in parallel, as most of the lighter bayesian models do, could be introduced. Possible further speedup could also be obtained integrating the GPU, if available, to release some load from the CPU. Needless to say, the road is already paved to perform such integration trough the various packages under the `JuliaGPU` collection.

# Appendix A

## Theoretical details

### A.1 Extended computations of the full conditionals

We propose here the extended computations which allowed to extract the full conditionals presented in Chapter 2. We report also the model graph to make it quickly accessible as a reference for the laws involved in the following computations.



- update  $\sigma_{jt}^{2*}$

for  $t = 1$ :

$$f(\sigma_{jt}^{2*} | -) \propto f(\sigma_{jt}^{2*}) f(\{Y_{it} : c_{it} = j\} | \sigma_{jt}^{2*}, -)$$

$$\begin{aligned}
&= \mathcal{L}_{\text{invGamma}(a_\sigma, b_\sigma)}(\sigma_{jt}^{2\star}) \prod_{i \in S_{jt}} \mathcal{L}_{\mathcal{N}(\mu_{c_{it}t}^* + \mathbf{x}_{it}^T \boldsymbol{\beta}_t, \sigma_{c_{it}1}^{2\star})}(Y_{it}) \\
&\propto \left[ \left( \frac{1}{\sigma_{jt}^{2\star}} \right)^{a_\sigma+1} \exp \left\{ -\frac{1}{\sigma_{jt}^{2\star}} b \right\} \right] \\
&\quad \cdot \left[ \prod_{i \in S_{jt}} \left( \frac{1}{\sigma_{jt}^{2\star}} \right)^{1/2} \exp \left\{ -\frac{1}{2\sigma_{jt}^{2\star}} (Y_{it} - \mu_{jt}^* - \mathbf{x}_{it}^T \boldsymbol{\beta}_t)^2 \right\} \right] \\
&\propto \left( \frac{1}{\sigma_{jt}^{2\star}} \right)^{(a_\sigma+|S_{jt}|/2)+1} \exp \left\{ -\frac{1}{\sigma_{jt}^{2\star}} \left( b_\sigma + \frac{1}{2} \sum_{i \in S_{jt}} (Y_{it} - \mu_{jt}^* - \mathbf{x}_{it}^T \boldsymbol{\beta}_t)^2 \right) \right\} \\
\implies f(\sigma_{jt}^{2\star} | -) &\propto \text{kernel of a } \text{invGamma}(a_{\sigma(\text{post})}, b_{\sigma(\text{post})}) \text{ with} \\
a_{\tau(\text{post})} &= a_\sigma + \frac{|S_{jt}|}{2} \\
b_{\tau(\text{post})} &= b_\sigma + \frac{1}{2} \sum_{i \in S_{jt}} (Y_{it} - \mu_{jt}^* - \mathbf{x}_{it}^T \boldsymbol{\beta}_t)^2
\end{aligned} \tag{A.1}$$

for  $t > 1$ :

$$\begin{aligned}
f(\sigma_{jt}^{2\star} | -) &\propto f(\sigma_{jt}^{2\star}) f(\{Y_{it} : c_{it} = j\} | \sigma_{jt}^{2\star}, -) \\
&= \mathcal{L}_{\text{invGamma}(a_\sigma, b_\sigma)}(\sigma_{jt}^{2\star}) \prod_{i \in S_{jt}} \mathcal{L}_{\mathcal{N}(\mu_{c_{it}t}^* + \eta_{1i} Y_{it-1} + \mathbf{x}_{it}^T \boldsymbol{\beta}_t, \sigma_{c_{it}1}^{2\star})}(Y_{it}) \\
&\propto \left[ \left( \frac{1}{\sigma_{jt}^{2\star}} \right)^{a_\sigma+1} \exp \left\{ -\frac{1}{\sigma_{jt}^{2\star}} b \right\} \right] \\
&\quad \cdot \left[ \prod_{i \in S_{jt}} \left( \frac{1}{\sigma_{jt}^{2\star}} \right)^{1/2} \exp \left\{ -\frac{1}{2\sigma_{jt}^{2\star}} (Y_{it} - \mu_{jt}^* - \eta_{1i} Y_{it-1} - \mathbf{x}_{it}^T \boldsymbol{\beta}_t)^2 \right\} \right] \\
&\propto \left( \frac{1}{\sigma_{jt}^{2\star}} \right)^{(a_\sigma+|S_{jt}|/2)+1} \\
&\quad \cdot \exp \left\{ -\frac{1}{\sigma_{jt}^{2\star}} \left( b_\sigma + \frac{1}{2} \sum_{i \in S_{jt}} (Y_{it} - \eta_{1i} Y_{it-1} - \mu_{jt}^* - \mathbf{x}_{it}^T \boldsymbol{\beta}_t)^2 \right) \right\} \\
\implies f(\sigma_{jt}^{2\star} | -) &\propto \text{kernel of a } \text{invGamma}(a_{\sigma(\text{post})}, b_{\sigma(\text{post})}) \text{ with} \\
a_{\tau(\text{post})} &= a_\sigma + \frac{|S_{jt}|}{2} \\
b_{\tau(\text{post})} &= b_\sigma + \frac{1}{2} \sum_{i \in S_{jt}} (Y_{it} - \mu_{jt}^* - \eta_{1i} Y_{it-1} - \mathbf{x}_{it}^T \boldsymbol{\beta}_t)^2
\end{aligned} \tag{A.2}$$

- update  $\mu_{jt}^*$

for  $t = 1$ :

$$f(\mu_{jt}^* | -) \propto f(\mu_{jt}^*) f(\{Y_{it} : c_{it} = j\} | \mu_{jt}^*, -)$$

$$\begin{aligned}
&= \mathcal{L}_{\mathcal{N}(\vartheta_t, \tau_t^2)}(\mu_{jt}^*) \prod_{i \in S_{jt}} \mathcal{L}_{\mathcal{N}(\mu_{c_{it}t}^* + \mathbf{x}_{it}^T \boldsymbol{\beta}_t, \sigma_{c_{it}t}^{2*})}(Y_{it}) \\
&\propto \exp \left\{ -\frac{1}{2\tau_t^2} (\mu_{jt}^* - \vartheta_t)^2 \right\} \exp \left\{ -\frac{1}{2\sigma_{jt}^{2*}} \left( \sum_{i \in S_{jt}} (\mu_{jt}^* - (Y_{i1} - \mathbf{x}_{it}^T \boldsymbol{\beta}_t))^2 \right) \right\} \\
&\propto \exp \left\{ -\frac{1}{2\tau_t^2} (\mu_{jt}^* - \vartheta_t)^2 \right\} \exp \left\{ -\frac{|S_{jt}|}{2\sigma_{jt}^{2*}} \left( \mu_{jt}^* - \frac{\text{SUM}_y}{|S_{jt}|} \right)^2 \right\} \\
&\text{where } \text{SUM}_y = \sum_{i \in S_{jt}} Y_{i1} - \mathbf{x}_{it}^T \boldsymbol{\beta}_t \\
\implies f(\mu_{jt}^* | -) &\propto \text{kernel of a } \mathcal{N}(\mu_{\mu_{jt}^*(\text{post})}, \sigma_{\mu_{jt}^*(\text{post})}^2) \text{ with} \\
\sigma_{\mu_{jt}^*(\text{post})}^2 &= \frac{1}{\frac{1}{\tau_t^2} + \frac{|S_{jt}|}{\sigma_{jt}^{2*}}} \\
\mu_{\mu_{jt}^*(\text{post})} &= \sigma_{\mu_{jt}^*(\text{post})}^2 \left( \frac{\vartheta_t}{\tau_t^2} + \frac{\text{SUM}_y}{\sigma_{jt}^{2*}} \right) \tag{A.3}
\end{aligned}$$

for  $t > 1$ :

$$\begin{aligned}
f(\mu_{jt}^* | -) &\propto f(\mu_{jt}^*) f(\{Y_{it} : c_{it} = j\} | \mu_{jt}^*, -) \\
&= \mathcal{L}_{\mathcal{N}(\vartheta_1, \tau_t^2)}(\mu_{jt}^*) \prod_{i \in S_{jt}} \mathcal{L}_{\mathcal{N}(\mu_{c_{it}t}^* + \eta_{1i} Y_{it-1} + \mathbf{x}_{it}^T \boldsymbol{\beta}_t, \sigma_{c_{it}t}^{2*})}(Y_{it}) \\
&\propto \exp \left\{ -\frac{1}{2\tau_t^2} (\mu_{jt}^* - \vartheta_t)^2 \right\} \\
&\cdot \exp \left\{ -\frac{1}{2\sigma_{jt}^{2*}} \left( \sum_{i \in S_{jt}} \frac{1}{1 - \eta_{1i}^2} (\mu_{jt}^* - (Y_{it} - \eta_{1i} Y_{i,t-1} - \mathbf{x}_{it}^T \boldsymbol{\beta}_t))^2 \right) \right\} \\
&\propto \exp \left\{ -\frac{1}{2\tau_t^2} (\mu_{jt}^* - \vartheta_t)^2 \right\} \exp \left\{ -\frac{\text{SUM}_{e2}}{2\sigma_{jt}^{2*}} \left( \mu_{jt}^* - \frac{\text{SUM}_y}{\text{SUM}_{e2}} \right)^2 \right\} \\
&\text{where } \text{SUM}_y = \sum_{i \in S_{jt}} \frac{Y_{it} - \eta_{1i} Y_{i,t-1} - \mathbf{x}_{it}^T \boldsymbol{\beta}_t}{1 - \eta_{1i}^2}, \text{SUM}_{e2} = \sum_{i \in S_{jt}} \frac{1}{1 - \eta_{1i}^2} \\
\implies f(\mu_{jt}^* | -) &\propto \text{kernel of a } \mathcal{N}(\mu_{\mu_{jt}^*(\text{post})}, \sigma_{\mu_{jt}^*(\text{post})}^2) \text{ with} \\
\sigma_{\mu_{jt}^*(\text{post})}^2 &= \frac{1}{\frac{1}{\tau_t^2} + \frac{\text{SUM}_{e2}}{\sigma_{jt}^{2*}}} \\
\mu_{\mu_{jt}^*(\text{post})} &= \sigma_{\mu_{jt}^*(\text{post})}^2 \left( \frac{\vartheta_t}{\tau_t^2} + \frac{\text{SUM}_y}{\sigma_{jt}^{2*}} \right) \tag{A.4}
\end{aligned}$$

- update  $\boldsymbol{\beta}_t$

for  $t = 1$ :

$$\begin{aligned}
f(\boldsymbol{\beta}_t | -) &\propto f(\boldsymbol{\beta}_t) f(\{Y_{1t}, \dots, Y_{nt}\} | \boldsymbol{\beta}_t, -) \\
&= \mathcal{L}_{\mathcal{N}(\mathbf{b}, s^2 I)}(\boldsymbol{\beta}_t) \prod_{i=1}^n \mathcal{L}_{\mathcal{N}(\mu_{c_{it}t}^* + \mathbf{x}_{it}^T \boldsymbol{\beta}_t, \sigma_{c_{it}t}^{2*})}(Y_{it})
\end{aligned}$$

$$\begin{aligned}
& \propto \exp \left\{ -\frac{1}{2} \left[ (\boldsymbol{\beta}_t^T - \mathbf{b})^T \frac{1}{s^2} (\boldsymbol{\beta}_t - \mathbf{b}) \right] \right\} \\
& \quad \cdot \exp \left\{ -\frac{1}{2} \sum_{i=1}^n (Y_{it} - \mu_{c_{it}t}^* - \mathbf{x}_{it}^T \boldsymbol{\beta}_t)^2 \right\} \\
& \propto \exp \left\{ -\frac{1}{2} \left[ \boldsymbol{\beta}_t^T \left( \frac{1}{s^2} I + \sum_{i=1}^n \frac{\mathbf{x}_{it} \mathbf{x}_{it}^T}{\sigma_{c_{it}t}^{2*}} \right) \boldsymbol{\beta}_t \right. \right. \\
& \quad \left. \left. - 2 \left( \frac{\mathbf{b}}{s^2} + \sum_{i=1}^n \frac{(Y_{it} - \mu_{c_{it}t}^*) \mathbf{x}_{it}}{\sigma_{c_{it}t}^{2*}} \right) \cdot \boldsymbol{\beta}_t \right] \right\} \\
\implies f(\boldsymbol{\beta}_t | -) & \propto \text{kernel of a } \mathcal{N}(\mathbf{b}_{(\text{post})}, A_{(\text{post})}) \text{ with} \\
A_{(\text{post})} & = \left( \frac{1}{s^2} I + \sum_{i=1}^n \frac{\mathbf{x}_{it} \mathbf{x}_{it}^T}{\sigma_{c_{it}t}^{2*}} \right)^{-1} \\
\mathbf{b}_{(\text{post})} & = A_{(\text{post})} \left( \frac{\mathbf{b}}{s^2} + \sum_{i=1}^n \frac{(Y_{it} - \mu_{c_{it}t}^*) \mathbf{x}_{it}}{\sigma_{c_{it}t}^{2*}} \right) \\
\iff f(\boldsymbol{\beta}_t | -) & \propto \text{kernel of a } \mathcal{N}_{\text{Canon}}(\mathbf{h}_{(\text{post})}, J_{(\text{post})}) \text{ with} \\
\mathbf{h}_{(\text{post})} & = \left( \frac{\mathbf{b}}{s^2} + \sum_{i=1}^n \frac{(Y_{it} - \mu_{c_{it}t}^*) \mathbf{x}_{it}}{\sigma_{c_{it}t}^{2*}} \right) \\
J_{(\text{post})} & = \left( \frac{1}{s^2} I + \sum_{i=1}^n \frac{\mathbf{x}_{it} \mathbf{x}_{it}^T}{\sigma_{c_{it}t}^{2*}} \right) \tag{A.5}
\end{aligned}$$

for  $t > 1$ :

$$\begin{aligned}
f(\boldsymbol{\beta}_t | -) & \propto f(\boldsymbol{\beta}_t) f(\{Y_{1t}, \dots, Y_{nt}\} | \boldsymbol{\beta}_t, -) \\
& = \mathcal{L}_{\mathcal{N}(\mathbf{b}, s^2 I)}(\boldsymbol{\beta}_t) \prod_{i=1}^n \mathcal{L}_{\mathcal{N}(\mu_{c_{it}t}^* + \eta_{1i} Y_{it-1} + \mathbf{x}_{it}^T \boldsymbol{\beta}_t, \sigma_{c_{it}t}^{2*})}(Y_{it}) \\
& \propto \exp \left\{ -\frac{1}{2} \left[ (\boldsymbol{\beta}_t^T - \mathbf{b})^T \frac{1}{s^2} (\boldsymbol{\beta}_t - \mathbf{b}) \right] \right\} \\
& \quad \cdot \exp \left\{ -\frac{1}{2} \sum_{i=1}^n (Y_{it} - \mu_{c_{it}t}^* - \eta_{1i} Y_{it-1} - \mathbf{x}_{it}^T \boldsymbol{\beta}_t)^2 \right\} \\
& \propto \exp \left\{ -\frac{1}{2} \left[ \boldsymbol{\beta}_t^T \left( \frac{1}{s^2} I + \sum_{i=1}^n \frac{\mathbf{x}_{it} \mathbf{x}_{it}^T}{\sigma_{c_{it}t}^{2*}} \right) \boldsymbol{\beta}_t \right. \right. \\
& \quad \left. \left. - 2 \left( \frac{\mathbf{b}}{s^2} + \sum_{i=1}^n \frac{(Y_{it} - \mu_{c_{it}t}^* - \eta_{1i} Y_{it-1}) \mathbf{x}_{it}}{\sigma_{c_{it}t}^{2*}} \right) \cdot \boldsymbol{\beta}_t \right] \right\}
\end{aligned}$$

$\implies f(\boldsymbol{\beta}_t | -) \propto \text{kernel of a } \mathcal{N}(\mathbf{b}_{(\text{post})}, A_{(\text{post})}) \text{ with}$

$$\begin{aligned}
A_{(\text{post})} & = \left( \frac{1}{s^2} I + \sum_{i=1}^n \frac{\mathbf{x}_{it} \mathbf{x}_{it}^T}{\sigma_{c_{it}t}^{2*}} \right)^{-1} \\
\mathbf{b}_{(\text{post})} & = A_{(\text{post})} \left( \frac{\mathbf{b}}{s^2} + \sum_{i=1}^n \frac{(Y_{it} - \mu_{c_{it}t}^* - \eta_{1i} Y_{it-1}) \mathbf{x}_{it}}{\sigma_{c_{it}t}^{2*}} \right)
\end{aligned}$$

$$\iff f(\beta_t | -) \propto \text{kernel of a } \mathcal{N}\text{Canon}(\mathbf{h}_{(\text{post})}, J_{(\text{post})}) \text{ with}$$

$$\begin{aligned} \mathbf{h}_{(\text{post})} &= \left( \frac{\mathbf{b}}{s^2} + \sum_{i=1}^n \frac{(Y_{it} - \mu_{c_{it}t}^* - \eta_{1i} Y_{it-1}) \mathbf{x}_{it}}{\sigma_{c_{it}t}^{2*}} \right) \\ J_{(\text{post})} &= \left( \frac{1}{s^2} I + \sum_{i=1}^n \frac{\mathbf{x}_{it} \mathbf{x}_{it}^T}{\sigma_{c_{it}t}^{2*}} \right) \end{aligned} \quad (\text{A.6})$$

- update  $\tau_t^2$

$$\begin{aligned} f(\tau_t^2 | -) &\propto f(\tau_t^2) f((\mu_{1t}^*, \dots, \mu_{k_t t}^*) | \tau_t^2, -) \\ &= \mathcal{L}_{\text{invGamma}(a_\tau, b_\tau)}(\tau_t^2) \prod_{j=1}^{k_t} \mathcal{L}_{\mathcal{N}(\vartheta_t, \tau_t^2)}(\mu_{jt}^*) \\ &\propto \left[ \left( \frac{1}{\tau_t^2} \right)^{a_\tau+1} \exp \left\{ -\frac{b_\tau}{\tau_t^2} \right\} \right] \left[ \prod_{j=1}^{k_t} \left( \frac{1}{\tau_t^2} \right)^{1/2} \exp \left\{ -\frac{1}{2\tau_t^2} (\mu_{jt}^* - \vartheta_t)^2 \right\} \right] \\ &\propto \left( \frac{1}{\tau_t^2} \right)^{\left( \frac{k_t}{2} + a_\tau \right) + 1} \exp \left\{ -\frac{1}{\tau_t^2} \left( \frac{\sum_{j=1}^{k_t} (\mu_{jt}^* - \vartheta_t)^2}{2} + b_\tau \right) \right\} \\ \implies f(\tau_t^2 | -) &\propto \text{kernel of a } \text{invGamma}(a_{\tau(\text{post})}, b_{\tau(\text{post})}) \text{ with} \\ a_{\tau(\text{post})} &= \frac{k_t}{2} + a_\tau \\ b_{\tau(\text{post})} &= \frac{\sum_{j=1}^{k_t} (\mu_{jt}^* - \vartheta_t)^2}{2} + b_\tau \end{aligned} \quad (\text{A.7})$$

- update  $\vartheta_t$

for  $t = T$ :

$$\begin{aligned} f(\vartheta_t | -) &\propto f(\vartheta_t) f((\mu_{1t}^*, \dots, \mu_{k_t t}^*) | \vartheta_t, -) \\ &= \mathcal{L}_{\mathcal{N}((1-\varphi_1)\varphi_0 + \varphi_1 \vartheta_{t-1}, \lambda^2(1-\varphi_1^2))}(\vartheta_t) \prod_{j=1}^{k_t} \mathcal{L}_{\mathcal{N}(\vartheta_t, \tau_t^2)}(\mu_{jt}^*) \\ &\propto \exp \left\{ -\frac{1}{2(\lambda^2(1-\varphi_1^2))} \left( \vartheta_t - ((1-\varphi_1)\varphi_0 + \varphi_1 \vartheta_{t-1}) \right)^2 \right\} \\ &\cdot \exp \left\{ -\frac{k_t}{2\tau_t^2} \left( \vartheta_t - \frac{\sum_{j=1}^{k_t} \mu_{jt}^*}{k_t} \right) \right\} \\ \implies f(\vartheta_t | -) &\propto \text{kernel of a } \mathcal{N}(\mu_{\vartheta_t(\text{post})}, \sigma_{\vartheta_t(\text{post})}^2) \text{ with} \\ \sigma_{\vartheta_t(\text{post})}^2 &= \frac{1}{\frac{1}{\lambda^2(1-\varphi_1^2)} + \frac{k_t}{\tau_t^2}} \\ \mu_{\vartheta_t(\text{post})} &= \sigma_{\vartheta_t(\text{post})}^2 \left( \frac{\sum_{j=1}^{k_t} \mu_{jt}^*}{\tau_t^2} + \frac{(1-\varphi_1)\varphi_0 + \varphi_1 \vartheta_{t-1}}{\lambda^2(1-\varphi_1^2)} \right) \end{aligned} \quad (\text{A.8})$$

for  $1 < t < T$ :

$$\begin{aligned}
f(\vartheta_t | -) &\propto \underbrace{f(\vartheta_t) f((\mu_{1t}^*, \dots, \mu_{kt}^*) | \vartheta_t, -)}_{\text{as in the case } t = T} f(\vartheta_{t+1} | \vartheta_t, -) \\
&= \mathcal{L}_{\mathcal{N}(\mu_{\vartheta_t(\text{post})}, \sigma_{\vartheta_t(\text{post})}^2)}(\vartheta_t) \mathcal{L}_{\mathcal{N}((1-\varphi_1)\varphi_0 + \varphi_1 \vartheta_t, \lambda^2(1-\varphi_1^2))}(\vartheta_{t+1}) \\
&\propto \exp \left\{ -\frac{1}{2\sigma_{\vartheta_t(\text{post})}^2} (\vartheta_t - \mu_{\vartheta_t(\text{post})})^2 \right\} \\
&\quad \cdot \exp \left\{ -\frac{1}{2\frac{\lambda^2(1-\varphi_1^2)}{\varphi_1^2}} \left( \vartheta_t - \frac{\vartheta_{t+1} - (1-\varphi_1)\varphi_0}{\varphi_1} \right)^2 \right\} \\
\implies f(\vartheta_t | -) &\propto \text{kernel of a } \mathcal{N}(\mu_{\vartheta_t(\text{post})}, \sigma_{\vartheta_t(\text{post})}^2) \text{ with} \\
\sigma_{\vartheta_t(\text{post})}^2 &= \frac{1}{\frac{1+\varphi_1^2}{\lambda^2(1-\varphi_1^2)} + \frac{k_t}{\tau_t^2}} \\
\mu_{\vartheta_t(\text{post})} &= \sigma_{\vartheta_t(\text{post})}^2 \left( \frac{\sum_{j=1}^{k_t} \mu_{jt}^*}{\tau_t^2} + \frac{\varphi_1(\vartheta_{t-1} + \vartheta_{t+1}) + \varphi_0(1-\varphi_1)^2}{\lambda^2(1-\varphi_1^2)} \right) \quad (\text{A.9})
\end{aligned}$$

for  $t = 1$ :

$$\begin{aligned}
f(\vartheta_t | -) &\propto f(\vartheta_t) f(\vartheta_{t+1} | \vartheta_t, -) f(\boldsymbol{\mu}_t^* | \vartheta_t, -) \\
&= \mathcal{L}_{\mathcal{N}(\varphi_0, \lambda^2)}(\vartheta_t) \mathcal{L}_{\mathcal{N}((1-\varphi_1)\varphi_0 + \varphi_1 \vartheta_{t-1}, \lambda^2(1-\varphi_1^2))}(\vartheta_{t+1}) \prod_{j=1}^{k_t} \mathcal{L}_{\mathcal{N}(\vartheta_t, \tau_t^2)}(\mu_{jt}^*) \\
&\propto \exp \left\{ -\frac{1}{2\lambda^2} (\vartheta_t - \varphi_0)^2 \right\} \\
&\quad \cdot \exp \left\{ -\frac{1}{2\frac{\lambda^2(1-\varphi_1^2)}{\varphi_1^2}} \left( \vartheta_t - \frac{\vartheta_{t+1} - (1-\varphi_1)\varphi_0}{\varphi_1} \right)^2 \right\} \\
&\quad \cdot \exp \left\{ -\frac{k_t}{2\tau_t^2} \left( \vartheta_t - \frac{\sum_{j=1}^{k_t} \mu_{jt}^*}{k_t} \right) \right\} \\
\implies f(\vartheta_t | -) &\propto \text{kernel of a } \mathcal{N}(\mu_{\vartheta_t(\text{post})}, \sigma_{\vartheta_t(\text{post})}^2) \text{ with} \\
\sigma_{\vartheta_t(\text{post})}^2 &= \frac{1}{\frac{1}{\lambda^2} + \frac{\varphi_1^2}{\lambda^2(1-\varphi_1^2)} + \frac{k_t}{\tau_t^2}} \\
\mu_{\vartheta_t(\text{post})} &= \sigma_{\vartheta_t(\text{post})}^2 \left( \frac{\varphi_0}{\lambda^2} + \frac{\varphi_1(\vartheta_{t+1} - (1-\varphi_1)\varphi_0)}{\lambda^2(1-\varphi_1^2)} + \frac{\sum_{j=1}^{k_t} \mu_{jt}^*}{\tau_t^2} \right) \quad (\text{A.10})
\end{aligned}$$

- update  $\varphi_0$

$$\begin{aligned}
f(\varphi_0 | -) &\propto f(\varphi_0) f((\vartheta_1, \dots, \vartheta_T) | \varphi_0, -) \\
&= \mathcal{L}_{\mathcal{N}(m_0, s_0^2)}(\varphi_0) \mathcal{L}_{\mathcal{N}(\varphi_0, \lambda^2)}(\vartheta_1) \prod_{t=2}^T \mathcal{L}_{\mathcal{N}((1-\varphi_1)\varphi_0 + \varphi_1 \vartheta_{t-1}, \lambda^2(1-\varphi_1^2))}(\vartheta_t) \\
&\propto \exp \left\{ \left\{ -\frac{1}{2s_0^2} (\varphi_0 - m_0)^2 \right\} \right\} \exp \left\{ \left\{ -\frac{1}{2\lambda^2} (\varphi_0 - \vartheta_1)^2 \right\} \right\}
\end{aligned}$$

$$\begin{aligned}
& \cdot \exp \left\{ \left\{ -\frac{1}{2 \frac{\lambda^2(1-\varphi_1^2)}{(T-1)(1-\varphi_1)^2}} \left( \varphi_0 - \frac{(1-\varphi_1)(\text{SUM}_t)}{(T-1)(1-\varphi_1)^2} \right)^2 \right\} \right\} \\
& \text{where } \text{SUM}_t = \sum_{t=2}^T (\vartheta_t - \varphi_1 \vartheta_{t-1}) \\
\implies f(\varphi_0 | -) & \propto \text{kernel of a } \mathcal{N}(\mu_{\varphi_0(\text{post})}, \sigma_{\varphi_0(\text{post})}^2) \text{ with} \\
\sigma_{\varphi_0(\text{post})}^2 &= \frac{1}{\frac{1}{s_0^2} + \frac{1}{\lambda^2} + \frac{(T-1)(1-\varphi_1)^2}{\lambda^2(1-\varphi_1^2)}} \\
\mu_{\varphi_0(\text{post})} &= \sigma_{\varphi_0(\text{post})}^2 \left( \frac{m_0}{s_0^2} + \frac{\vartheta_1}{\lambda^2} + \frac{1-\varphi_1}{\lambda^2(1-\varphi_1^2)} \text{SUM}_t \right) \tag{A.11}
\end{aligned}$$

- update  $\lambda^2$

$$\begin{aligned}
f(\lambda^2 | -) & \propto f(\lambda^2) f(\vartheta_1, \dots, \vartheta_T | \lambda^2, -) \\
& = \mathcal{L}_{\text{invGamma}(a_\lambda, b_\lambda)}(\lambda^2) \mathcal{L}_{\mathcal{N}(\varphi_0, \lambda^2)}(\vartheta_1) \prod_{t=2}^T \mathcal{L}_{\mathcal{N}((1-\varphi_1)\varphi_0 + \varphi_1 \vartheta_{t-1}, \lambda^2(1-\varphi_1^2))}(\vartheta_t) \\
& \propto \left[ \left( \frac{1}{\lambda_t^2} \right)^{a_\lambda+1} \exp \left\{ -\frac{b_\lambda}{\lambda^2} \right\} \right] \left[ \left( \frac{1}{\lambda^2} \right)^{1/2} \exp \left\{ -\frac{1}{2\lambda^2} (\vartheta_1 - \varphi_0)^2 \right\} \right] \\
& \cdot \left[ \prod_{t=2}^T \left( \frac{1}{\lambda^2} \right)^{1/2} \exp \left\{ -\frac{1}{2\lambda^2} (\vartheta_t - (1-\varphi_1)\varphi_0 - \varphi_1 \vartheta_{t-1})^2 \right\} \right] \\
& \propto \left( \frac{1}{\lambda^2} \right)^{\left( \frac{T}{2} + a_\lambda \right) + 1} \\
& \cdot \exp \left\{ -\frac{1}{\lambda^2} \left( \frac{(\vartheta_1 - \varphi_0)^2}{2} + \sum_{t=2}^T \frac{(\vartheta_t - (1-\varphi_1)\varphi_0 - \varphi_1 \vartheta_{t-1})^2}{2} + b_\lambda \right) \right\}
\end{aligned}$$

$\implies f(\lambda^2 | -) \propto \text{kernel of a } \text{invGamma}(a_{\lambda(\text{post})}, b_{\lambda(\text{post})}) \text{ with}$

$$\begin{aligned}
a_{\lambda(\text{post})} &= \frac{T}{2} + a_\lambda \\
b_{\lambda(\text{post})} &= \frac{(\vartheta_1 - \varphi_0)^2}{2} + \sum_{t=2}^T \frac{(\vartheta_t - (1-\varphi_1)\varphi_0 - \varphi_1 \vartheta_{t-1})^2}{2} + b_\lambda \tag{A.12}
\end{aligned}$$

- update  $\alpha$

if global  $\alpha$ : prior is  $\alpha \sim \text{Beta}(a_\alpha, b_\alpha)$

$$\begin{aligned}
f(\alpha | -) & \propto f(\alpha) f((\gamma_{11}, \dots, \gamma_{1T}, \dots, \gamma_{n1}, \dots, \gamma_{nT}) | \alpha) \\
& \propto \alpha^{a_\alpha-1} (1-\alpha)^{b_\alpha-1} \prod_{i=1}^n \prod_{t=1}^T \alpha^{\gamma_{it}} (1-\alpha)^{1-\gamma_{it}} \\
& = \alpha^{(a_\alpha + \sum_{i=1}^n \sum_{t=1}^T \gamma_{it}) - 1} (1-\alpha)^{(b_\alpha + nT - \sum_{i=1}^n \sum_{t=1}^T \gamma_{it}) - 1} \\
\implies f(\alpha | -) & \propto \text{kernel of a } \text{Beta}(a_{\alpha(\text{post})}, b_{\alpha(\text{post})}) \text{ with}
\end{aligned}$$

$$a_{\alpha(\text{post})} = a_\alpha + \sum_{i=1}^n \sum_{t=1}^T \gamma_{it} \quad b_{\alpha(\text{post})} = b_\alpha + nT - \sum_{i=1}^n \sum_{t=1}^T \gamma_{it} \quad (\text{A.13})$$

if time specific  $\alpha$ : prior is  $\alpha_t \sim \text{Beta}(a_\alpha, b_\alpha)$

$$\begin{aligned} f(\alpha_t | -) &\propto f(\alpha_t) f((\gamma_{1t}, \dots, \gamma_{nt}) | \alpha_t) \\ &\propto \alpha_t^{a_\alpha-1} (1-\alpha_t)^{b_\alpha-1} \prod_{i=1}^n \alpha_t^{\gamma_{it}} (1-\alpha_t)^{1-\gamma_{it}} \\ &= \alpha_t^{(a_\alpha + \sum_{i=1}^n \gamma_{it})-1} (1-\alpha_t)^{(b_\alpha + n - \sum_{i=1}^n \gamma_{it})-1} \end{aligned}$$

$\implies f(\alpha_t | -) \propto \text{kernel of a Beta}(a_{\alpha(\text{post})}, b_{\alpha(\text{post})})$  with

$$a_{\alpha(\text{post})} = a_\alpha + \sum_{i=1}^n \gamma_{it} \quad b_{\alpha(\text{post})} = b_\alpha + n - \sum_{i=1}^n \gamma_{it} \quad (\text{A.14})$$

if unit specific  $\alpha$ : prior is  $\alpha_i \sim \text{Beta}(a_{\alpha i}, b_{\alpha i})$

$$\begin{aligned} f(\alpha_i | -) &\propto f(\alpha_i) f((\gamma_{i1}, \dots, \gamma_{iT}) | \alpha_i) \\ &\propto \alpha_i^{a_{\alpha i}-1} (1-\alpha_i)^{b_{\alpha i}-1} \prod_{t=1}^T \alpha_i^{\gamma_{it}} (1-\alpha_i)^{1-\gamma_{it}} \\ &= \alpha_i^{(a_{\alpha i} + \sum_{t=1}^T \gamma_{it})-1} (1-\alpha_i)^{(b_{\alpha i} + T - \sum_{t=1}^T \gamma_{it})-1} \end{aligned}$$

$\implies f(\alpha_i | -) \propto \text{kernel of a Beta}(a_{\alpha(\text{post})}, b_{\alpha(\text{post})})$  with

$$a_{\alpha(\text{post})} = a_{\alpha i} + \sum_{t=1}^T \gamma_{it} \quad b_{\alpha(\text{post})} = b_{\alpha i} + T - \sum_{t=1}^T \gamma_{it} \quad (\text{A.15})$$

if time and unit specific  $\alpha$ : prior is  $\alpha_{it} \sim \text{Beta}(a_{\alpha i}, b_{\alpha i})$

$$\begin{aligned} f(\alpha_{it} | -) &\propto f(\alpha_{it}) f(\gamma_{it} | \alpha_{it}) \\ &\propto \alpha_{it}^{a-1} (1-\alpha_{it})^{b-1} \alpha_{it}^{\gamma_{it}} (1-\alpha_{it})^{1-\gamma_{it}} \\ &= \alpha_i^{(a+\gamma_{it})-1} (1-\alpha_i)^{(b+1+\gamma_{it})-1} \end{aligned}$$

$\implies f(\alpha_{it} | -) \propto \text{kernel of a Beta}(a_{\alpha(\text{post})}, b_{\alpha(\text{post})})$  with

$$a_{\alpha(\text{post})} = a_{\alpha i} + \gamma_{it} \quad b_{\alpha(\text{post})} = b_{\alpha i} + 1 - \gamma_{it} \quad (\text{A.16})$$

- update a missing observation  $Y_{it}$

for  $t = 1$ :

$$\begin{aligned} f(Y_{it} | -) &\propto f(Y_{it}) f(Y_{it+1} | Y_{it}, -) \\ &= \mathcal{L}_{\mathcal{N}(\mu_{c_{it} t}^* + \mathbf{x}_{it}^T \boldsymbol{\beta}_t, \sigma_{c_{it} t}^{2*})}(Y_{it}) \\ &\cdot \mathcal{L}_{\mathcal{N}(\mu_{c_{it+1} t+1}^* + \eta_{1i} Y_{it} + \mathbf{x}_{it+1}^T \boldsymbol{\beta}_{t+1}, \sigma_{c_{it+1} t+1}^{2*} (1 - \eta_{1i}^2))}(Y_{it+1}) \\ &\propto \exp \left\{ -\frac{1}{2\sigma_{c_{it} t}^{2*}} (Y_{it} - \mu_{c_{it} t}^* - \mathbf{x}_{it}^T \boldsymbol{\beta}_t)^2 \right\} \\ &\cdot \exp \left\{ -\frac{1}{2\sigma_{c_{it+1} t+1}^{2*} (1 - \eta_{1i}^2)} (Y_{it+1} - \mu_{c_{it+1} t+1}^* - \eta_{1i} Y_{it} - \mathbf{x}_{it+1}^T \boldsymbol{\beta}_{t+1})^2 \right\} \end{aligned}$$

$$\begin{aligned}
&= \exp \left\{ -\frac{1}{2\sigma_{c_{it}t}^{2\star}} (Y_{it} - (\mu_{c_{it}t}^* + \mathbf{x}_{it}^T \boldsymbol{\beta}_t))^2 \right\} \\
&\cdot \exp \left\{ -\frac{\eta_{1i}^2}{2\sigma_{c_{it+1}t+1}^{2\star}(1-\eta_{1i}^2)} \left( Y_{it} - \frac{Y_{it+1} - \mu_{c_{it+1}t+1}^* - \mathbf{x}_{it+1}^T \boldsymbol{\beta}_{t+1}}{\eta_{1i}} \right)^2 \right\} \\
\implies f(Y_{it} | -) &\propto \text{kernel of a } \mathcal{N}(\mu_{Y_{it}(\text{post})}, \sigma_{Y_{it}(\text{post})}^2) \text{ with} \\
\sigma_{Y_{it}(\text{post})}^2 &= \frac{1}{\frac{1}{\sigma_{c_{it}t}^{2\star}} + \frac{\eta_{1i}^2}{2\sigma_{c_{it+1}t+1}^{2\star}(1-\eta_{1i}^2)}} \\
\mu_{Y_{it}(\text{post})} &= \sigma_{Y_{it}(\text{post})}^2 \left( \frac{\mu_{c_{it}t}^* + \mathbf{x}_{it}^T \boldsymbol{\beta}_t}{\sigma_{c_{it}t}^{2\star}} + \frac{\eta_{1i}(Y_{it+1} - \mu_{c_{it+1}t+1}^* - \mathbf{x}_{it+1}^T \boldsymbol{\beta}_{t+1})}{\sigma_{c_{it+1}t+1}^{2\star}(1-\eta_{1i}^2)} \right) \tag{A.17}
\end{aligned}$$

for  $1 < t < T$ :

$$\begin{aligned}
f(Y_{it} | -) &\propto f(Y_{it}) f(Y_{it+1} | Y_{it}, -) \\
&= \mathcal{L}_{\mathcal{N}(\mu_{c_{it}t}^* + \eta_{1i} Y_{it-1} + \mathbf{x}_{it}^T \boldsymbol{\beta}_t, \sigma_{c_{it}t}^{2\star})}(Y_{it}) \\
&\cdot \mathcal{L}_{\mathcal{N}(\mu_{c_{it+1}t+1}^* + \eta_{1i} Y_{it} + \mathbf{x}_{it+1}^T \boldsymbol{\beta}_{t+1}, \sigma_{c_{it+1}t+1}^{2\star}(1-\eta_{1i}^2))}(Y_{it+1}) \\
&\propto \exp \left\{ -\frac{1}{2\sigma_{c_{it}t}^{2\star}(1-\eta_{1i}^2)} (Y_{it} - \mu_{c_{it}t}^* - \eta_{1i} Y_{it-1} - \mathbf{x}_{it}^T \boldsymbol{\beta}_t)^2 \right\} \\
&\cdot \exp \left\{ -\frac{1}{2\sigma_{c_{it+1}t+1}^{2\star}(1-\eta_{1i}^2)} (Y_{it+1} - \mu_{c_{it+1}t+1}^* - \eta_{1i} Y_{it} - \mathbf{x}_{it+1}^T \boldsymbol{\beta}_{t+1})^2 \right\} \\
&= \exp \left\{ -\frac{1}{2\sigma_{c_{it}t}^{2\star}(1-\eta_{1i}^2)} (Y_{it} - (\mu_{c_{it}t}^* + \eta_{1i} Y_{it-1} + \mathbf{x}_{it}^T \boldsymbol{\beta}_t))^2 \right\} \\
&\cdot \exp \left\{ -\frac{\eta_{1i}^2}{2\sigma_{c_{it+1}t+1}^{2\star}(1-\eta_{1i}^2)} \left( Y_{it} - \frac{Y_{it+1} - \mu_{c_{it+1}t+1}^* - \mathbf{x}_{it+1}^T \boldsymbol{\beta}_{t+1}}{\eta_{1i}} \right)^2 \right\} \\
\implies f(Y_{it} | -) &\propto \text{kernel of a } \mathcal{N}(\mu_{Y_{it}(\text{post})}, \sigma_{Y_{it}(\text{post})}^2) \text{ with} \\
\sigma_{Y_{it}(\text{post})}^2 &= \frac{1 - \eta_{1i}^2}{\frac{1}{\sigma_{c_{it}t}^{2\star}} + \frac{\eta_{1i}^2}{\sigma_{c_{it+1}t+1}^{2\star}}} \\
\mu_{Y_{it}(\text{post})} &= \sigma_{Y_{it}(\text{post})}^2 \left( \frac{\mu_{c_{it}t}^* + \eta_{1i} Y_{it-1} + \mathbf{x}_{it}^T \boldsymbol{\beta}_t}{\sigma_{c_{it}t}^{2\star}(1-\eta_{1i}^2)} + \frac{\eta_{1i}(Y_{it+1} - \mu_{c_{it+1}t+1}^* - \mathbf{x}_{it+1}^T \boldsymbol{\beta}_{t+1})}{\sigma_{c_{it+1}t+1}^{2\star}(1-\eta_{1i}^2)} \right) \tag{A.18}
\end{aligned}$$

for  $t = T$ :

$$\begin{aligned}
f(Y_{it} | -) &\propto f(Y_{it}) \\
&= \mathcal{L}_{\mathcal{N}(\mu_{c_{it}t}^* + \eta_{1i} Y_{it-1} + \mathbf{x}_{it}^T \boldsymbol{\beta}_t, \sigma_{c_{it}t}^{2\star}(1-\eta_{1i}^2))}(Y_{it}) \\
\implies f(Y_{it} | -) &\text{ is just the likelihood of } Y_{it} \tag{A.19}
\end{aligned}$$



# Appendix B

## Computational details

### B.1 Fitting algorithm code

We report here part of the code of the `MCMC_fit` function which implements the updated DRPM model described in this work. We include it to let the readers appreciate the ease, clarity and even elegance of the Julia language in translating the mathematical formulation into code. Together with what said in Chapter 3, we also note that the productivity offered by the Julia language is not only obtained through the vast land of packages and documentation, but even through an online active forum<sup>1</sup>, where I wrote myself some questions (and received answers) during the development of the thesis.

All this with the hope for Julia to become the new natural choice in the statistical, or in general scientific, computing field, giving to it a refreshing approach.

**Listing 3:** Julia code which implements the fitting model algorithm. We report here just the “functional” part, i.e. not all the setup lines regarding the function definition, variable preallocations, input arguments checks, etc.

```
##### start MCMC algorithm #####
println("Starting MCMC algorithm")

t_start = now()
progresso = Progress(round(Int64(draws)),
    showspeed=true,
    output=stdout, # not stderr, to make it work nicer on R
    dt=1, # every how many seconds update the feedback
    barlen=0 # no progress bar, just time feedback
)

for i in 1:draws

##### sample the missing values #####
# from the "update rho" section onwards also the Y[j,t] will be needed (to
# compute weights, update laws, etc)
# so we need now to simulate the values (from their full conditional) for the
# data which are missing
if Y_has_NA
```

---

<sup>1</sup><https://discourse.julialang.org/>

```

# we have to use the missing_idxs to remember which units and at which
→ times had a missing value,
# in order to simulate just them and instead use the given value for the
→ other units and times
for (j,t) in missing_idxs
    # What if when filling a NA we occur in another NA value? eg when we
    → also need Y[j,t+1]?
    # I decided here to set that value to 0, if occurs, since anyway target
    → should be centered
    # so it seems a reasonable patch, and I think there was no other
    → solution

    c_it = Si_iter[j,t]
    Xlk_term_t = (lk_xPPM ? dot(view(Xlk_covariates,j,:,:t), beta_iter[t]) :
    → 0)
    aux1 = eta1_iter[j]^2

    if t==1
        c_itp1 = Si_iter[j,t+1]
        Xlk_term_tp1 = (lk_xPPM ? dot(view(Xlk_covariates,j,:,:t+1),
        → beta_iter[t+1]) : 0)

        sig2_post = 1 / (1/sig2h_iter[c_it,t] +
        → aux1/(sig2h_iter[c_itp1,t+1]*(1-aux1)))
        mu_post = sig2_post * (
            (1/sig2h_iter[c_it,t])*(muh_iter[c_it,t] + Xlk_term_t) +
            (eta1_iter[j]/(sig2h_iter[c_itp1,t+1]*(1-aux1)))*((ismissing(Y[j,t+1])
            → ? 0 : Y[j,t+1]) - muh_iter[c_itp1,t+1] - Xlk_term_tp1)
        )

        Y[j,t] = rand(Normal(mu_post,sqrt(sig2_post)))

    elseif 1<t<T
        c_itp1 = Si_iter[j,t+1]
        Xlk_term_tp1 = (lk_xPPM ? dot(view(Xlk_covariates,j,:,:t+1),
        → beta_iter[t+1]) : 0)

        sig2_post = (1-aux1) / (1/sig2h_iter[c_it,t] +
        → aux1/sig2h_iter[c_itp1,t+1])
        mu_post = sig2_post * (
            (1/(sig2h_iter[c_it,t]*(1-aux1)))*(muh_iter[c_it,t] +
            → eta1_iter[j]*(ismissing(Y[j,t-1]) ? 0 : Y[j,t-1]) +
            → Xlk_term_t) +
            (eta1_iter[j]/(sig2h_iter[c_itp1,t+1]*(1-aux1)))*((ismissing(Y[j,t+1])
            → ? 0 : Y[j,t+1]) - muh_iter[c_itp1,t+1] - Xlk_term_tp1)
        )

        Y[j,t] = rand(Normal(mu_post,sqrt(sig2_post)))

    else # t==T
        Y[j,t] = rand(Normal(
            muh_iter[c_it,t] + eta1_iter[j]*(ismissing(Y[j,t-1]) ? 0 :
            → Y[j,t-1]) + Xlk_term_t,
            sqrt(sig2h_iter[c_it,t]*(1-aux1))
        ))
    end
end
end

for t in 1:T
    ##### update gamma #####

```

```

for j in 1:n
    if t==1
        gamma_iter[j,t] = 0
        # at the first time units get reallocated
    else
        # we want to find rho_t^{\{R_t(-j)\}} ...
        indexes = findall_faster(jj -> jj != j && gamma_iter[jj, t] == 1,
                                  ↵ 1:n)
        Si_red = Si_iter[indexes, t]
        copy!(Si_red1, Si_red)
        push!(Si_red1, Si_iter[j,t]) # ... and rho_t^{\{R_t(+j)\}}
```

# get also the reduced spatial info if sPPM model

```

if sPPM
    sp1_red = @view sp1[indexes]
    sp2_red = @view sp2[indexes]
end
# and the reduced covariates info if cl_xPPM model
if cl_xPPM
    Xcl_covariates_red = @view Xcl_covariates[indexes,:,:t]
end
```

# compute n\_red's and nclus\_red's and relabel

```

n_red = length(Si_red) # = "n" relative to here, i.e. the
                        ↵ sub-partition size
n_red1 = length(Si_red1)
relabel!(Si_red,n_red)
relabel!(Si_red1,n_red1)
nclus_red = isempty(Si_red) ? 0 : maximum(Si_red) # = number of
                        ↵ clusters
nclus_red1 = maximum(Si_red1)
```

# save the label of the current working-on unit j

```

j_label = Si_red1[end]
```

# compute also nh\_red's

```

nh_red .= 0
nh_red1 .= 0
for jj in 1:n_red
    nh_red[Si_red[jj]] += 1 # = numerosities for each cluster label
    nh_red1[Si_red1[jj]] += 1
end
nh_red1[Si_red1[end]] += 1 # account for the last added unit j, not
                            ↵ included in the above loop
```

# start computing weights

```

lg_weights .= 0
```

# unit j can enter an existing cluster...

```

for k in 1:nclus_red
    aux_idxs = findall(Si_red .== k) # fast
    lC .= 0.
    if sPPM
        # filter the spatial coordinates of the units of label k
        copy!(s1o, sp1_red[aux_idxs])
        copy!(s2o, sp2_red[aux_idxs])
        copy!(s1n,s1o); push!(s1n, sp1[j])
        copy!(s2n,s2o); push!(s2n, sp2[j])
        spatial_cohesion!(spatial_cohesion_idx, s1o, s2o,
                          ↵ sp_params_struct, true, M_dp, S, 1, false, lC)
        spatial_cohesion!(spatial_cohesion_idx, s1n, s2n,
                          ↵ sp_params_struct, true, M_dp, S, 2, false, lC)
```

```

    end
    lS .= 0.
    if cl_xPPM
        # and the covariates of the units of label k
        for p in 1:p_cl
            copy!(Xo, @view Xcl_covariates_red[aux_idx[p]])
            copy!(Xn, Xo); push!(Xn,Xcl_covariates[j,p,t])
            covariate_similarity!(covariate_similarity_idx, Xo,
                → cv_params, true, 1, true, lS)
            covariate_similarity!(covariate_similarity_idx, Xn,
                → cv_params, true, 2, true, lS)
        end
    end
    lg_weights[k] = log(nh_red[k]) + lC[2] - lC[1] + lS[2] - lS[1]
end
# ... or unit j can create a singleton
lC .= 0.
if sPPM
    spatial_cohesion!(spatial_cohesion_idx, SVector(sp1[j]),
        → SVector(sp2[j]), sp_params_struct, true, M_dp, S, 2, false,
        → lC)
end
lS .= 0.
if cl_xPPM
    for p in 1:p_cl
        covariate_similarity!(covariate_similarity_idx,
            → SVector(Xcl_covariates[j,p,t]), cv_params, true, 2, true,
            → lS)
    end
end
lg_weights[nclus_red+1] = log_Mdp + lC[2] + lS[2]

# now use the weights towards sampling the new gamma_jt
max_ph = maximum(@view lg_weights[1:(nclus_red+1)])
sum_ph = 0.0
# exponentiate...
for k in 1:(nclus_red+1)
    # for numerical purposes we subtract max_ph
    lg_weights[k] = exp(lg_weights[k] - max_ph)
    sum_ph += lg_weights[k]
end
# ... and normalize
lg_weights ./= sum_ph

# compute probh
probh = 0.0
if time_specific_alpha==false && unit_specific_alpha==false
    probh = alpha_iter / (alpha_iter + (1 - alpha_iter) *
        → lg_weights[j_label])
elseif time_specific_alpha==true && unit_specific_alpha==false
    probh = alpha_iter[t] / (alpha_iter[t] + (1 - alpha_iter[t]) *
        → lg_weights[j_label])
elseif time_specific_alpha==false && unit_specific_alpha==true
    probh = alpha_iter[j] / (alpha_iter[j] + (1 - alpha_iter[j]) *
        → lg_weights[j_label])
elseif time_specific_alpha==true && unit_specific_alpha==true
    probh = alpha_iter[j,t] / (alpha_iter[j,t] + (1 -
        → alpha_iter[j,t]) * lg_weights[j_label])
end

# compatibility check for gamma transition
if gamma_iter[j, t] == 0

```

```

# we want to find rho_(t-1)^{R_t(+j)} ...
indexes = findall_faster(jj -> jj==j gamma_iter[jj, t]==1, 1:n)
Si_comp1 = @view Si_iter[indexes, t-1]
Si_comp2 = @view Si_iter[indexes, t] # ... and rho_t^{R_t(+j)})

rho_comp = compatibility(Si_comp1, Si_comp2)
if rho_comp == 0
    probh = 0.0
end
end
# sample the new gamma
gt = rand(Bernoulli(probh))
gamma_iter[j, t] = gt
end
end # for j in 1:n

##### update rho #####
# we only update the partition for the units which can move (i.e. with
# gamma_jt=0)
movable_units = findall(gamma_iter[:,t] .== 0)

for j in movable_units
    # remove unit j from the cluster she is currently in

    if nh[Si_iter[j,t],t] > 1 # unit j does not belong to a singleton
    # cluster
        nh[Si_iter[j,t],t] -= 1
        # no nclus_iter[t] change since j's cluster is still alive
    else # unit j belongs to a singleton cluster
        j_label = Si_iter[j,t]
        last_label = nclus_iter[t]

        if j_label < last_label
            # here we enter if j_label is not the last label, so we need to
            # relabel clusters in order to then remove j's cluster
            # eg: units 1 2 3 4 5 j 7 -> units 1 2 3 4 5 j 7
            #      label 1 1 2 2 2 3 4      label 1 1 2 2 2 4 3

            # swap cluster labels...
            for jj in 1:n
                if Si_iter[jj, t] == last_label
                    Si_iter[jj, t] = j_label
                end
            end
            Si_iter[j, t] = last_label
            # ... and cluster-specific parameters
            sig2h_iter[j_label, t], sig2h_iter[last_label, t] =
            # sig2h_iter[last_label, t], sig2h_iter[j_label, t]
            muh_iter[j_label, t], muh_iter[last_label, t] =
            # muh_iter[last_label, t], muh_iter[j_label, t]
            nh[j_label, t] = nh[last_label, t]
            nh[last_label, t] = 1
        end
        # remove the j-th observation and the last cluster (being j in a
        # singleton)
        nh[last_label, t] -= 1
        nclus_iter[t] -= 1
    end

    # setup probability weights towards the sampling of rho_jt

```

```

ph .= 0.0
resize!(ph, nclus_iter[t]+1)
copy!(rho_tmp, @view Si_iter[:,t])

# compute nh_tmp (numerosities for each cluster label)
copy!(nh_tmp, @view nh[:,t])
# unit j contribute is already absent from the change we did above
nclus_temp = 0

# we now simulate the unit j to be assigned to one of the existing
# clusters...
for k in 1:nclus_iter[t]
    rho_tmp[j] = k
    indexes = findall(gamma_iter[:,t+1] .== 1)
    # we check the compatibility between rho_t^{h=k, R_{(t+1)}} ...
    Si_comp1 = @view rho_tmp[indexes]
    Si_comp2 = @view Si_iter[indexes,t+1] # and rho_{(t+1)}^{R_{(t+1)}}
```

rho\_comp = compatibility(Si\_comp1, Si\_comp2)

```

    if rho_comp != 1
        ph[k] = log(0) # assignment to cluster k is not compatible
    else
        # update params for "rho_jt = k" simulation
        nh_tmp[k] += 1
        nclus_temp = count(a->(a>0), nh_tmp)

        lPP .= 0.
        for kk in 1:nclus_temp
            aux_idxs = findall(rho_tmp .== kk)
            if sPPM
                copy!(s1n, @view sp1[aux_idxs])
                copy!(s2n, @view sp2[aux_idxs])
                spatial_cohesion!(spatial_cohesion_idx, s1n, s2n,
                    → sp_params_struct, true, M_dp, S, 1, true, lPP)
            end
            if cl_xPPM
                for p in 1:p_cl
                    Xn_view = @view Xcl_covariates[aux_idxs,p,t]
                    covariate_similarity!(covariate_similarity_idx, Xn_view,
                        → cv_params, true, 1, true, lPP)
                end
            end
            lPP[k] += log_Mdp + lgamma(nh_tmp[kk])
        end

        if t==1
            ph[k] = loglikelihood(Normal(
                muh_iter[k,t] + (lk_xPPM ? dot(view(Xlk_covariates,j,:,:t),
                    → beta_iter[t]) : 0),
                sqrt(sig2h_iter[k,t])),
                Y[j,t]) + lPP[1]
        else
            ph[k] = loglikelihood(Normal(
                muh_iter[k,t] + eta1_iter[j]*Y[j,t-1] + (lk_xPPM ?
                    → dot(view(Xlk_covariates,j,:,:t), beta_iter[t]) : 0),
                sqrt(sig2h_iter[k,t]*(1-eta1_iter[j]^2))),
                Y[j,t]) + lPP[1]
        end

        # restore params after "rho_jt = k" simulation
        nh_tmp[k] -= 1
    end
end

```

```

    end
    # ... plus the case of being assigned to a new (singleton for now)
    ↪ cluster
    k = nclus_iter[t]+1
    rho_tmp[j] = k
    # declare (for later scope accessibility) the new params here
    muh_draw = 0.0; sig2h_draw = 0.0

    indexes = findall(gamma_iter[:,t+1] .== 1)
    Si_comp1 = @view rho_tmp[indexes]
    Si_comp2 = @view Si_iter[indexes,t+1]
    rho_comp = compatibility(Si_comp1, Si_comp2)

    if rho_comp != 1
        ph[k] = log(0) # assignment to a new cluster is not compatible
    else
        # sample new params for this new cluster
        muh_draw = rand(Normal(theta_iter[t], sqrt(tau2_iter[t])))
        sig2h_draw = rand(InverseGamma(sig2h_priors[1],sig2h_priors[2]))

        # update params for "rho_jt = k" simulation
        nh_tmp[k] += 1
        nclus_temp = count(a->(a>0), nh_tmp)

        lPP .= 0.
        for kk in 1:nclus_temp
            aux_idx = findall(rho_tmp .== kk)
            if sPPM
                copy!(sin, @view sp1[aux_idx])
                copy!(s2n, @view sp2[aux_idx])
                spatial_cohesion!(spatial_cohesion_idx, sin, s2n,
                    ↪ sp_params_struct, true, M_dp, S, 1, true, lPP)
            end
            if cl_xPPM
                for p in 1:p_cl
                    Xn_view = @view Xcl_covariates[aux_idx,p,t]
                    covariate_similarity!(covariate_similarity_idx, Xn_view,
                        ↪ cv_params, true, 1, true, lPP)
                end
            end
            lPP[1] += log_Mdp + lgamma(nh_tmp[kk])
        end

        if t==1
            ph[k] = loglikelihood(Normal(
                muh_draw + (lk_xPPM ? dot(view(Xlk_covariates,j,:,:t),
                    ↪ beta_iter[t]) : 0),
                sqrt(sig2h_draw)),
                Y[j,t]) + lPP[1]
        else
            ph[k] = loglikelihood(Normal(
                muh_draw + eta1_iter[j]*Y[j,t-1] + (lk_xPPM ?
                    ↪ dot(view(Xlk_covariates,j,:,:t), beta_iter[t]) : 0),
                sqrt(sig2h_draw*(1-eta1_iter[j]^2))),
                Y[j,t]) + lPP[1]
        end

        # restore params after "rho_jt = k" simulation
        nh_tmp[k] -= 1
    end

    # now exponentiate the weights...
end

```

```

max_ph = maximum(ph)
sum_ph = 0.0
for k in eachindex(ph)
    # for numerical purposes we subtract max_ph
    ph[k] = exp(ph[k] - max_ph)
    sum_ph += ph[k]
end
# ... and normalize them
ph ./= sum_ph

# now sample the new label Si_iter[j,t]
u = rand(Uniform(0,1))
cph = cumsum(ph)
cph[end] = 1 # fix numerical problems of having sums like 0.999999etc
new_label = 0
for k in eachindex(ph)
    if u <= cph[k]
        new_label = k
        break
    end
end

if new_label <= nclus_iter[t]
    # we enter an existing cluster
    Si_iter[j, t] = new_label
    nh[new_label, t] += 1
else
    # we create a new singleton cluster
    nclus_iter[t] += 1
    cl_new = nclus_iter[t]
    Si_iter[j, t] = cl_new
    nh[cl_new, t] = 1
    muh_iter[cl_new, t] = muh_draw
    sig2h_iter[cl_new, t] = sig2h_draw
end

# now we need to relabel after the possible mess created by the
# sampling
# eg: (before sampling) (after sampling)
#      units j 2 3 4 5 -> units j 2 3 4 5
#      labels 1 1 1 2 2      labels 3 1 1 2 2
# the after case has to be relabelled
Si_tmp = @view Si_iter[:,t]

relabel_full!(Si_tmp, n, Si_relab, nh_reordered, old_lab)
# - Si_relab gives the relabelled partition
# - nh_reordered gives the numerosities of the relabelled partition, ie
#   "nh_reordered[k] = #(units of new cluster k)"
# - old_lab tells "the index in position i (which before was cluster i)"
#   is now called cluster old_lab[i]"
# eg:          Original labels (Si): 4 2 1 1 1 3 1 4 5
#           Relabeled groups (Si_relab): 1 2 3 3 3 4 3 1 5
# Reordered cluster sizes (nh_reordered): 2 1 4 1 1 0 0 0 0
#           Old labels (old_lab): 4 2 1 3 5 0 0 0 0

# now fix everything (morally permute params)
Si_iter[:,t] = Si_relab
copy!(muh_iter_copy, muh_iter)
copy!(sig2h_iter_copy, sig2h_iter)
len = findlast(x -> x != 0, nh_reordered)
for k in 1:nclus_iter[t]
    muh_iter[k,t] = muh_iter_copy[old_lab[k],t]

```

```

        sig2h_iter[k,t] = sig2h_iter_copy[old_lab[k],t]
        nh[k,t] = nh_reordered[k]
    end

end # for j in movable_units

##### update muh #####
if t==1
    for k in 1:nclus_iter[t]
        sum_Y = 0.0
        for j in 1:n
            if Si_iter[j,t]==k
                sum_Y += Y[j,t] - (lk_xPPM ? dot(view(Xlk_covariates,j,:,:),t),
                                     ↳ beta_iter[t]) : 0.0)
            end
        end
        sig2_star = 1 / (1/tau2_iter[t] + nh[k,t]/sig2h_iter[k,t])
        mu_star = sig2_star * (theta_iter[t]/tau2_iter[t] +
                               ↳ sum_Y/sig2h_iter[k,t])
        muh_iter[k,t] = rand(Normal(mu_star,sqrt(sig2_star)))
    end

else # t>1
    for k in 1:nclus_iter[t]
        sum_Y = 0.0
        sum_e2 = 0.0
        for j in 1:n
            if Si_iter[j,t]==k
                aux1 = 1 / (1-eta1_iter[j]^2)
                sum_e2 += aux1
                sum_Y += (Y[j,t] - eta1_iter[j]*Y[j,t-1] - (lk_xPPM ?
                                                               ↳ dot(view(Xlk_covariates,j,:,:),t), beta_iter[t]) : 0.0)) *
                           ↳ aux1
            end
        end
        sig2_star = 1 / (1/tau2_iter[t] + sum_e2/sig2h_iter[k,t])
        mu_star = sig2_star * (theta_iter[t]/tau2_iter[t] +
                               ↳ sum_Y/sig2h_iter[k,t])
        muh_iter[k,t] = rand(Normal(mu_star,sqrt(sig2_star)))
    end
end

##### update sigma2h #####
if t==1
    for k in 1:nclus_iter[t]
        a_star = sig2h_priors[1] + nh[k,t]/2
        sum_Y = 0.0
        S_kt = findall(Si_iter[:,t] .== k)
        for j in S_kt
            sum_Y += (Y[j,t] - muh_iter[k,t] - (lk_xPPM ?
                                                 ↳ dot(view(Xlk_covariates,j,:,:),t), beta_iter[t]))^2
        end

        b_star = sig2h_priors[2] + sum_Y/2
        sig2h_iter[k,t] = rand(InverseGamma(a_star, b_star))
    end

else # t>1

```

```

    for k in 1:nclus_iter[t]
        a_star = sig2h_priors[1] + nh[k,t]/2
        sum_Y = 0.0
        S_kt = findall(Si_iter[:,t] .== k)
        for j in S_kt
            sum_Y += (Y[j,t] - muh_iter[k,t] - eta1_iter[j]*Y[j,t-1] -
            ↳ (lk_xPPM ? dot(view(Xlk_covariates,j,:,:t), beta_iter[t]) :
            ↳ 0.0))^2
        end

        b_star = sig2h_priors[2] + sum_Y/2
        sig2h_iter[k,t] = rand(InverseGamma(a_star, b_star))
    end
end

#####
# update beta #####
# if lk_xPPM && i>=beta_update_threshold # conditional update version
if lk_xPPM
    if t==1
        sum_Y = zeros(p_lk)
        A_star = I(p_lk)/s2_beta
        for j in 1:n
            X_jt = @view Xlk_covariates[j,:,:t]
            sum_Y += (Y[j,t] - muh_iter[Si_iter[j,t],t]) * X_jt /
            ↳ sig2h_iter[Si_iter[j,t],t]
            A_star += (X_jt * X_jt') / sig2h_iter[Si_iter[j,t],t]
        end
        b_star = beta0/s2_beta + sum_Y
        A_star = Symmetric(A_star)
        # Symmetric is needed for numerical problems
        # but A_star is indeed symm and pos def (by construction) so there
        ↳ is no problem
        beta_iter[t] = rand(MvNormalCanon(b_star, A_star))
        # quicker and more accurate method
        # old method with the MvNormal and the inversion required was
        # beta_iter[t] = rand(MvNormal(inv(Symmetric(A_star))*b_star,
        ↳ inv(Symmetric(A_star))))
    else
        sum_Y = zeros(p_lk)
        A_star = I(p_lk)/s2_beta
        for j in 1:n
            X_jt = @view Xlk_covariates[j,:,:t]
            sum_Y += (Y[j,t] - muh_iter[Si_iter[j,t],t] -
            ↳ eta1_iter[j]*Y[j,t-1]) * X_jt / sig2h_iter[Si_iter[j,t],t]
            A_star += (X_jt * X_jt') / sig2h_iter[Si_iter[j,t],t]
        end
        b_star = beta0/s2_beta + sum_Y
        A_star = Symmetric(A_star)
        beta_iter[t] = rand(MvNormalCanon(b_star, A_star))
    end
end

#####
# update theta #####
aux1 = 1 / (lambda2_iter*(1-phi1_iter^2))
kt = nclus_iter[t]
sum_mu = 0.0
for k in 1:kt
    sum_mu += muh_iter[k,t]
end

```

```

if t==1
    sig2_post = 1 / (1/lambda2_iter + phi1_iter^2*aux1 + kt/tau2_iter[t])
    mu_post = sig2_post * (phi0_iter/lambda2_iter + sum_mu/tau2_iter[t] +
    ↵ (phi1_iter*(theta_iter[t+1] - (1-phi1_iter)*phi0_iter))*aux1)

    theta_iter[t] = rand(Normal(mu_post, sqrt(sig2_post)))

elseif t==T
    sig2_post = 1 / (aux1 + kt/tau2_iter[t])
    mu_post = sig2_post * (sum_mu/tau2_iter[t] + ((1- phi1_iter)*phi0_iter
    ↵ + phi1_iter*theta_iter[t-1])*aux1)

    theta_iter[t] = rand(Normal(mu_post, sqrt(sig2_post)))

else # 1<t<T
    sig2_post = 1 / ((1+phi1_iter^2)*aux1 + kt/tau2_iter[t])
    mu_post = sig2_post * (sum_mu/tau2_iter[t] +
    ↵ (phi1_iter*(theta_iter[t-1]+theta_iter[t+1]) +
    ↵ phi0_iter*(1-phi1_iter)^2)*aux1)

    theta_iter[t] = rand(Normal(mu_post, sqrt(sig2_post)))
end

#####
# update tau2 #####
kt = nclus_iter[t]
aux1 = 0.0
for k in 1:kt
    aux1 += (muh_iter[k,t] - theta_iter[t])^2
end
a_star = tau2_priors[1] + kt/2
b_star = tau2_priors[2] + aux1/2
tau2_iter[t] = rand(InverseGamma(a_star, b_star))

end # for t in 1:T

#####
# update eta1 #####
# the input argument eta1_priors[2] is already the std dev
if update_eta1
    for j in 1:n
        eta1_old = eta1_iter[j]
        eta1_new = rand(Normal(eta1_old, eta1_priors[2])) # proposal value

        if (-1 <= eta1_new <= 1)
            ll_old = 0.0
            ll_new = 0.0
            for t in 2:T
                # likelihood contribution
                ll_old += loglikelihood(Normal(
                    muh_iter[Si_iter[j,t],t] + eta1_old*Y[j,t-1] + (lk_xPPM ?
                    ↵ dot(view(Xlk_covariates,j,:,:t), beta_iter[t]) : 0),
                    sqrt(sig2h_iter[Si_iter[j,t],t]*(1-eta1_old^2))
                ), Y[j,t])
                ll_new += loglikelihood(Normal(
                    muh_iter[Si_iter[j,t],t] + eta1_new*Y[j,t-1] + (lk_xPPM ?
                    ↵ dot(view(Xlk_covariates,j,:,:t), beta_iter[t]) : 0),
                    sqrt(sig2h_iter[Si_iter[j,t],t]*(1-eta1_new^2))
                ), Y[j,t])
            end
            logit_old = aux_logit(eta1_old)
            logit_new = aux_logit(eta1_new)
        end
    end
end

```

```

# prior contribution
ll_old += -log(2*eta1_priors[1]) -1/eta1_priors[1]*abs(logit_old)
ll_new += -log(2*eta1_priors[1]) -1/eta1_priors[1]*abs(logit_new)

ll_ratio = ll_new-ll_old
u = rand(Uniform(0,1))
if (ll_ratio > log(u))
    eta1_iter[j] = eta1_new # accept the candidate
    acceptance_ratio_eta1 += 1
end
end
end
end

##### update alpha #####
if update_alpha
    if time_specific_alpha==false && unit_specific_alpha==false
        # a scalar
        sumg = sum(@view gamma_iter[:,1:T])
        a_star = alpha_priors[1] + sumg
        b_star = alpha_priors[2] + n*T - sumg
        alpha_iter = rand(Beta(a_star, b_star))

    elseif time_specific_alpha==true && unit_specific_alpha==false
        # a vector in time
        for t in 1:T
            sumg = sum(@view gamma_iter[:,t])
            a_star = alpha_priors[1] + sumg
            b_star = alpha_priors[2] + n - sumg
            alpha_iter[t] = rand(Beta(a_star, b_star))
        end

    elseif time_specific_alpha==false && unit_specific_alpha==true
        # a vector in units
        for j in 1:n
            sumg = sum(@view gamma_iter[j,1:T])
            a_star = alpha_priors[1,j] + sumg
            b_star = alpha_priors[2,j] + T - sumg
            alpha_iter[j] = rand(Beta(a_star, b_star))
        end

    elseif time_specific_alpha==true && unit_specific_alpha==true
        # a matrix
        for j in 1:n
            for t in 1:T
                sumg = gamma_iter[j,t] # nothing to sum in this case
                a_star = alpha_priors[1,j] + sumg
                b_star = alpha_priors[2,j] + 1 - sumg
                alpha_iter[j,t] = rand(Beta(a_star, b_star))
            end
        end
    end
end

##### update phi0 #####
aux1 = 1/lambda2_iter
aux2 = 0.0
for t in 2:T
    aux2 += theta_iter[t] - phi1_iter*theta_iter[t-1]
end

```

```

sig2_post = 1 / ( 1/phi0_priors[2] + aux1 * (1 +
    ↵ (T-1)*(1-phi1_iter)/(1+phi1_iter)) )
mu_post = sig2_post * ( phi0_priors[1]/phi0_priors[2] + theta_iter[1]*aux1 +
    ↵ aux1/(1+phi1_iter)*aux2 )
phi0_iter = rand(Normal(mu_post, sqrt(sig2_post)))

#####
# update phi1 #####
# the input argument phi1_priors is already the std dev
if update_phi1
    phi1_old = phi1_iter
    phi1_new = rand(Normal(phi1_old, phi1_priors)) # proposal value

    if (-1 <= phi1_new <= 1)
        ll_old = 0.0; ll_new = 0.0
        for t in 2:T
            # likelihood contribution
            ll_old += loglikelihood(Normal(
                (1-phi1_old)*phi0_iter + phi1_old*theta_iter[t-1],
                sqrt(lambda2_iter*(1-phi1_old^2))
            ), theta_iter[t])
            ll_new += loglikelihood(Normal(
                (1-phi1_new)*phi0_iter + phi1_new*theta_iter[t-1],
                sqrt(lambda2_iter*(1-phi1_new^2))
            ), theta_iter[t])
        end

        # prior contribution
        ll_old += loglikelihood(Uniform(-1,1), phi1_old)
        ll_new += loglikelihood(Uniform(-1,1), phi1_new)

        ll_ratio = ll_new-ll_old
        u = rand(Uniform(0,1))
        if (ll_ratio > log(u))
            phi1_iter = phi1_new # accept the candidate
            acceptance_ratio_phi1 += 1
        end
    end
end

#####
# update lambda2 #####
aux1 = 0.0
for t in 2:T
    aux1 += (theta_iter[t] - (1-phi1_iter)*phi0_iter -
        ↵ phi1_iter*theta_iter[t-1])^2
end
a_star = lambda2_priors[1] + T/2
b_star = lambda2_priors[2] + ((theta_iter[1] - phi0_iter)^2 + aux1) / 2
lambda2_iter = rand(InverseGamma(a_star,b_star))

#####
# save MCMC iterates #####
if i>burnin && i%thin==0
    Si_out[:, :, i_out] = Si_iter[:, 1:T]
    gamma_out[:, :, i_out] = gamma_iter[:, 1:T]
    if time_specific_alpha==false && unit_specific_alpha==false
        # for each iterate, a scalar
        alpha_out[i_out] = alpha_iter
    elseif time_specific_alpha==true && unit_specific_alpha==false
        # for each iterate, a vector in time
        alpha_out[:, i_out] = alpha_iter[1:T]
    end
end

```

```

    elseif time_specific_alpha==false && unit_specific_alpha==true
        # for each iterate, a vector in units
        alpha_out[:,i_out] = alpha_iter
    elseif time_specific_alpha==true && unit_specific_alpha==true
        # for each iterate, a matrix
        alpha_out[:, :, i_out] = alpha_iter[:, 1:T]
    end
    for t in 1:T
        for j in 1:n
            sigma2h_out[j, t, i_out] = sig2h_iter[Si_iter[j, t], t]
            muh_out[j, t, i_out] = muh_iter[Si_iter[j, t], t]
        end
    end
    eta1_out[:, i_out] = eta1_iter
    if lk_xPPM
        for t in 1:T
            beta_out[t, :, i_out] = beta_iter[t]
        end
    end
    theta_out[:, i_out] = theta_iter[1:T]
    tau2_out[:, i_out] = tau2_iter[1:T]
    phi0_out[i_out] = phi0_iter
    phi1_out[i_out] = phi1_iter
    lambda2_out[i_out] = lambda2_iter

##### save fitted values and metrics #####
for j in 1:n
    for t in 1:T
        muh_jt = muh_iter[Si_iter[j, t], t]
        sig2h_jt = sig2h_iter[Si_iter[j, t], t]
        X_lk_term = lk_xPPM ? dot(view(Xlk_covariates, j, :, t), beta_iter[t])
        → : 0.0

        if t==1
            llike[j, t, i_out] = logpdf(Normal(
                muh_jt + X_lk_term,
                sqrt(sig2h_jt)
            ), Y[j, t])
            fitted[j, t, i_out] = muh_jt + X_lk_term
        else # t>1
            llike[j, t, i_out] = logpdf(Normal(
                muh_jt + eta1_iter[j]*Y[j, t-1] + X_lk_term,
                sqrt(sig2h_jt*(1-eta1_iter[j]^2))
            ), Y[j, t])
            fitted[j, t, i_out] = muh_jt + eta1_iter[j]*Y[j, t-1] + X_lk_term
        end
        mean_likelhd[j, t] += exp(llike[j, t, i_out])
        mean_loglikelhd[j, t] += llike[j, t, i_out]
        CPO[j, t] += exp(-llike[j, t, i_out])
    end
    end

    i_out += 1
end

next!(progresso)

end # for i in 1:draws

println("\ndone!")

```

```

t_end = now()
println("Elapsed time: ",
    ↪ Dates.canonicalize(Dates.CompoundPeriod(t_end-t_start)))

##### compute LPML and WAIC #####
for j in 1:n
    for t in 1:T
        LPML += log(CPO[j,t])
    end
end
LPML -= n*T*log(nout) # scaling factor
LPML = -LPML # fix sign
println("LPML: ", LPML, " (the higher the better)")

# adjust mean variables
mean_likelhd ./= nout
mean_loglikelhd./= nout
for j in 1:n
    for t in 1:T
        WAIC += 2*mean_loglikelhd[j,t] - log(mean_likelhd[j,t])
    end
end
WAIC *= -2
println("WAIC: ", WAIC, " (the lower the better)")

if update_eta1 @printf "acceptance ratio eta1: %.2f%%\n"
    ↪ acceptance_ratio_eta1/(n*draws)*100 end
if update_phi1 @printf "acceptance ratio phi1: %.2f%%"
    ↪ acceptance_ratio_phi1/draws*100 end
println()

if perform_diagnostics
    chn = Chains(
        hcat(lambda2_out,phi0_out,tau2_out',theta_out',eta1_out',alpha_out'),
        ["lambda2","phi0",
        [string("tau2_t", i) for i in 1:T]...,
        [string("theta_t", i) for i in 1:T]...,
        [string("eta1_j", i) for i in 1:n]...,
        [string("alpha_t", i) for i in 1:T]...,
        ])
    ss = DataFrame(summarystats(chn))
    println("\nDiagnostics:")
    @show ss[!, [1,4,5,6,7]];
    if logging CSV.write(log_file,ss[!, [1,4,5,6,7]]) end
end

close(log_file)

if simple_return
    return Si_out, LPML, WAIC
else
    return Si_out, Int.(gamma_out), alpha_out, sigma2h_out, muh_out, include_eta1
    ↪ ? eta1_out : NaN, lk_xPPM ? beta_out : NaN, theta_out, tau2_out,
    ↪ phi0_out, include_phi1 ? phi1_out : NaN, lambda2_out, fitted, llike,
    ↪ LPML, WAIC
end

```

## B.2 Interface

Now some more technical details about the whole implementation design. The fitting code was written in Julia, but its main intended use is from R. This choice was made because R is currently the best language for statistical purposes, or at least the most spread; in fact all other models “competitors” to the DRPM are available through some R package. Therefore we thought that letting our work be also accessible from R, and not only from Julia, would have eased the possibilities of testing and comparisons with other models or datasets.

To do so, we relied on the `JuliaConnectoR` library [LHB22] on R, which allows the interaction between the two languages. In this sense, we can load in R the Julia package `JDRPM`, which stores the Julia project (i.e. all codes and packages dependencies) about the improved version of the DRPM model, and call it using data and arguments from R. The output produced by the Julia functions has then to be converted back into R structures, which is done automatically through a dedicated function of the package. The structure of this workflow is summarized in Listing 4.

**Listing 4:** Instructions on how to use the `JDRPM` model from R.

```
#####
# Requirements #####
# install the required package
install.packages("JuliaConnectoR")

#####
# Setup #####
# load the package
library(JuliaConnectoR)
# check it returns TRUE
juliaSetupOk()

# load the Package manager on Julia
juliaEval("using Pkg")
# enter into the JDRPM project
juliaEval("Pkg.activate(\"<path/to/where/you/stored/JDRPM>\")")

# downloads and install, only once, all the dependencies
juliaEval("Pkg.instantiate()")
# now, as a check, this should print the list of packages that JDRPM uses,
# such as Distributions, Statistics, LinearAlgebra, SpecialFunctions, etc.
juliaEval("Pkg.status()")

# locate the "main" file
module = normalizePath("<path/to/where/you/stored/JDRPM>/src/JDRPM.jl")
# load the "main" file into a callable R object
module_JDRPM = juliaImport(juliaCall("include", module))

# trigger the compilation of the function, otherwise all first runs
# will be slow since the function still would have to be compiled
module_JDRPM$trigger_compilation()

#####
# Fit #####
# perform the fit
out = module_JDRPM$MCMC_fit(...)
```

```

# convert the output to R structures
rout = juliaGet(out)
names(rout) = c("Si", "gamma", "alpha", "sigma2h", "muh", "eta1", "beta", "theta",
← "tau2", "phi0", "phi1", "lambda2", "fitted", "llike", "lpml", "waic")

# and reshape it to uniform to the DRPM output form
rout$Si = apperm(rout$Si, c(2, 1, 3))
rout$gamma = apperm(rout$gamma, c(2, 1, 3))
rout$sigma2h = apperm(rout$sigma2h, c(2, 1, 3))
rout$muh = apperm(rout$muh, c(2, 1, 3))
rout$fitted = apperm(rout$fitted, c(2, 1, 3))
rout$llike = apperm(rout$llike, c(2, 1, 3))
rout$alpha = apperm(rout$alpha, c(2, 1))
rout$theta = apperm(rout$theta, c(2, 1))
rout$tau2 = apperm(rout$tau2, c(2, 1))
rout$eta1 = apperm(rout$eta1, c(2, 1))
rout$phi0 = matrix(rout$phi0, ncol = 1)
rout$phi1 = matrix(rout$phi1, ncol = 1)
rout$lambda2 = matrix(rout$lambda2, ncol = 1)
# this reshape works in the case of full model fit, but in the case of special
# fitting options (e.g. unit_specific_alpha=true) it needs to be adjusted

```

The `trigger_compilation` function runs the fitting function on a small test case to simply give Julia a friendly nudge to compile the function, making all the subsequent and more serious fits faster. In fact, especially for more complex projects, there are packages such as `PrecompileTools` and `PackageCompiler` which helps to solve this “time to first execution” problem of Julia.

Regarding instead the visual interface, in the sense of the feedback provided by the function, we decided to make it more user-friendly and possibly informative than the original C implementation. The most relevant add-ons are the possibility to perform diagnostics on a subset of the sampled parameters, and the real-time progress monitoring, which updates itself every second to show the estimated remaining time to complete the fit. As a further proof of the ease of this language, these features were just a simple insertion of few lines of code, thanks to the Julia packages `MCMCChains` and `ProgressMeter`.

**Listing 5:** Feedback from the JDRPM implementation.

```

# if verbose=true this initial parameter section is also printed
Parameters:
sig2h ~ invGamma(0.01, 0.01)
Logit(1/2(eta1+1)) ~ Laplace(0, 0.9)
tau2 ~ invGamma(1.9, 0.4)
phi0 ~ Normal(mu=0.0, sigma=10.0)
lambda2 ~ invGamma(1.9, 0.4)
alpha ~ Beta(2.0, 2.0)

- using seed 113.0 -
fitting 100000 total iterates (with burnin=80000, thinning=5)
thus producing 4000 valid iterates in the end

on n=105 subjects
for T=12 time instants

```

[✓] with space? true (cohesion 3.0)  
[X] with covariates in the likelihood? false  
[X] with covariates in the clustering process? false  
[X] are there missing data in Y? false

2024-10-14 09:33:11  
Starting MCMC algorithm  
Progress: 100% Time: 0:25:39 (15.40 ms/it)

done!  
Elapsed time: 25 minutes, 39 seconds, 569 milliseconds  
LPML: 517.182456879369 (the higher the better)  
WAIC: -1283.8930457498177 (the lower the better)  
acceptance ratio eta1: 74.66%

```
# if perform_diagnostics=true this final diagnostics section is also printed
Diagnostics:
ss[!, [1, 4, 5, 6, 7]] = 143×5 DataFrame
  Row | parameters      mcse      ess_bulk      ess_tail      rhat
      | Symbol          Float64     Float64     Float64     Float64
-----|-----
  1 | lambda2        0.000817173  4243.04    3970.25    0.999769
  2 | phi0           0.00218706   3533.95    3675.99    1.00018
  3 | tau2_t1        0.00540064   3716.56    3645.99    0.999968
  :
  14 | tau2_t12       0.00259168   3965.77    3655.55    0.999951
  15 | theta_t1       0.00404988   3603.34    3765.78    0.999834
  :
  26 | theta_t12       0.00337843   3588.83    3907.13    0.999866
  27 | eta1_j1         0.0112187    451.588   1107.96    1.00163
  :
  131 | eta1_j105      0.00328424   1539.36    2194.83    1.00002
  132 | alpha_t1        0.000213087  3774.24    3920.48    1.00044
  :
  143 | alpha_t12       0.00266005   541.427   1867.54    1.0084
```

# Bibliography

- [Bar+12] Luis E Nieto Barajas et al. “A Time-Series DDP for Functional Proteomics Profiles”. In: *Biometrics* 68.3 (Jan. 2012), pp. 859–868. DOI: 10.1111/j.1541-0420.2011.01724.x. URL: <https://doi.org/10.1111/j.1541-0420.2011.01724.x> (cit. on p. 3).
- [AW15] Isadora Antoniano Villalobos and Stephen Walker. “A Nonparametric Model for Stationary Time Series”. In: *Journal of Time Series Analysis* 63 (Aug. 2015). DOI: 10.1111/jtsa.12146 (cit. on p. 3).
- [GMR16] Luis Gutiérrez, Ramsés H. Mena, and Matteo Ruggiero. “A time dependent Bayesian nonparametric model for air quality analysis”. In: *Computational Statistics & Data Analysis* 95.C (2016), pp. 161–175. DOI: 10.1016/j.csda.2015.10.00. URL: <https://ideas.repec.org/a/eee/csdana/v95y2016icp161-175.html> (cit. on p. 3).
- [Jo+16] Seongil Jo et al. “Dependent Species Sampling Models for Spatial Density Estimation”. In: *Bayesian Analysis* 12 (May 2016). DOI: 10.1214/16-BA1006 (cit. on p. 3).
- [KG18] Maria Kalli and Jim Griffin. “Bayesian nonparametric vector autoregressive models”. In: *Journal of Econometrics* 203 (Jan. 2018). DOI: 10.1016/j.jeconom.2017.11.009 (cit. on p. 3).
- [DK18] Maria De Iorio and Athanasios Kottas. “Modeling for Dynamic Ordinal Regression Relationships: An Application to Estimating Maturity of Rockfish in California”. In: *Journal of the American Statistical Association* 113.521 (2018), pp. 68–80. DOI: 10.1080/01621459.2017.1328357. eprint: <https://doi.org/10.1080/01621459.2017.1328357>. URL: <https://doi.org/10.1080/01621459.2017.1328357> (cit. on p. 3).
- [De +19] Maria De Iorio et al. *Bayesian nonparametric temporal dynamic clustering via autoregressive Dirichlet priors*. Oct. 2019. DOI: 10.48550/arXiv.1910.10443 (cit. on p. 3).
- [Car+17] François Caron et al. “Generalized póya urn for time-varying pitman-yor processes”. In: *J. Mach. Learn. Res.* 18.1 (Jan. 2017), pp. 836–867. ISSN: 1532-4435 (cit. on p. 3).
- [PQD22] Garrit L. Page, Fernando A. Quintana, and David B. Dahl. “Dependent Modeling of Temporal Sequences of Random Partitions”. In: *Journal of Computational and Graphical Statistics* 31.2 (2022), pp. 614–627. DOI: 10.1080/10618600.2021.1987255. eprint: <https://doi.org/>

- 10.1080/10618600.2021.1987255. URL: <https://doi.org/10.1080/10618600.2021.1987255> (cit. on pp. 3, 6, 29, 30).
- [Chr+10] Ronald Christensen et al. *Bayesian ideas and data analysis. An introduction for scientists and statisticians*. CRC Press, 2010. DOI: 10.1201/9781439894798 (cit. on p. 10).
- [GHV13] Andrew Gelman, Jessica Hwang, and Aki Vehtari. “Understanding predictive information criteria for Bayesian models”. In: *Statistics and Computing* 24 (July 2013). DOI: 10.1007/s11222-013-9416-2 (cit. on p. 10).
- [PQ15] Garrett Page and Fernando Quintana. “Spatial Product Partition Models”. In: *Bayesian Analysis* 11 (Apr. 2015). DOI: 10.1214/15-BA971 (cit. on p. 10).
- [DH01] D. Denison and C Holmes. “Bayesian Partitioning for Estimating Disease Risk”. In: *Biometrics* 57 (Apr. 2001), pp. 143–9. DOI: 10.1111/j.0006-341X.2001.00143.x (cit. on p. 12).
- [De +15] Pierpaolo De Blasi et al. “Are Gibbs-Type Priors the Most Natural Generalization of the Dirichlet Process?” In: *IEEE Trans. Pattern Anal. Mach. Intell.* 37.2 (Feb. 2015), pp. 212–229. ISSN: 0162-8828. DOI: 10.1109/TPAMI.2013.217. URL: <https://doi.org/10.1109/TPAMI.2013.217> (cit. on p. 15).
- [MQR11] Peter Müller, Fernando Quintana, and Gary Rosner. “A Product Partition Model With Regression on Covariates”. In: *Journal of computational and graphical statistics: a joint publication of American Statistical Association, Institute of Mathematical Statistics, Interface Foundation of North America* 20 (Mar. 2011), pp. 260–278. DOI: 10.1198/jcgs.2011.09066 (cit. on p. 15).
- [QMP15] Fernando Quintana, Peter Müller, and Ana Luisa Papoila. “Cluster-Specific Variable Selection for Product Partition Models”. In: *Scandinavian Journal of Statistics* 42 (Mar. 2015). DOI: 10.1111/sjos.12151 (cit. on p. 15).
- [PQ18] Garrett Page and Fernando Quintana. “Calibrating covariate informed product partition models”. In: *Statistics and Computing* 28 (Sept. 2018), pp. 1–23. DOI: 10.1007/s11222-017-9777-z (cit. on p. 15).
- [Gow71] J. C. Gower. “A General Coefficient of Similarity and Some of Its Properties”. In: *Biometrics* 27.4 (1971), pp. 857–871. ISSN: 0006341X, 15410420. URL: <http://www.jstor.org/stable/2528823> (visited on 10/16/2024) (cit. on p. 17).
- [Bez+17] Jeff Bezanson et al. “Julia: A fresh approach to numerical computing”. In: *SIAM Review* 59.1 (2017), pp. 65–98. DOI: 10.1137/141000671. URL: <https://epubs.siam.org/doi/10.1137/141000671> (cit. on p. 21).

- [Law+79] C. L. Lawson et al. “Basic Linear Algebra Subprograms for Fortran Usage”. In: *ACM Trans. Math. Softw.* 5.3 (Sept. 1979), pp. 308–323. ISSN: 0098-3500. DOI: 10.1145/355841.355847. URL: <https://doi.org/10.1145/355841.355847> (cit. on p. 21).
- [Bes+21] Mathieu Besançon et al. “Distributions.jl: Definition and Modeling of Probability Distributions in the JuliaStats Ecosystem”. In: *Journal of Statistical Software* 98.16 (2021), pp. 1–30. ISSN: 1548-7660. DOI: 10.18637/jss.v098.i16. URL: <https://www.jstatsoft.org/v098/i16> (cit. on p. 21).
- [Lin+19] Dahua Lin et al. *JuliaStats/Distributions.jl: a Julia package for probability distributions and associated functions*. July 2019. DOI: 10.5281/zenodo.2647458. URL: <https://doi.org/10.5281/zenodo.2647458> (cit. on p. 21).
- [CR16] Jiahao Chen and Jarrett Revels. “Robust benchmarking in noisy environments”. In: *arXiv e-prints*, arXiv:1608.04295 (Aug. 2016). arXiv: 1608.04295 [cs.PF] (cit. on p. 23).
- [HA85] Lawrence J. Hubert and Phipps Arabie. “Comparing partitions”. In: *Journal of Classification* 2 (1985), pp. 193–218. URL: <https://api.semanticscholar.org/CorpusID:189915041> (cit. on p. 29).
- [Fas+23] A. Fassò et al. *AgrImOnIA: Open Access dataset correlating livestock and air quality in the Lombardy region, Italy (3.0.0)*. 2023. DOI: <https://doi.org/10.5281/zenodo.7956006> (cit. on p. 31).
- [Gel04] Andrew Gelman. “Prior Distributions for Variance Parameters in Hierarchical Models”. In: *Economics and Econometrics Research Institute (EERI), EERI Research Paper Series* 1 (Jan. 2004) (cit. on p. 58).
- [LHB22] Stefan Lenz, Maren Hackenberg, and Harald Binder. “The JuliaConnectoR: A Functionally-Oriented Interface for Integrating Julia in R”. In: *Journal of Statistical Software* 101.6 (2022), pp. 1–24. DOI: 10.18637/jss.v101.i06 (cit. on p. 84).



# Acknowledgements

*"This is to be my haven for many long years, my niche which I enter with such a mistrustful, such a painful sensation... And who knows? Maybe when I come to leave it many years hence I may regret it!"*

— Fëdor Dostoevskij, *The House of the Dead*

I would like to thank my advisors Alessandra Guglielmi and Alessandro Carminati, primarily for having made me feel, during the entire course of the thesis, in a very calm and lovely atmosphere, in which I have been able to feel completely at ease (which is notoriously a NP-hard problem). The epigraphs of my beloved author Dostoevsky and the title inspired by the Star Wars films, as well as some poetic licenses and easter eggs scattered in the various chapters (which they have kindly allowed me to keep) I think prove this feeling of sweet confidence.

I thank professor Alessandra Guglielmi for the faith she put on myself and my skills, as perhaps witnessed by the relatively few meetings that we made to monitor the development of the thesis. At least, this is how I interpreted the autonomy and independence given to me, but it could have been easily due the fact that she had better things to do than follow the adventures of a young grad student. Jokes aside, my a-posteriori beliefs still support the idea of the faith.

I thank Alessandro Carminati for having helped me in many of the most critical phases of the thesis. His action always precise and effective has been necessary to solve the various theoretical puddles in which I got mired. Moreover, we share the same passion for Julia and, I believe, the delight for having overthrown the not-so-missed C of the old model implementation.

I thank my family for having helped me during these years of university, and my friends and fellows who have always and wisely brought to light my highest potential and resources. The passion for solving problems, inventing creative solutions, getting lost in calculations, wandering trough the magical world of the most advanced mathematics, sharing doubts and reasonings: all this has always found in you a great companion.



# Ringraziamenti

*“Ecco il mio ponte d’approdo per molti lunghi anni, il mio angioletto, nel quale faccio il mio ingresso con una sensazione così diffidente, così morbosa... Ma chi lo sa? Forse, quando tra molti anni mi toccherà abbandonarlo, magari potrei anche rimiangerlo!”*

— Fëdor Dostoevskij, *Memorie da una casa di morti*

Vorrei ringraziare innanzitutto i miei relatori Alessandra Guglielmi e Alessandro Carminati, principalmente per avermi fatto sentire, durante l’intero svolgimento della tesi, in un clima molto tranquillo, sereno, in cui ho avuto modo di trovarmi pienamente a mio agio. Le epigrafi del mio caro autore Dostoevskij e il titolo ispirato alla saga di Star Wars, nonché alcune licenze poetiche sparse nei vari capitoli (che loro mi hanno gentilmente concesso di tenere) credo dimostrino questa atmosfera di piacevole confidenza.

Ringrazio la professoressa Alessandra Guglielmi per la fiducia che ha riposto in me e nelle mie capacità, come forse testimoniato dai relativamente pochi incontri che abbiamo fatto per gestire il lavoro della tesi. O almeno, così ho interpretato questa autonomia e indipendenza che mi è stata concessa, ma poteva tranquillamente trattarsi del fatto che avesse di meglio da fare che seguire le avventure di un giovane laureando. In ogni caso, le mie convinzioni a posteriori sostengono apertamente la visione della fiducia.

Ringrazio Alessandro Carminati per avermi aiutato in molte delle fasi più critiche della tesi. Il suo intervento sempre preciso e puntuale è stato necessario per risolvere le varie pozanghere teoriche in cui mi ero impantanato. Inoltre, condividiamo la stessa passione per Julia e, credo, la soddisfazione per aver battuto il non-così-compianto C della vecchia implementazione del modello.

Ringrazio la mia famiglia per avermi aiutato durante questi anni di università, e i miei amici e compagni di studio, i quali hanno sempre sapientemente fatto emergere le mie migliori potenzialità e risorse. La passione per risolvere problemi, ideare soluzioni creative, perdersi nei calcoli, addentrarsi nel magico mondo della matematica più avanzata, condividere dubbi e ragionamenti: tutto questo ha sempre trovato in voi un’ottima compagnia.